MAP GP-1001

U.S. DEPARTMENT OF THE INTERIOR
U.S. GEOLOGICAL SURVEY

GEOPHYSICAL LOGS AND CORE MEASUREMENTS FROM FORTY BOREHOLES AT YUCCA MOUNTAIN, NEVADA

By Philip H. Nelson, Douglas C. Muller, Ulrich Schimschal, and Joyce E. Kibler

Prepared in cooperation with the
U.S. DEPARTMENT OF ENERGY

GEOPHYSICAL INVESTIGATIONS MAP
Published by the U.S. Geological Survey, 1991

NELSON AND OTHERS—GEOPHYSICAL LOGS AND CORE MEASUREMENTS FROM FORTY BOREHOLES AT YUCCA MOUNTAIN, NEVADA MAP GP-1001

U.S. DEPARTMENT OF THE INTERIOR
U.S. GEOLOGICAL SURVEY

GEOPHYSICAL LOGS AND CORE MEASUREMENTS FROM FORTY BOREHOLES AT YUCCA MOUNTAIN, NEVADA

By

Philip H. Nelson, Douglas C. Muller, Ulrich Schimschal, and Joyce E. Kibler

Prepared in cooperation with the U.S. Department of Energy

Pamphlet to accompany
GEOPHYSICAL INVESTIGATIONS
MAP GP–1001

CONTENTS

PLATES

FIGURES

TABLES

Geophysical Logs and Core Measurements from Forty Boreholes at Yucca Mountain, Nevada

By Philip H. Nelson, Douglas C. Muller, Ulrich Schimschal, *and* Joyce E. Kibler

Abstract

A data base of geophysical logs and core measurements acquired in boreholes at Yucca Mountain, Nevada, has been established. We used this data set to generate log plots from 40 boreholes at a scale of 1:1,200 for reference and for correlation. Log headers summarize the drilling and logging sequence. We describe the logging tools, the sources of core data, and the editing procedures. We illustrate the adverse effects of casing on the gamma-ray log, of borehole rugosity on the density log, and of borehole diameter and fluid resistivity on the resistivity logs.

Welding and alteration of the tuffs are the dominant geological controls on the response of the density, velocity, neutron, and resistivity logs. Density, resistivity, gamma-ray, and, in particular, the magnetic-field logs are useful for correlation of stratigraphy and alteration. A few zones in which the matrix is moderately permeable have produced log responses indicating invasion of the rock by drilling fluid. Readings from the density log were confirmed with core measurements. It appears that the epithermal-neutron and dielectric-permittivity logs can be used to estimate water content providing calibration methods are established.

INTRODUCTION

During the last 10 years, the U.S. Geological Survey has participated in the geological characterization of Yucca Mountain as a potential site for the emplacement of radioactive waste. Drilling and logging of boreholes have been a major component of this effort. Logs have been routinely acquired in any hole that was drilled to the depth of the proposed repository. By the end of 1984, 40 boreholes had been completed and logged (fig. 1). Logs from water well J–13, which was drilled in 1963, are included in the set of 40 boreholes.

Manuscript approved for publication May 4, 1990.

Objectives of the logging program are to provide data and interpretations for locating and characterizing lithostratigraphic units and contacts, and for determining the distribution of rock properties. This report describes a major step toward these objectives: the consolidation of the logs into a computerized data base. The data base facilitates presentation of the logs in a format that permits easy inspection of the data and allows comparison among logs from different boreholes. Because the logs are most effectively evaluated by considering geological and hydrological information and core measurements, these other forms of data have been incorporated into the data base and are presented with the geophysical logs.

Table 1 lists all holes for which logs are presented in this report. We will refer to boreholes by their "short name" in the text; the correct long name is given in table 1 for reference. The prefix UE–25 in the long name is used for holes in area 25 of the Nevada Test Site. The prefix USW designates holes outside the boundary of the Nevada Test Site.

Note that the holes are not listed in table 1 in the order in which they were logged but are grouped in the following way: holes from which substantial lengths of core have been recovered (G-series, A–1, B–1H, P–1); holes for hydrological tests (H-series and C-series); holes for monitoring the water table and characterizing the unsaturated zone (WT-series and UZ-series); short holes in Drillhole Wash (A–4 through A–7); and holes that are some distance away from the proposed repository but that still penetrate the tuff sequence (J–13, VH–1, VH–2).

We have omitted logs from hole UE–29a#2 in Fortymile Wash because they are incomplete. We have also omitted UE–25a#3 in the Calico Hills, which penetrated argillite of the Upper Devonian to Lower

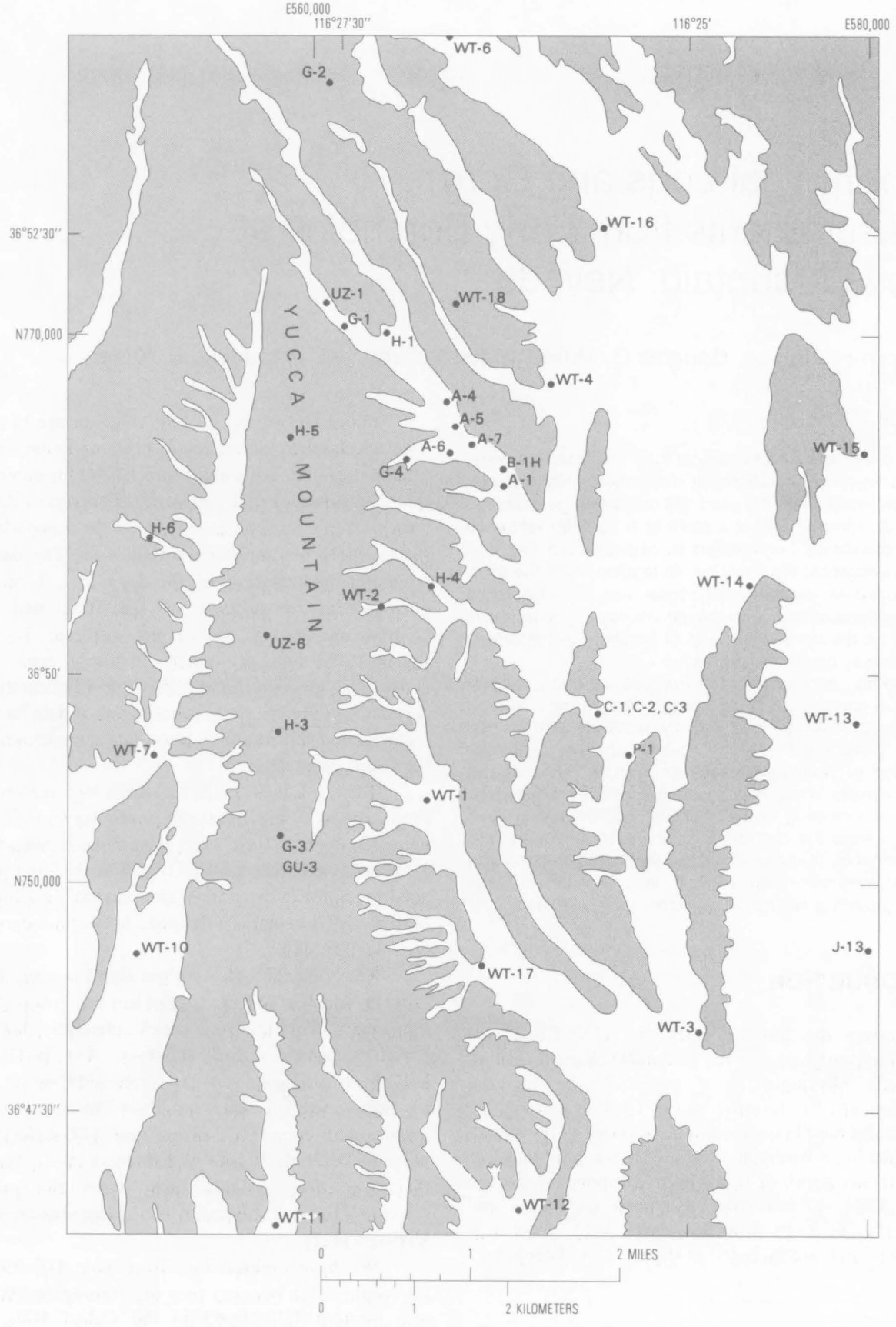

Figure 1. Index map showing location of 38 of 40 logged boreholes at Yucca Mountain, Nev. Boreholes USW VH-1 and USW VH-2 are located approximately 6 mi west of Yucca Mountain.

Table 1. Descriptions of boreholes at Yucca Mountain, Nev.

[Y, yes; N, no; B, bottom; ---, static water level not reached or not measured]

Short name	Long name	Coordinates X	Coordinates Y	Elevation (ft)	Total depth (ft)	Static water level (ft)	Date of last log	Core	Minimum hole diameter (in)
G-1	USW G-1	770500	561000	4349	6000	1876	9/80	Y	3.875
G-2	USW G-2	778824	560504	5098	6006	1722	10/81	Y	2.98
GU-3	USW GU-3	752690	558501	4857	2644	2462	5/82	Y	2.98
G-3	USW G-3	752780	558483	4857	5031	2462	3/82	Y	3.937
G-4	USW G-4	765807	563082	4167	3003	1770	11/82	Y	4.25
A-1	UE-25a#1	764900	566350	3934	2501	1538	8/78	Y	2.98
B-1H	UE-25b#1	765243	566416	3939	4002	1542	8/81	Y	8.5
P-1	UE-25p#1	756171	571485	3655	5923	1188	6/83	Y	6.75
H-1	USW H-1	770254	562388	4274	6000	1876	12/80	Y	8.75
H-3	USW H-3	756542	558452	4866	4000	2464	3/82	N	8.75
H-4	USW H-4	761644	563911	4097	4000	1700	5/82	N	8.75
H-5	USW H-5	766634	558909	4851	4000	2309	6/82	N	8.75
H-6	USW H-6	763299	554075	4271	4002	1729	10/82	Y	8.75
C-1	UE-25c#1	757096	569680	3709	3000	1315	10/83	Y	9.875
C-2	UE-25c#2	756849	569634	3714	3000	---	2/84	Y	9.875
C-3	UE-25c#3	756910	569555	3714	3000	---	4/84	Y	9.875
WT-1	USW WT-1	753941	563739	3942	1689	1545	5/83	B	8.75
WT-2	USW WT-2	760661	561924	4270	2060	1873	7/83	B	8.75
WT-3	UE-25WT#3	745995	573384	3380	1142	986	5/83	B	8.75
WT-4	UE-25WT#4	768512	568040	3835	1580	1440	6/83	B	8.75
WT-6	UE-25WT#6	780576	564524	4312	1256	931	6/83	B	6.75
WT-7	USW WT-7	755570	553891	3927	1610	1382	7/83	B	8.75
WT-10	USW WT-10	748771	553302	3686	1413	1141	7/83	B	8.75
WT-11	USW WT-11	739070	558377	3591	1446	1194	8/83	B	8.75
WT-12	UE-25WT#12	739726	567011	3527	1308	1133	8/83	B	8.75
WT-13	UE-25WT#13	756715	578757	3386	1160	995	7/83	B	8.75
WT-14	UE-25WT#14	761651	575210	3530	1310	1136	9/83	B	8.75
WT-15	UE-25WT#15	766117	579806	3553	1360	1162	11/83	B	8.75
WT-16	UE-25WT#16	774420	570395	3971	1710	1551	11/83	B	8.75
WT-17	UE-25WT#17	748420	566212	3689	1453	1295	10/83	N	8.75
WT-18	UE-25WT#18	771167	564855	4383	2043	DRY	5/84	B	8.75
UZ-1	USW UZ-1	771276	560221	4426	1270	---	7/83	Y	5.0
UZ-6	USW UZ-6	759731	558325	4925	1887	---	9/84	N	17.5
A-4	UE-25a#4	767972	564472	4101	500	---	9/79	Y	6.125
A-5	UE-25a#5	766956	564755	4057	487	---	9/79	Y	6.125
A-6	UE-25a#6	765899	564501	4053	500	---	9/79	Y	5.5
A-7	UE-25a#7	766250	565469	4005	1002	---	10/80	Y	3.875
J-13	J-13	749209	579651	3318	3498	929	12/62	Y	7.625
VH-1	USW VH-1	743356	533626	3161	2501	604	1/81	Y	6.25
VH-2	USW VH-2	748319	526264	3197	4000	---	4/83	Y	3.937

Mississippian Eleana Formation. References to publications giving data on logs and core measurements for UE-25a#3 are included in Appendix 1.

Geophysical logs were previously published for boreholes A-1 (Hagstrum and others, 1980a; Spengler and others, 1979), G-1 (Muller and Kibler, 1983), G-4 (Spengler and Chornack, 1984), A-4 through A-7 (Daniels and others, 1981), P-1 (Muller and Kibler, 1984), and 15 boreholes in the WT series (Muller and Kibler, 1986). With this report, we alter the previous style of reporting and present the geophysical logs for all boreholes drilled as recently as the end of 1984, including the ones previously reported. This change allows us to report all the logs at a uniform scale and move on to log interpretation. In order to accomplish this task, we include less ancillary data and less discussion of each individual hole than was included in the earlier reports.

Drilling and logging of many of the holes in stages required that the individual runs be merged to provide continuous logs. Gaps can be observed in the well-log plots where logging runs failed to overlap. Not all logs that were run are presented here. Some were redundant, such as the gamma-ray log obtained on several logging runs; some were unsuccessful due to tool failure; and some were experimental and failed to yield data of interest. Obviously, we have made many choices regarding which logs to retain and present. These choices are documented on the headers of the individual logs.

The amount of editing of the logs varied greatly with log type. Most logs are essentially as they appeared on the final paper print delivered by the contractor or investigator, except for the previously mentioned questions of merging and redundancy. However, some logs, such as dielectric, magnetic field, and sonic travel-time, contain erroneous data in the form of spikes or dropouts that are clearly attributable to improper equipment response and that would obscure valid information if not removed by editing. The editing criteria for these cases are stated in "Sources of Data and Editing Procedures."

We have not yet applied borehole corrections to account for the influence of hole size and borehole fluid, nor have the logs been shifted to adjust for depth so that the same deviations in log and core occur at the same depth. Both these steps require meticulous care and have been left to subsequent analysis, since they were not required for all logs.

The log data from all wells were loaded onto a VAX 780 computer using a commercial log analysis software package called ESLOG[1]. All log and core data were loaded in increments of 0.5 ft, a null value being inserted for missing data. Thus, each individual physical measurement is stored separately and is referred to as a "trace." The software package serves as a data manager, making it easy to access a particular log in any given well. The software was used to generate the plots accompanying this report.

In "Sources of Data and Editing Procedures" and "Format of the Log Plots," we concentrate on the mechanics of organizing, editing, and plotting the logs, followed by a discussion on the "Effects of Borehole Environment." In "Log Characteristics," we examine the ramifications of the logs as to geological and physical properties of the strata in order to indicate the benefits of further log analysis. Readers interested in more detail concerning the physics of logging tools and interpretation of logs are advised to consult Hearst and Nelson (1985) and Ellis (1987). For a short description of log characteristics relevant to Yucca Mountain, consult Muller and Kibler (1986).

SOURCES OF DATA AND EDITING PROCEDURES

There are two primary sources for the data incorporated in the well-log plots: the paper prints and magnetic tape recordings of the logs themselves and the published reports dealing with stratigraphy, core measurements, and hydrological tests. To aid the reader in referring to the published reports, we include a guide to the information published prior to 1989 on Yucca Mountain boreholes (Appendix 1). Tables 2 and 3 summarize the types of log and core data that are available for each borehole.

Logs were acquired by government agencies (U.S. Geological Survey and Lawrence Livermore National Laboratory) and by commercial contractors. The primary commercial contractor on the Nevada Test Site for many years was Birdwell, which developed expertise in logging holes of large diameter. At Yucca Mountain, Dresser-Atlas tools were used in the holes of smaller diameter. As a consequence, most holes were logged with a mix of Birdwell and Dresser-Atlas tools. In 1985, Dresser-Atlas purchased Birdwell and became the primary logging contractor. In 1987, Dresser-Atlas was renamed "Atlas Wireline Services."

Caliper Logging

Three types of caliper tools are used at Yucca Mountain: a three-arm tool that measures average diameter, a four-arm tool that measures two orthogonal diameters, and a six-arm tool that measures three

[1]Tradename of Energy Systems, Denver, Colo.

Table 2. Types of logs run in boreholes at Yucca Mountain, Nev.

[CAL, caliper; GR, gamma ray; SP, self potential; DBC, density; NBC, thermal neutron; CVL, sonic; IND, induction; RES, resistivity; ENP, epithermal neutron; NNL, thermal neutron; DIE, dielectric; KUT, spectral gamma; MAG, magnetic field; MS, magnetic susceptibility; IP, induced polarization; FLO, radioactive tracer; GRV, gravimeter]

Borehole	CAL	GR	SP	DBC	NBC	CVL	IND	RES	ENP	NNL	DIE	KUT	MAG	MS	IP	FLO	GRV
G-1	*	*	*	*	*	*	*	*	*	*							
G-2	*	*	*	*	*	*	*	*	*	*		*					
GU-3	*	*	*	*	*	*	*	*									
G-3	*	*	*	*	*	*	*	*	*	*		*	*	*	*		*
G-4	*	*	*	*	*	*	*	*		*		*				*	*
A-1	*	*	*	*		*		*		*				*	*		
B-1H	*	*	*	*	*	*	*	*	*			*				*	
P-1	*	*	*	*	*	*	*	*	*		*	*	*			*	*
H-1	*	*	*	*	*	*	*	*	*	*		*	*			*	*
H-3	*	*	*	*	*	*	*	*	*	*		*	*			*	
H-4	*	*	*	*	*	*	*	*	*			*	*			*	
H-5	*	*	*	*	*	*	*	*	*			*	*			*	
H-6	*	*	*	*	*	*	*	*	*			*	*			*	
C-1	*	*	*	*	*	*	*	*	*		*	*					*
C-2	*	*	*	*	*	*	*	*	*		*	*					
C-3	*	*	*	*	*	*	*	*	*		*	*					
WT-1	*	*	*	*			*	*	*		*	*					
WT-2	*	*	*	*			*	*	*		*	*					
WT-3	*	*	*	*			*	*	*		*	*					
WT-4	*	*	*	*			*	*	*		*	*					
WT-6	*	*	*	*			*	*	*		*	*					
WT-7	*	*	*	*			*	*	*		*	*					
WT-10	*	*	*	*			*	*	*		*	*					
WT-11	*	*	*	*			*	*	*		*	*					
WT-12	*	*	*	*			*	*	*		*	*					
WT-13	*	*	*	*			*	*	*		*	*					
WT-14	*	*	*	*			*	*	*		*	*	*	*			
WT-15	*	*	*	*			*	*	*		*	*					
WT-16	*	*	*	*			*	*	*		*	*					
WT-17	*	*	*	*			*	*	*		*	*					
WT-18	*	*	*	*			*	*	*		*	*					
UZ-1	*	*		*			*		*		*	*					
UZ-6	*	*		*			*		*		*	*	*	*			
A-4	*	*	*	*			*	*	*					*	*		
A-5	*	*	*	*			*	*	*					*	*		
A-6	*	*	*	*			*	*	*					*	*		
A-7	*	*	*	*			*	*	*	*				*	*		
J-13	*	*	*			*	*	*		*							
VH-1	*	*	*	*	*	*	*	*	*	*							
VH-2	*	*	*	*	*	*	*	*	*			*	*				

Table 3. Boreholes for which measurements of physical properties of core are available, Yucca Mountain, Nev.

[References are cited in Appendix 1]

Borehole	Bulk density	Grain density	Porosity	Water saturation	Resistivity	Induced polarization	Magnetic properties	Sonic velocity
G-1	*	*	*				*	
G-2	*	*	*				*	
GU-3	*	*	*		*	*	*	*
G-3	*	*	*		*	*	*	*
G-4	*	*	*		*	*		*
A-1	*	*	*		*	*	*	*
B-1H	*	*	*	*				
P-1	*	*	*					
H-1	*	*	*	*				
J-13	*	*	*					
VH-1							*	

equiangular diameters. The six-arm tool is used in holes greater than 4 in. in diameter, and the four-arm and three-arm tools are used in holes less than 4 in. in diameter.

The logging service company presents an average diameter along with the multi-diameter data; we store and present only the average diameter. Users interested in determining hole eccentricity must consult the original field logs.

Gamma-Ray Logging

Total-Count Gamma-Ray Logging

A gamma-ray tool giving a standard total count is ordinarily run singly, a standard practice at the Nevada Test Site. Some gamma-ray logs were run in combination with neutron or density tools. Output is presented in American Petroleum Institute (API) units.

Spectral Gamma-Ray Logging

Spectral gamma-ray logging requires a special tool and a separate logging run. Wichmann and others (1975) described the Dresser-Atlas spectral tool, which provides estimates of the potassium (K), uranium (U), and thorium (Th) concentrations by counting gamma-rays in specific energy windows emitted by radioactive potassium and by radioactive daughter elements of uranium and thorium. Daughter elements result from radioactive decay of a parent element, and the volume percent of the parent element can be related to the number of gamma rays emitted by the daughter, assuming the parent and daughter are in equilibrium.

Because the spectral gamma-ray counting rates are limited by detector sensitivity, the log is typically run at the minimum logging rate of 8–10 ft per minute with time constants of 4–6 seconds in order to improve accuracy. In spite of these precautions, the repeatability of the three channels is less than satisfactory.

We corrected spectral logs acquired prior to April 20, 1983, using correction factors provided by Dresser-Atlas that required division of the original log by 2.20, 2.26, and 1.94 for the K, U and Th traces, respectively. Logs obtained after that date required no correction.

Density Logging

Rock density was measured by three different methods: by continuous logs that measure gamma-ray scattering, by borehole gravimetry from which an interval density can be calculated, and by laboratory measurements of the weight and volume of core samples.

Single-Detector Density Logging

The log from a single-detector gamma-gamma density tool (Birdwell) was recorded in counts per second. The density was then computed in the office by conversion algorithms furnished by Birdwell for wet and

dry holes. Tools of 2.25 and 3.625 in. in diameter were used. Proximity wheels provided a continuous measurement of separation between the tool and the borehole wall (referred to as the "standoff") for the larger tool but never worked properly for the smaller tool. For the larger tool, a correction was calculated on the basis of the standoff. Where the standoff exceeded 0.25 in., the density measurement was discarded. Single-detector tools were used early in the program, then were phased out and replaced by the compensated-density tools.

Compensated-Density Logging

Density tools incorporating two detectors utilize a corrective algorithm to compensate for tool standoff from the borehole wall. This correction is applied in the truck while running the log. Both Birdwell and Dresser Atlas compensated-density tools were run in Yucca Mountain boreholes. The field logs incorporate a correction trace to show the density correction that was applied to the resulting density trace. The magnitude of this correction can be taken as indicative of intervals where large corrections were needed and where tool response may therefore not be reliable.

Gravity Logging

Drill holes G–3, G–4, H–1, P–1, and C–1 were logged with a borehole gravity meter (Healey, Clutsom, and others, 1984, 1986; Robbins and others, 1982), which is influenced by a much larger volume of rock than is the gamma-gamma density tool. Gravity was measured at stations usually spaced 30 ft or more apart. An "interval density" was computed from the difference between the free-air gradient and the measured vertical-gravity gradient. Healey and others (1986) reported that the free-air gradient varies several percentage points at the Nevada Test Site and that an error of 1 percent in the free-air gradient shifts the calculated interval density by 0.037 g/cm^3. Thus, a tower should be used at each drill hole in measuring the free-air gradient. This was done at G–4, P–1, and C–1, but not at G–3 or H–1, for which a value for the free-air gradient was assumed, thereby increasing the uncertainty of the interval densities in those two holes.

Core Data

Bulk density, grain density, and porosity of core samples have been measured by a number of laboratories. Thus far we have incorporated core measurements made by Holmes and Narver in Mercury, Nev.; Terra Tek in Salt Lake City, Utah; Sandia Laboratories in Albuquerque, N. Mex.; and the USGS in Denver, Colo. Because these data are important for log analysis, they are presented in Appendix 2.

Three of the four laboratories (Holmes and Narver, Terra Tek, and Sandia) appear to have measured dry bulk density (DBD) and grain density (GD) and to have computed porosity as 1–(DBD/GD). Nimick and Schwartz (1987, Appendix 1) discussed the methods and uncertainties in the drying and measurement process.

Anderson (1981a,b; 1984) measured core densities in three saturation states: as received from the core barrel (referred to as "natural bulk density," or NBD), after heating to drive off the water (referred to as "dry bulk density," or DBD), and after resaturation (referred to as "saturated bulk density," or SBD). Rather than measure the grain density by the pycnometer method, Anderson calculated the porosity and the grain density from the saturated and dry bulk densities.

Neutron Logging

Three types of neutron-logging tools have been run at Yucca Mountain by Dresser-Atlas and Birdwell. These tools are very sensitive to the type of fluid filling the wellbore, so the change in their response above and below the water level can be dramatic.

Uncompensated Thermal-Neutron Logging

The uncompensated neutron-logging tool has a single thermal-neutron detector. It is a Birdwell tool, is designated NNL (neutron-neutron logging), is run uncentralized (without centralizers or with decentralizers), and is usually recorded in API units. It was tried early in the program in order to obtain data in air-filled boreholes, but was eventually dropped from the logging suite and supplanted by the epithermal tool. In cases where no NNL log was recorded above the water table, the long-spaced detector counts from the compensated tool are reported as NNL (see "Compensated Thermal-Neutron Logging," below).

Compensated Thermal-Neutron Logging

Compensated neutron tools using short and long-spaced detectors have been run mostly by Dresser-Atlas, but some were run by Birdwell. Both are run decentralized with a bowspring that forces the mandrel against the side of the borehole. Where tools from both suppliers were run over the same interval, the Dresser logs were usually retained in the data set. Whether the log was run by Birdwell or by Dresser, it is designated "NBC" for "neutron-borehole compensated" and is

recorded on a "sandstone scale," meaning that the porosity scale is referenced to a calibration facility of clean, water-filled sandstone. The NBC porosity log is reported only for the fluid-filled boreholes. However, the long-spacing counts have been retained and reported as NNL in air-filled holes. This is done because the long-spaced thermal-detector spacing is similar to that of the uncompensated thermal tool.

Epithermal-Neutron Logging

The single-detector epithermal-neutron-logging tool, designated "ENP," is a Birdwell tool. In boreholes as much as 6 in. in diameter, it is held against the borehole wall by extending a pad that contains the source and sensors. In holes greater than 6 in. in diameter, a rigid skid is attached to the tool body in order to maintain contact with the wall. It is too large to be operated in a 4-in. hole, so many boreholes (for example, G–3) have an ENP only in the upper part of the hole. It is run singly, not in combination, and has a proximity wheel that rides against the wall to measure offset of the skid from the borewall. We did not retain the proximity trace, but it is recorded on the original prints. The output of the ENP is presented in API units and is run in both fluid-filled and air-filled boreholes.

Sonic-Velocity Logging

Sonic logging tools can be operated only in fluid-filled boreholes; clamped geophones can provide data for velocity over a given interval in both air-filled and water-filled boreholes.

Compensated Acoustic Logging

Travel times of compressional waves (inverse velocity) are logged with the Dresser Atlas compensated acoustic-logging tool, which employs two transmitters firing alternately to minimize borehole effects. Travel time is recorded as the time difference between two receivers spaced 2 ft apart. The receiver mid-point is spaced 5 ft from the lower and upper transmitters. The recorded travel time (microseconds per foot) was converted to velocity (meters per second) in the log data base. This tool is also used to obtain shear velocities by recording the full waveform on film (see "Sonic Waveform Logging").

Travel time of compressional waves is also recorded with the USGS acoustic-logging tool. This tool consists of a single transmitter and two receivers spaced 2 ft apart, and hence does not compensate for tool standoff and misalignment in the borehole. Only one log (borehole A–1) recorded with the USGS system is presented in this data set.

Sonic-Waveform Logging

Sonic waveforms are recorded as a variable density plot in coordinates of time (for example, 500 microseconds per inch) versus depth (20 ft per inch). Positive areas of the wavelet are dark, and negative areas are white, so the waveform log is essentially a pictorial representation of the position of zero values. Arrivals of compressional and shear waves on both the short-spaced and long-spaced records are picked and digitized. Velocities are then computed from the time differences and the receiver spacing. Where the waveform record is disrupted by fracturing or borehole washout, no arrivals can be picked and consequently there is a gap in the velocity traces.

The Birdwell sonic-waveform log is generally run in small boreholes (4 in. or less in diameter), and the Dresser-Atlas tool is run in large holes. Receiver spacing on the Dresser-Atlas tool is 2 ft, and receiver spacing on the Birdwell tool is 3 ft.

Geophone Survey

Geophones clamped against the borewall are used to record sonic arrivals from a surface source using sweep frequencies from 15 to 75 Hz. These are sometimes called "check shot" surveys and are used to provide near-surface velocity information for seismic surveys. When differences in arrival time between successive geophones are taken, the data can be used to compute velocities over a given interval. Geophones are typically spaced 25 ft apart, so the method yields average velocities over that vertical distance.

Unfortunately, the precision with which arrivals can be determined is inadequate for determining average velocities over intervals of 25 ft, so the contractor provided averages over 50-ft spacings. Even so, the uncertainty is about 20 percent as reflected in the variation of velocity. Consequently, the data were not entered into the data base and are not shown here. Examples of the data have been previously reported by Muller and Kibler (1984, 1986).

Improvements in source technology or signal extraction are required to produce useful velocity data over 25- or 50-ft intervals. From the data acquired thus far, it appears that velocities can be determined only over relatively thick intervals (greater than 100 ft).

Electrical Resistivity

Electrical resistivity can be measured with induction tools that use coils as sensors or with tools using electrodes as sensors. Both types have been employed at Yucca Mountain. Neither type can be operated inside metal casing. An induction tool can be operated either in air-filled or water-filled boreholes. Tools with electrodes can operate only in water-filled boreholes.

Induction Logging

An induction tool is best suited to measurements at low resistivities (<10 ohm-meters), but is limited in range at higher resistivities: data quality begins to erode above 200 ohm-meters, and higher values can be suspect.

Birdwell's tool is a single deep-induction tool combined with a 16-in. tool for normal and self-potential (SP) logging. The Dresser-Atlas version is a dual-induction (medium and deep) tool combined with a focussed-array, a self-potential (SP), and (in some cases) a gamma-ray tool.

Normal and Self-Potential Logging

The Birdwell electrical logging tool is a combination of 16-in. and 64-in. normal-resistivity (single-source and single-potential electrodes) sensors, an 18-ft, 8-in. lateral-resistivity sensor, and self-potential (SP) sensors. The lateral-resistivity measurement is rather difficult to interpret, is considered obsolete, and was not retained in the data base. The normal-resistivity measurement is quite simple and reliable, but it can require substantial corrections for the borehole diameter and the resistivity of the fluid. The SP is a single-electrode measurement of electrical potential in the borehole fluid.

Water-Resistivity Measurements

Good measurements of the resistivity of water in a formation are important to subsequent analysis of the electrical logs. Benson and McKinley (1985) tabulated the specific conductance of 25 water samples taken from 15 wells. We combined their on-site measurements into 11 well-site samples, excluding the samples taken from the Paleozoic rocks in P–1 and a low-volume, high-conductance sample from well H–3. The specific conductance averaged 305.3 microsiemens/cm at 25 °C, the standard deviation being 45.3. Converted to units of electrical resistivity, the mean value is 32.8 ohm-meters, the range being 26.0–40.2 ohm-meters.

Induced-Polarization Logging

Induced-polarization (IP) logs have been obtained by the USGS in six boreholes (A–1, A–4, A–5, A–6, A–7, and G–3). Logs from the A-series of holes were obtained during 1978 and 1979 by means of a Mt. Sopris Series 2 analog IP system. The G–3 log was obtained with a newer Mt. Sopris tool utilizing downhole digitization of the received waveform.

Both tools operate in a current-on, current-off excitation mode. During the off cycle the decay voltage is integrated for a fixed time following a dead time to allow switching transients to decay. The integrated signal is presented as millivolts of decay signal per volt of primary on-time signal. Because the integration times vary between the tools and no calibration standards are available for IP logging tools, the absolute values cannot be compared among the six holes. However, the four holes A–4 through A–7 were run during September 13 and 14, 1979, and hence the tool, the settings, and resultant logs should be quite comparable.

Induced-polarization measurements are available on core from three holes: A–1 (Anderson, 1981a) and G–3 and G–4 (Anderson, 1984). The measurement method, as described by Anderson (1981a) is similar to that of the logging tools. After two seconds of current excitation and a 15-millisecond dead time, the decay voltage is integrated for 30 milliseconds. This measurement sequence continues with alternating positive and negative polarity of the excitation current. Anderson's core measurements were presented in terms of received signal as a percentage of primary (on-time) voltage. We have multiplied his data by 10.0 to convert to millivolts per volt for consistency with the units used for the logs.

Dielectric Logging

The dielectric-logging tool records a resistivity and dielectric trace from measurements of amplitude and phase shift of a 47–MHz electromagnetic wave. Most spurious spikes were edited from both the dielectric and resistivity traces. The hole most adversely affected was WT–17. Although the measurement frequency and mode of operation is quite different from other resistivity tools, we plotted the resistivity trace (RDIEL) in track 4 along with the other resistivity traces.

Magnetic-Susceptibility Logging

Magnetic-susceptibility logs were obtained in eight boreholes: A–1 (Hagstrum and others, 1980a); A–4, A–5, A–6, and A–7 (Daniels and others, 1981); and WT–14, UZ–6, and G–3 (no prior reference). The tool

incorporates a temperature-regulated solenoid wound on a core of high magnetic permeability (Scott and others, 1981). Regulation of the temperature of the sensor is sometimes inadequate, and measurements must then be corrected for an approximately linear temperature drift caused by the thermal gradient in the borehole. The logs were also corrected for borehole diameter, but the overall accuracy of the measurement depends chiefly upon the correction for temperature drift.

Core values are available for G–1, G–2, G–3, and VH–1 (Rosenbaum and Snyder, 1984). These data, available at roughly 10-ft intervals, were also incorporated into the data set.

Although magnetic susceptibility is a ratio and therefore dimensionless, its numerical values in the centimeter-gram-second (cgs) system differ from those in the International System of Units (SI). A susceptibility value expressed in cgs units must be multiplied by 4π to be converted to SI units. Even in highly susceptible rocks, the values are a small fraction of unity, so we have chosen to express the values in units of mSI, so that a susceptibility of 7 mSI is equivalent to 0.007 SI units, for example.

Magnetic-Field Logging

Lawrence Livermore National Laboratory Logs

During the years 1980–1982, researchers at Lawrence Livermore National Laboratory (LLNL) acquired magnetometer logs of eight boreholes at Yucca Mountain. Four boreholes were logged with a total-field, proton-precession magnetometer: H–1, H–5, H–6, and P–1. Four other boreholes were logged with a triaxial fluxgate magnetometer: H–3, GU–3/G–3, H–4, and VH–2. Douglas and Millett (1978) described the LLNL proton magnetometer.

Magnetic tapes of the logs recorded by LLNL were made available to the U.S. Geological Survey (USGS) by M. Millett (oral commun., 1988). An exception was the H–1 log, which was digitized from a paper copy. In the case of the three-component fluxgate logs, the three measured components (x, y, z) and four computed components (total field, horizontal field, magnetic dip, and magnetic azimuth) were all loaded into the well-log data set.

Before loading into ESLOG format, the data were linearly interpolated to even 0.5-ft spacings from the uneven spacings of the original data. Because the original data were recorded at spatial densities of 2–4 points per foot, the interpolated data are quite accurate, the check plots showing excellent replication of the original paper copies. Next, severe spikes in the vertical, horizontal, and total field components were removed from the data. These spikes were so large (greater than 2 μT) and so narrow (occurring on only one or two 0.5-ft samples) that they could be attributed to measurement or sampling problems. As a final editing step, the proton magnetometer logs were multiplied by 0.001 to convert from gammas to microteslas (μT) for consistency with the three-component logs.

In general, the x and y components have a higher noise component (which could be due to borehole irregularities) than does the z component. In addition, the x and y components exhibit a sinusoidal oscillation caused by tool rotation. Both the noise and the sinusoidal oscillation appear in the computed horizontal and total field components. For this reason, it was more desirable to plot the z component rather than the total field component. An exception is borehole G–3, for which the z component exhibits a steady decrease from 3,850 to 5,000 ft due to deviation of the hole from vertical. Thus, for holes H–3, H–4, and VH–2, we present the vertical component and for G–3 the computed total field. For the four holes logged with the proton magnetometer, the measured total field is presented.

U.S. Geological Survey Logs

In 1983 and 1984 the USGS ran an experimental three-component fluxgate magnetometer in holes G–3, UZ–6, and WT–14. This magnetometer probe differed from the two LLNL probes in that it incorporated a gyroscopic compass and an inclinometer from which the probe tilt and orientation can be determined (Scott and Olson, 1986). Knowing the probe tilt and orientation, the three measured magnetic components (one along the hole and two in the plane orthogonal to the hole) can be converted to three spatial field components (vertical, magnetic north-south, and magnetic east-west). These conversions were done by Scott, and they are of considerable interest in studying the magnetic properties. However, here we present only the vertical magnetic field component for comparison with other logs.

Quality of Data

Both three-component magnetometer probes were under development when run in the boreholes. As already mentioned, spikes appearing in the records are attributed to tool problems and to field inhomogeneities caused by a rough borehole. Our checks on repeatability are limited to the two USGS logs that were recorded both logging down and logging up. The tool was run without centralizers, so the tool position was probably not the same on the two runs. Differences between the vertical component from the up and down runs were as much as 1.5 μT in G–3 and WT–14; in UZ–6 the difference was less than 0.5 μT.

Both LLNL and USGS magnetic tools were run in G–3, providing our only check on overall accuracy. The vertical component from the LLNL three-component tool systematically reads about 1.0 μT higher than the vertical component from the USGS tool over the depth range 2,600–3,400 ft. Once this shift is accounted for, the logs generally track to within 0.5 μT.

Remanent Magnetization Measured on Core

Measurements of remanent magnetization on core samples were reported by Rosenbaum and Snyder (1984). Values generally ranged between 0 and 10 amperes/meter. Spacing between samples was generally about 10 ft.

Temperature Measurements

Temperature is measured in two ways. A single maximum temperature is determined with a mercury-in-glass thermometer when open-hole logs are run. This measurement is called the bottom hole temperature (BHT). It is useful for making temperature corrections to the logs.

Temperature is also measured by installing thermistor strings into the wellbore and waiting for thermal equilibration between the fluid and the formation. Sass and others (1988) reported such data for many of the Yucca Mountain boreholes. These measurements do not lend themselves to the format for well-log plotting adopted in this report and were not incorporated into the well-log data base.

Flow Profiles

Radioactive-tracer measurements were carried out in eight test wells by USGS investigators while pump or injection tests were underway.

During pumping or injection, a tool that combines an iodine ejector and a gamma-ray detector is lowered on a wireline to a specified depth. Radioactive iodine is ejected into the water column. The movement of the iodine is tracked by pulling the gamma-logging tool through the borehole, detecting the gamma peak emitted by the iodine slug, and noting the time and depth. From several such determinations, the flow velocity at a given depth is estimated. After computing the hole volume from caliper logs, an estimate of volumetric flow rate is obtained. From estimates at a number of depths, a volumetric flow profile is obtained over the depth interval of the injection test. These flow profiles, presented as a percentage of total flow (defined as 100 percent in casing) have been presented in various reports by USGS authors (see Appendix 1) and in summary form for seven wells by Benson and others (1983).

Numerical values for the profiles were obtained from USGS files. Flow values were linearly interpolated between measurement depths by means of ESLOG programmed logic before plotting in well-log format.

Stratigraphic Units

We entered the depth to the top of each stratigraphic unit into the data set for each borehole. The depths were taken from relevant publications cited in Appendix 1.

Static Water Level

Static water level data provided by J. Robison (written commun., 1988) are given in table 1. These values include some small corrections to those published previously (Robison, 1984). The water level for each hole was entered and a trace created for subsequent plotting in track 2.

Directional Surveys

Directional surveys were provided by Eastman Whipstock, who used a multishot gyroscopic instrument occupying stations spaced 50 ft apart on an "in run" and again spaced 50 ft apart (but staggered 25 ft with respect to the in run) on an "out run." The hole coordinates are computed on 25-ft intervals by either an angle-averaging method or a radius-of-curvature method to project the measurements of inclination, azimuth, and depth to another depth level. Because of the modest borehole deviations encountered at Yucca Mountain, the choice of computational model does not affect the computed locations. We excerpted data from the combined run, which is usually an average of the in and out runs, for entry on the log headers.

FORMAT OF THE LOG PLOTS

The log plots on plates 1–40 are presented at a scale of 100 ft per inch (1,200:1), a scale judged suitable to show sufficient detail. The plot width was constrained by the criterion of providing a z-fold log compatible with 8.5 x 11-in. paper.

Each header contains a list of logs displayed, the physical units, type of log run, the log originator, and the date of the log.

The header also contains an excerpt of the directional survey results, showing the inclination (drift angle), the azimuth (drift direction), the true vertical depth, and the x and y coordinates relative to the surface location. These values are listed for 1,000-ft increments and for the deepest computed point.

Each plot is composed of as many as nine tracks showing the "traces." Caliper, gamma-ray, and SP are plotted in the left-most track (track 1). Track 2 shows the height of the static water level and the porosity-dependent density and neutron logs. Track 3 shows sonic velocities, and track 4 shows electrical resistivity. Track 5 shows the sidewall neutron and dielectric logs. Tracks 6 and 7 show the spectral gamma traces where they are available. Tracks 8 and 9 are used for a variety of traces including magnetic field, magnetic susceptibility, flow profiles, and induced polarization. Where core data are available, they are plotted in the appropriate track. If a log was not run, the track is retained but left empty.

We followed the conventions of oil-well logging in plotting the four logs (density, neutron, velocity, and resistivity) that respond to changes in porosity. For example, the density scale increases to the right. If grain density is unvarying in a formation, but porosity increases, then the log responds to the reduced bulk density by deflecting to the left. The other three logs are in general similarly affected by a porosity increase, with a consequent deflection to the left. Of course, not all deflections to the left are due to porosity increases.

A plotting range of 16 μT was chosen for the magnetic logs to accommodate the large swings caused by remanent magnetization and still preserve uniformity from borehole to borehole. Where the remanent magnetization is low, the field in the borehole is relatively unperturbed. The scales were shifted so that the unperturbed field (approximately 52 μT for the total field (MAGT) logs and 46 μT for the vertical component (MAGZ, MAGV) logs) plots at one-fourth of the track width.

The tops of geologic units are designated by horizontal lines and by symbols at the right edge of the plots. The corresponding geologic names and symbols are listed in table 4.

EFFECTS OF BOREHOLE ENVIRONMENT

Borehole measurements are affected by the type and density of fluid in the borehole, the diameter of the hole, and its roughness (rugosity). Logging tools are usually calibrated in a hole of a specified diameter that is filled with drilling mud of specified properties. The

Table 4. Stratigraphic chart showing geologic names and unit symbols used in this report

Name of unit	Symbol
Quaternary and younger Tertiary	
Alluvium	Qac
Alluvium and colluvium	QTac
Miocene	
Basalt	Tb
Timber Mountain Tuff	
Ammonia Tanks Member	Tma
Rainier Mesa Member	Tmr
Bedded tuff	Tba
Paintbrush Tuff	
Tiva Canyon Member	Tpc
Bedded tuff	Tba
Yucca Mountain Member	Tpy
Bedded tuff	Tba
Bedded tuff (ash flow)	Tpb
Bedded tuff	Tba
Pah Canyon Member	Tpp
Bedded tuff	Tba
Topopah Spring Member	Tpt
Bedded tuff	Tba
Rhyolite of Calico Hills	
(tuffs and lavas of Calico Hills)	Tht
Crater Flat Tuff	
Prow Pass Member	Tcp
Bedded tuff	Tba
Bullfrog Member	Tcb
Bedded tuff	Tba
Tram Member	Tct
Bedded tuff	Tba
Lavas and flow breccias	Tll
Bedded tuff	Tba
Lithic Ridge Tuff	Tlr
Bedded tuff	Tba
Lava	Tll
Bedded tuff	Tba
Older tuffs in borehole USW G-1	Tt
Unit A	Tta
Unit B	Ttb
Unit C	Ttc
Older units	
Sedimentary deposits	Tsd
Calcified tuff	Tca
Tuff of Yucca Flat(?)	Tyf
Lone Mountain Dolomite	Slm
Roberts Mountain Formation	Srm

logging contractor supplies charts to correct for hole conditions different from standard conditions. These corrections are known collectively as "environmental corrections." Environmental corrections have not yet been applied to any logs presented in the accompanying plates. In the following discussion we consider some of the effects manifest in the logs due to the borehole environment.

Static Water Level and Air-Filled Boreholes

The static water level is unusually deep at Yucca Mountain (table 1), a circumstance that played a large role in its selection as a potential waste repository. As a consequence of the deep water table, logs are acquired in both water-filled and air-filled boreholes. The latter case is unusual in logging; only on the neighboring Nevada Test Site are logs routinely (although with difficulty) acquired in air-filled holes. Different kinds of logs are affected in different ways by the absence of liquid.

Some logging tools, such as those for logging sonic velocity, SP, and normal resistivity, operate very well in a fluid-filled borehole but not at all in an air-filled borehole. These logs require a liquid to transmit acoustic energy or electrical current into the formation and, as can be seen in the plates, these logs are not shown above some depth near the static water level. The precise depth at which these logs commence depends on the liquid level at the time of logging. Water or drilling fluid were added to G–1, H–1, and GU–3 in order to facilitate logging, but most holes were logged without inducing any change in the liquid level.

The neutron tools can be operated in an air-filled hole, but the count rates and calibration factors are drastically different from those in a liquid-filled hole due to the absence of a neutron-moderating liquid. As the plates show, the response of the ENP and NNL traces increases dramatically going from a water-filled to an air-filled hole. The two-detector neutron tool (NBC) is affected so adversely that it is not run in an air-filled hole.

The gamma-ray, density, dielectric, and induction tools can be run successfully in air-filled holes but require correction for the change in fluid type. The magnitude of these corrections depends upon hole size and may or may not be visible in the plates.

A few tools, such as caliper, magnetometer, magnetic susceptibility, and gravimeter, are not affected by the presence or absence of liquid in the hole and hence no corrections are needed.

Drilling Methods and Drilling Fluids

The 40 drill holes listed in table 1 were drilled according to several criteria developed by various investigators participating in the Yucca Mountain Project. As a result, boreholes were drilled with a variety of bit types and sizes using different drilling fluids and resulting in a range of diameters. A further complication is the evolution of the drilling strategy, primarily to protect the unsaturated zone from contamination by drilling fluids that affect the on-site hydrologic flow tests.

Drilling Methods

Four methods of drilling have been used at Yucca Mountain: conventional drilling, conventional coring, wireline coring, and reaming. In conventional drilling a roller- or cone-type bit rotates to crush and pulverize all of the rock as the hole is deepened. The bits for conventional drilling range from 6.25 in. to 24 in. in diameter.

In conventional coring a bit consisting of industrial diamonds embedded in hardened steel erodes away the annulus of rock and leaves a cylindrical core of rock that is captured in a tubular core barrel just above the bit. Core barrels typically range from 10 to 30 ft in length. The core in the core barrel is retrieved by pulling the entire drill string from the hole, a time-consuming and tedious process for deep holes. The H-series and C-series of boreholes were drilled with a combination of conventional drilling and conventional coring.

Holes that were 100 percent cored over very long intervals (G-series, VH-series, A-series, and P–1) were drilled by wireline coring. Wireline coring is done with diamond bits and drill pipe only slightly smaller in diameter than the bit. The core barrel with the core is retrieved through the drill pipe with a wireline cable, eliminating the time-consuming round trip to pull the drill string and put it back in the hole. Bits 3 and 4 in. in diameter were used, and then the holes were partially or completely reamed to larger diameters for hydrologic tests and instrumentation. Reaming is done with special bits that follow the existing hole and increase its diameter.

Drilling Fluids

Fluids of various kinds are circulated into drill holes through the drill string during drilling to cool and lubricate the drill bit and to evacuate the cuttings with the mud that returns to the surface by flowing up the annulus around the drill string. The fluid in the drill hole also dampens the vibration of the drill string during drilling,

lessening the wear on the drill pipe and slowing the aging of the steel, which becomes brittle with use. The most commonly used fluids at Yucca Mountain are air-foam and polymer mud.

Air-foam is the viscous foam created by circulating a detergent slurry while aerating with compressed air through the drill string. The foam is viscous enough to carry cuttings from the hole. In the unsaturated zone at Yucca Mountain the light weight of the foam produces a lower hydrostatic head than a column of mud, thus decreasing circulation losses to the formation. All conventionally drilled and conventionally cored holes at Yucca Mountain were drilled with air foam, and G–4 was wireline cored with air foam.

Polymer mud is a viscous slurry that becomes a gel after sitting motionless for a period of time and then reverts to a slurry when stirred by the drill string. In porous, permeable rock the mud penetrates the pore space, and then it gels, effectively sealing the rock from further invasion of borehole fluid. In the unsaturated zone at Yucca Mountain polymer mud is ineffective for maintaining circulation because the hydrostatic head of the mud column is great enough to overcome the gelling effects in the highly permeable fractured zones. Polymer mud was used for all wireline coring

Bentonite mud and polymer-bentonite mud mixtures were used in GU–3. Bentonite mud is a slurry that forms a bentonite mud cake on the borehole wall in porous, permeable rock that prevents or retards invasion. Potash and other additives were added to the mud to increase the viscosity, and slugs of material to control circulation loss were injected in fracture zones to clog the fractures and seal them.

Drill holes UZ–1 and UZ–6 were drilled by means of a vacuum with compressed air instead of fluid. The compressed air was circulated through the drill string to blow the cuttings out of the drill holes. This method is limited to holes of large diameter and relatively shallow depths. The air blowing at high velocity past the formation in the annulus has a desiccating action and deposits dust on the hole walls, obscuring the rock from television camera view and clogging the pores for permeability tests. The method is being refined for future drilling to use dual-string reverse-circulation methods so that the air will travel through an inner pipe and the annulus between an inner and outer pipe, leaving the borehole walls undisturbed by the drilling fluid (air).

Drilling Strategy

Early in the drilling program, the strategy was to use whatever drilling methods and muds were effective to create a stable drill hole that would hold fluid for open-hole geophysical logging. The almost impermeable rock matrix and very high fracture permeability in the unsaturated zone rendered the muds ineffective for sealing the walls of the borehole and for maintaining circulation to remove drill cuttings from the hole. In drill hole G–1, more than 56,000 barrels of fluid carrying rock cuttings were lost into the formation fracture systems. Attempts to maintain a fluid-filled hole in the unsaturated zone for geophysical logging by pumping water and mud into drill holes G–1 and H–1 while logging were ineffective, gaining only a few hundred feet of fluid above the static water level and never raising the level much above the base of the Topopah Spring Member of the Miocene Paintbrush Tuff. In drill hole GU–3 extreme measures were taken to successfully obtain a fluid-filled hole above the static water level by using very viscous muds and injecting slugs of fluid containing shredded swelling fibrous materials to clog and seal fractures.

An intermediate strategy was to drill the unsaturated zone with air-foam, log the open air-filled hole, case to the water table, and drill the saturated zone with water, air-foam, or polymer mud. Even with casing in place, drilling the saturated zone with mud or water was difficult because of continued fluid loss, and air-foam therefore is preferred. The present strategy is to drill the unsaturated zone with a dual-string reverse-circulation air method and the unsaturated zone with water or air-foam after casing to the water table.

Drilling Problems and Related Logging Problems

Continuous wireline coring has been a difficult enterprise at Yucca Mountain. The drilling history of A–1 and the four G-boreholes is filled with tales of lost circulation, dropped pipe, and logging through drill pipe. Drilling problems required reaming and repeated logging of the upper section of holes. After completion of coring, some holes (G–4) were reamed to total depth to allow for hydrological testing. This complicated sequence, which caused logs to be acquired piecemeal rather than in one or two continuous runs, is reflected in the tabulation of logs and hole sizes on the log headers. The user of the logs must be careful in associating a hole diameter with a particular log.

Two sets of paired holes were drilled in which one hole was cored in the unsaturated zone and a second, adjacent hole was cored in the saturated zone. Boreholes A–1 and B–1H are one such pair, GU–3 and G–3 are another. The drilling history of boreholes GU–3 and G–3, which are 30 m apart, was summarized by Scott and Castellanos (1984, p. 5):

> The coordinated pair of drill holes, USW GU–3 and USW G–3, were cored in two stages: USW GU–3 was cored in the unsaturated zone and USW G–3 was cored largely in the saturated zone. This two-stage coring program was designed to obtain maximum hole stability and to

optimize conditions for wet-hole geophysical logging above the zone of saturation. Drill hole USW G–3 was spudded January 8, 1982, and completed March 21, 1982; this was followed by drill hole USW GU–3 that was spudded January 26, 1982, and completed June 12, 1982. USW GU–3 was continuously cored from about 10 m to 806 m, and USW G–3 was continuously cored from about 795 m to 1,533 m.

To this account we should add that GU–3 was drilled with polymer and bentonite mud, whereas G–3 was drilled with air-foam from 38 to 2,600 ft (11.6 to 792 m) and with polymer mud from 2,600 to 5,031 ft (792 to 1,533 m).

These accountings should persuade the user of logs and core to look carefully at the headers and to consult the drilling histories if necessary.

Borehole Deviation and Dip of Bedding

In order to use core and log data to determine the true vertical thickness of units and true vertical depth to mappable horizons such as the static water level, a large deviation of the borehole away from vertical must be taken into account. The actual borehole coordinates as a function of depth are required when comparing deep borehole data to surface geophysical data. Surveys of borehole deviation to determine the coordinates as a function of depth are discussed in "Directional Surveys." Thirty-five of the forty boreholes discussed in this report were surveyed for borehole deviation.

Some general observations can be made from the deviation surveys. Most of the holes maintained a nearly vertical attitude for at least several hundred feet and some holes for more than 2,000 ft. With few exceptions, the deviation was gradual and became progressively greater with depth. All holes less than 2,000 ft deep have bottom hole coordinates within 100 ft of the surface collar. Most holes followed a relatively direct path to total depth, some exceptions being the almost spiral route of H-1 and the sharp dogleg of VH–2 and of G–3.

Figure 2 shows the bottom-hole coordinates referred to the surface collar location. Boreholes are grouped according to drilling method: twenty-three conventionally drilled and cored holes (A) and twelve remaining holes (B), ten of which were partly or totally drilled by wireline coring and two of which were drilled by an air-vacuum method. Note the change in scale between A and B. None of the conventionally drilled holes deviates more than 100 ft. The wireline-cored holes deviate as much as nearly 700 ft. Total depth does not appear to be a factor in causing the difference because all ten of the wireline-cored holes are 2,500–6,000 ft deep, and eight of the conventionally drilled holes are 3,000–6,000 ft deep. It is clear that the conventionally drilled holes having an 8.75-in. diameter deviate less than the wireline-cored holes that were drilled with drill strings having 3- and 4-in. diameters.

Most of the holes on both plots fall in the southwest quadrant. The surface locations of the holes shown on figure 1 indicate that most of the holes in the southwest quadrants were drilled in the repository structural block where surface features tend to have a northwest bearing, and most of the outliers, such as C–1, C–2, C–3, P–1, H–3, WT–11, VH–1, and others, are located in or near adjoining structural blocks, where surface features tend

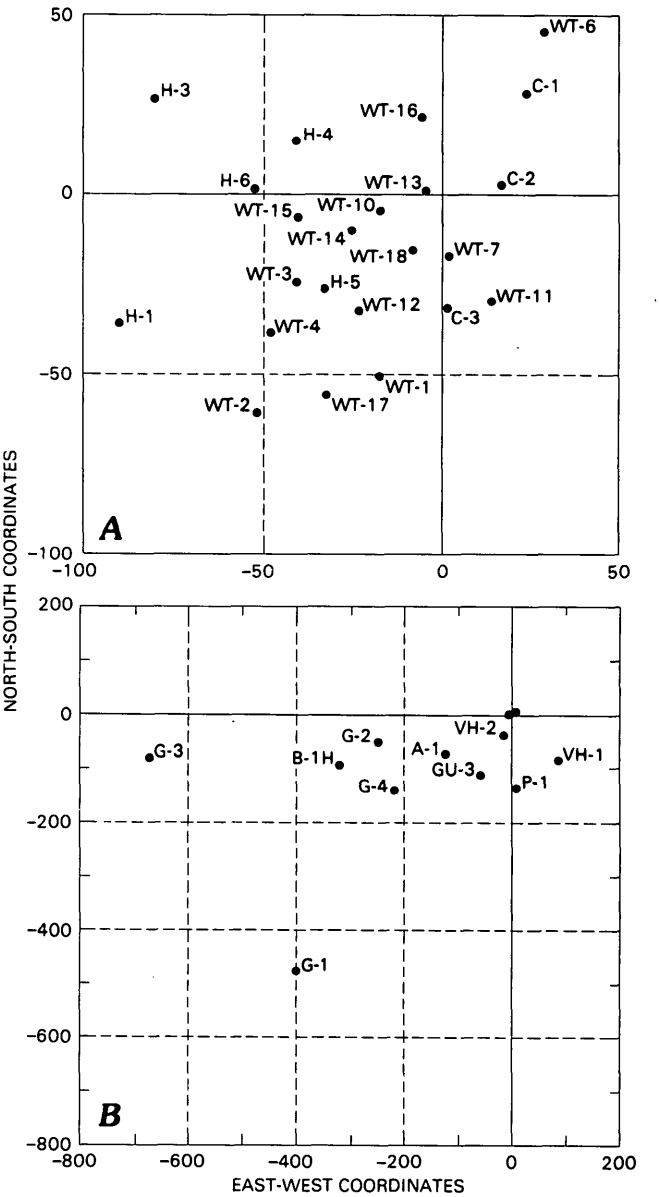

Figure 2. Bottom-hole coordinates, in feet, referred to surface collar location (0,0) of boreholes at Yucca Mountain, Nev. *A*, Conventionally drilled and cored holes. *B*, Wireline-cored holes. UZ–1 and UZ–6, unlabelled near the origin (*B*), were drilled by a dual-string, reverse-vacuum method.

to have a north-northeast bearing. The outlier G–3 sustained drilling problems that probably outweigh any geologic factors in causing the deviation.

It is hard to isolate and measure the effect of geologic factors that cause boreholes to deviate from vertical and to drift in a preferred direction. Scott and Castellanos (1984) discounted the role of bedding dip and concluded that fracturing is the dominant geologic factor influencing the direction of borehole deviation at the repository site. Borehole deviation deserves further study if it is to contribute to the characterization of the site.

True stratigraphic thickness will not be represented by the core or logs if the hole does not orthogonally intersect the bed. At Yucca Mountain the dip of the beds is about 12 degrees; borehole deviation is typically no more than several degrees (refer to log headers on plates 1–40). The resulting angle between bed and borehole is modest, eliminating the need for correction to true stratigraphic thickness in most Yucca Mountain boreholes.

The logs presented in this report have not been converted to true vertical depth. All depths are measured depths, also referred to as "depth along hole."

Hole Rugosity

The unusually high hole rugosity (rough hole, irregular diameter greater than bit size) in the upper part of most holes is due to several related factors. Because the water table is deep, most holes are drilled without a supporting column of mud, which helps prevent sloughing of rock from the wall of the borehole. When drilling above the water table, drilling fluid is lost through fractures. Mud cake would prevent the loss of fluid, but the densely welded rock units have very low permeability, so no mud cake forms. With no fluid to lubricate the bit or dampen the vibrating drill string, mechanical damage to the formation is high. The brittle nature of the densely welded Topopah Spring member further contributes to the development of a rough hole. The readings of almost all logs, and particularly the compensated-density and compensated-neutron logs, are adversely affected by hole rugosity, primarily because it causes standoff between the tool and the rock. Although changes in borehole diameter can be compensated for, in general it is not possible to compensate completely for standoff in highly rugose holes.

Hole Eccentricity

The average caliper curve is the best indicator of hole rugosity, but it must be kept in mind that the hole can also be eccentric. If a four-arm or six-arm tool was run, the original log can be inspected for eccentricity. Two examples of logs obtained with the six-arm caliper are shown in figure 3. From 750 to 795 ft in borehole G–1 two caliper arms are reading the bit diameter of 6.25 in. while the third indicates an elongated hole of about 8 in. It can be said that this zone is eccentric but not rugose. Borehole H–4 is enlarged from the 14.75-in. bit diameter throughout almost the entire section shown, and from 1,660 to 1,710 ft it is both washed out and eccentric.

The examples of figure 3 are typical of those zones where borehole eccentricity results in the long axis being 1–2 in. greater than the short axis. This amount of borehole distortion is unlikely to be significant in correcting tool response. Eccentric zones appear to constitute about 5–20 percent of the total hole length. No work has been done to determine if the eccentric zones are related to existing fractures or to "breakout" zones caused by horizontal stress anisotropy. Directional devices were not run with the caliper, so it is not possible to determine the orientation of the zones.

Only the average caliper log has been retained in the data base and plotted on plates 1–40. The original paper copies must be consulted in order to inspect the multi-arm caliper traces.

Casing and the Gamma-Ray Log

The gamma-ray and its spectral version can be run in either cased or open holes; the spectral log has been routinely run from total depth up through casing to surface. This procedure provides continuous data, but the casing reduces the count rate. The gamma-ray traces from hole H–5 are reproduced in figure 4, in which an open-hole gamma-ray log (GR) can be compared with one run in a cased hole (TC). The hole is cased to 2,585 ft, where an abrupt decrease in gamma-ray activity can be observed as the tool rises from open hole into cased hole. From surface to 2,585 ft, the casing diminished the TC gamma-ray activity with respect to the open-hole GR. A second decrease in TC can be seen at 311 ft at the base of surface casing. In addition, spikelike amplitude decreases occur at 40-ft intervals where the TC tool passed increased steel thickness at casing joints. Water in the borehole also attenuates gamma rays as can be seen in figure 4 by the increase in both TC and GR above the static water level at 2,300 ft. The steplike changes in both TC and GR at 2,010 and 2,130 ft are attributed to lithology.

Rugosity and the Density Log

Examination of a selected set of density and caliper logs (figs. 5 and 6) demonstrates for an extreme case the combined effects of hole rugosity, hole size, and fluid

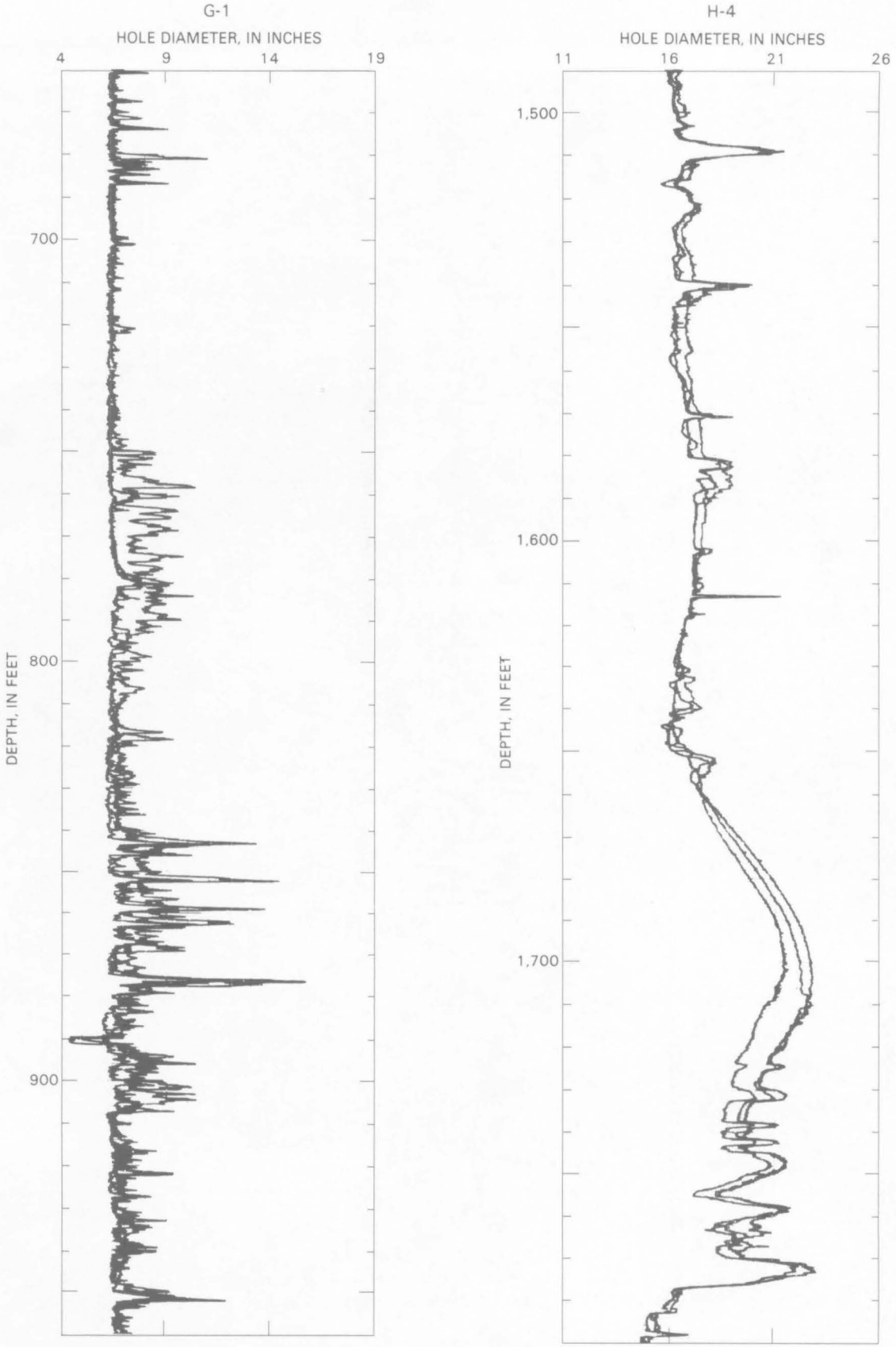

Figure 3. Six-arm caliper logs from boreholes G–1 and H–4, Yucca Mountain, Nev. Each pair of caliper arms produces a trace. Bit diameter is 6.25 in. in G–1 and 14.75 in. in H–4.

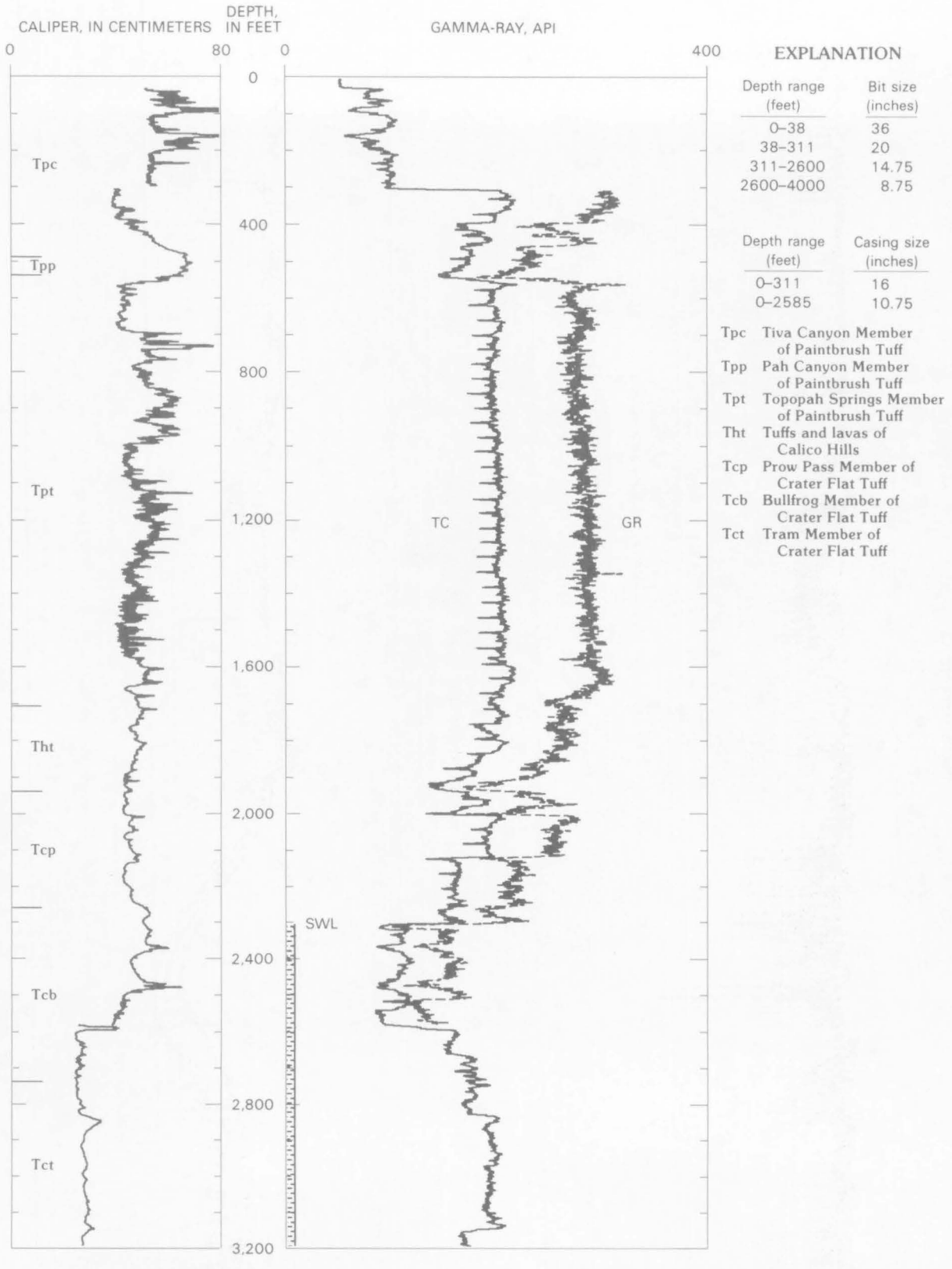

Figure 4. Gamma-ray log (GR) run in open borehole H–5, Yucca Mountain, Nev. A total-count log from the spectral gamma-ray tool (TC) was obtained in casing from surface to 2,585 ft and in open hole below 2,585 ft. SWL, static water level.

type on log response. All five examples are from the densely welded part of the Topopah Spring Member, which tends to produce a rugose hole in which the tool cannot maintain contact with the wall, leaving an air gap between the rock and tool so that an unrealistically low density is recorded. Contrast the three density logs obtained in air-filled boreholes (fig. 5) with the two logs obtained in liquid-filled boreholes (fig. 6). In particular, note the correspondence between caliper openings and low-density peaks on the logs from the air-filled boreholes, especially in the upper part of WT–2.

Density is computed from count rates measured by the short and long detectors. To correct for the gap between the tool and the wall, a compensation algorithm is applied to the short and long count rates. Lacking a compensation algorithm for an air-filled borehole, the algorithm for the water-filled borehole was used instead. The incorrect alogorithm, coupled with the high rugosity, produced erroneous spikes on the density logs. The erratic nature of the density logs can be suppressed to some degree with the application of an algorithm appropriate to the air-filled borehole.

Borehole size also affects the density measurement because of a mismatch between the tool curvature and the borehole curvature as borehole size departs from the design size of the tool. This results in an erroneously low density measurement in holes that are either too large or too small for the curvature of the tool. This effect is most apparent in the mirroring of the caliper and density traces in well H–4 (fig. 5) and in the overall density recorded in H–4, which is lower than in GU–3 or WT–2. Clearly, borehole size must be taken into account.

By way of summary, the density logs from the liquid-filled parts of the boreholes provide density readings that agree with core measurements. However, the density logs from the upper parts of the boreholes (generally speaking, above the static water level) give unrealistically low density values, particularly where the borehole is rugose, and require correction.

Borehole Diameter, Mud Resistivity, and the Resistivity Logs

Above the water level in air-filled boreholes, only the induction and dielectric tools can be used to determine resistivity. In addition to these, all conventional resistivity devices may be used below the water level. Below the water level, the resistivity traces from different tools in some cases overlie one another (for example, holes H–3 and H–5) and in other cases maintain a consistent separation (for example, holes C–1 and A–4). Figure 7 shows the range of curve separation of five resistivity logs from borehole P–1: long-normal, short-normal, deep-induction, medium-induction, and dielectric logs, in order of decreasing resistivity.

The normal-resistivity logs are quite sensitive to borehole size and mud resistivity changes. Among the holes cited above, bit diameter ranges from 6 to 10 in. and mud resistivity ranges from 4 to 22 ohm-meters. Under these conditions, the short (16-in. spacing) and long (64-in. spacing) normal logs can overestimate the formation resistivity because of current channelling in the wellbore (refer to figure 5–24 of Hearst and Nelson, 1985). We observe overestimation in P–1 and in the A- and C-series boreholes. It is also possible for the long- and short-normal logs to agree with one another, as we observe in the H-series boreholes.

The resistivity recorded by the dielectric logging is the lowest resistivity estimate because it incorporates a dielectric loss. In addition, the operating frequency of 47 MHz, much higher than the 20-kHz induction frequency, assures that the resistivity will be lower due to frequency-dependent polarization effects. Thus, the dielectric-derived resistivity will be incorrectly lower than the induction resistivity.

The resistivity recorded by the induction tool should be very nearly correct because at mud resistivities greater than 2 ohm-meters, the signal from the mud is negligible (Dresser-Atlas, 1985). This factor also applies in air-filled boreholes, except where the formation resistivity becomes so high (see "Induction") that the uncertainty in the reading approaches the signal magnitude.

Consequently, in air-filled boreholes the induction log provides the best estimate of formation resistivity as long as formation resistivity is less than 200 ohm-meters. The dielectric tool provides a minimum value of resistivity.

In fluid-filled boreholes and in the absence of borehole corrections, the best estimate of formation resistivity can be obtained in the following way:

1. If an induction log is present, it provides the best estimate if the resistivity is less than 200 ohm-meters.
2. If no induction log is present, or if the resistivity is greater than 200 ohm-meters, and the short- and long-normal logs agree, then the short- and long-normal logs provide the best estimate.
3. If no induction log is present, or if the resistivity is greater than 200 ohm-meters, and the short- and long-normal logs are separated, then the lesser of the two is the better estimate. However, it is likely that this estimate is greater than true formation resistivity. It is not likely that the formation resistivity is underestimated. A dielectric log, if present, provides a lower limit on resistivity.

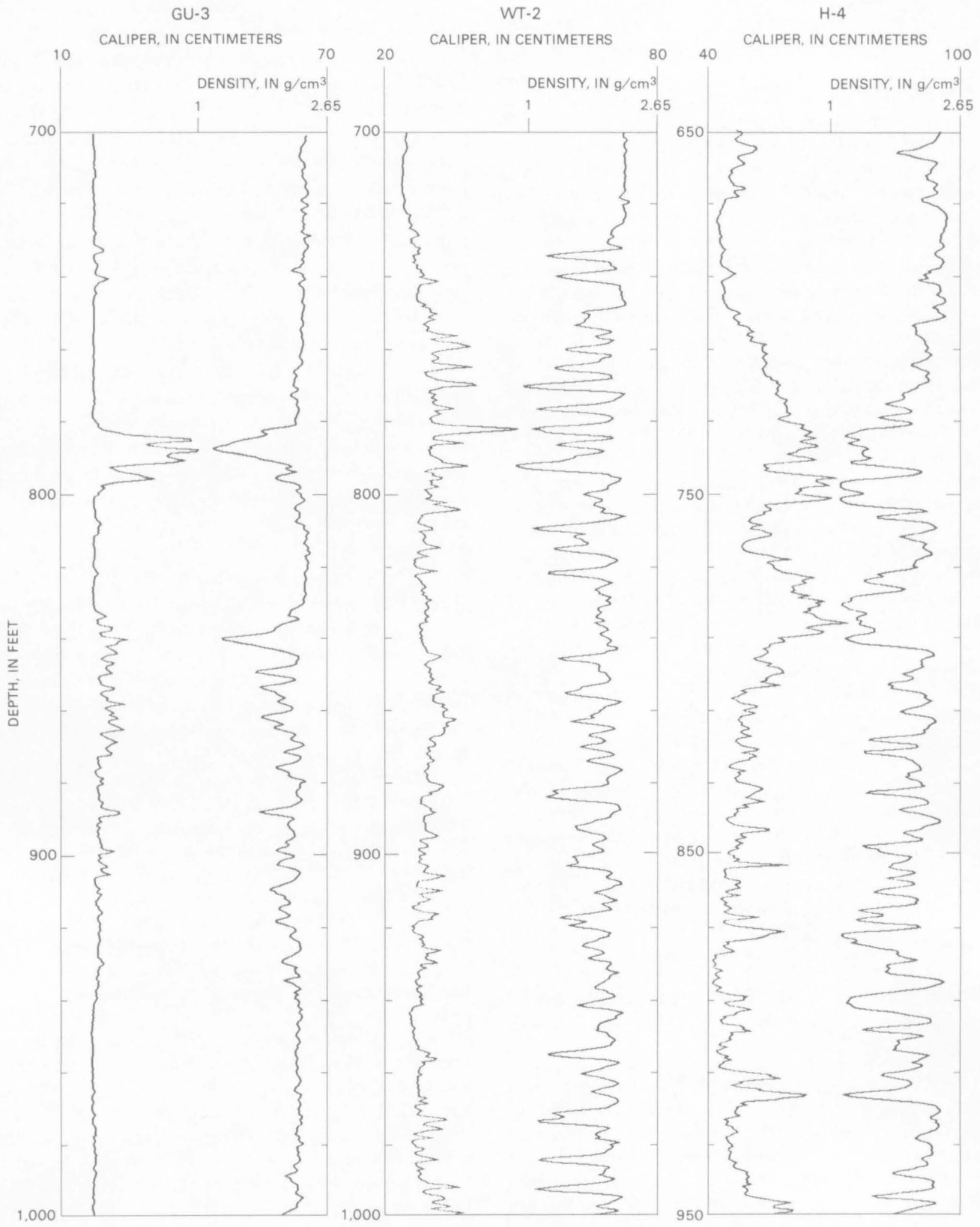

Figure 5. Caliper and density logs of the Topopah Spring Member in air-filled boreholes, Yucca Mountain, Nev. Nominal bit diameter is 6.75 in. (17.1 cm) in GU–3, 8.75 in. (22.2 cm) in WT–2, and 14.75 in. (37.5 cm) in H–4.

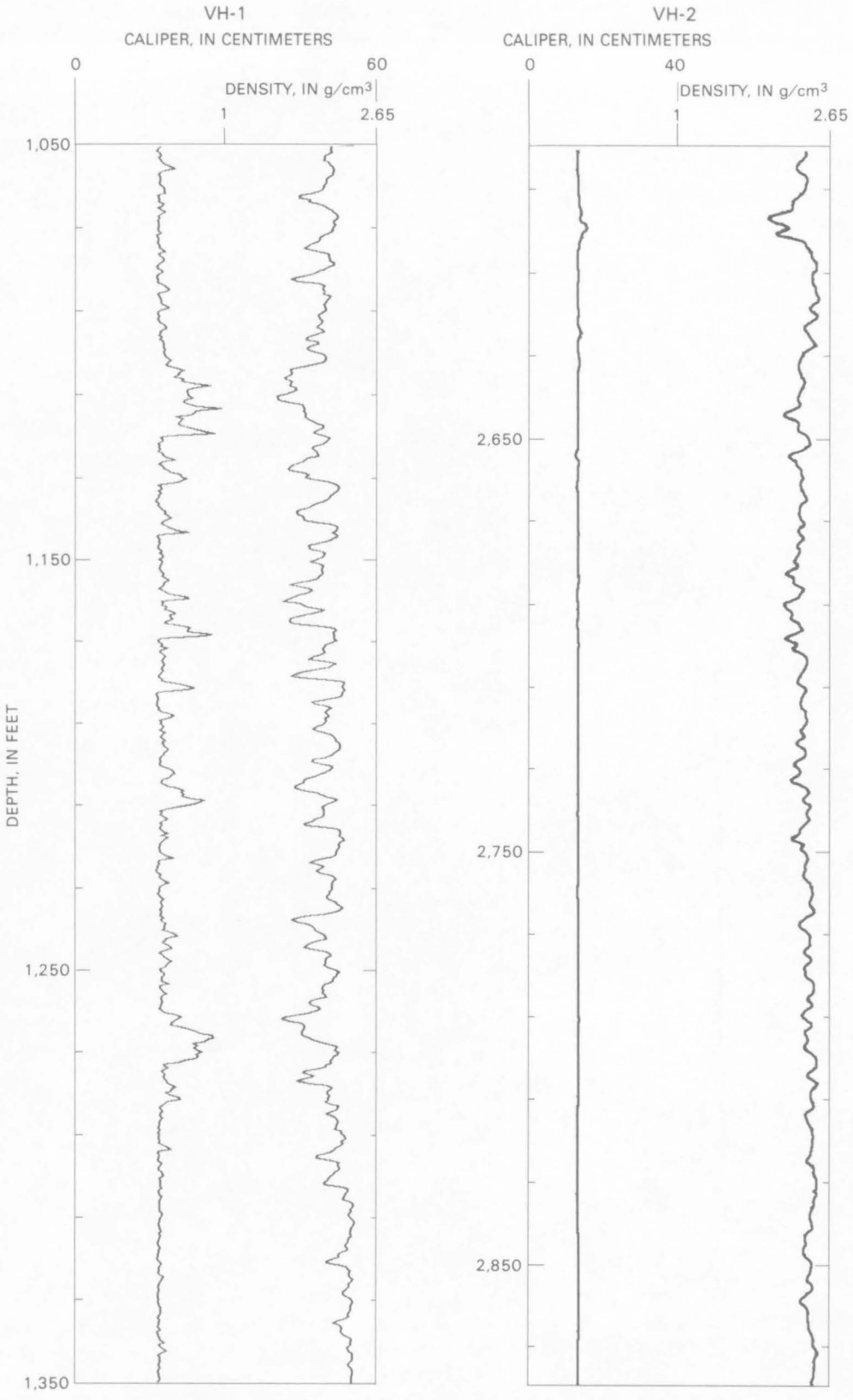

Figure 6. Caliper and density logs of the Topopah Spring Member in water-filled boreholes, Yucca Mountain, Nev. Nominal bit diameter is 6.25 in. (15.9 cm) in VH–1 and 3.94 in. (10.0 cm) in VH–2.

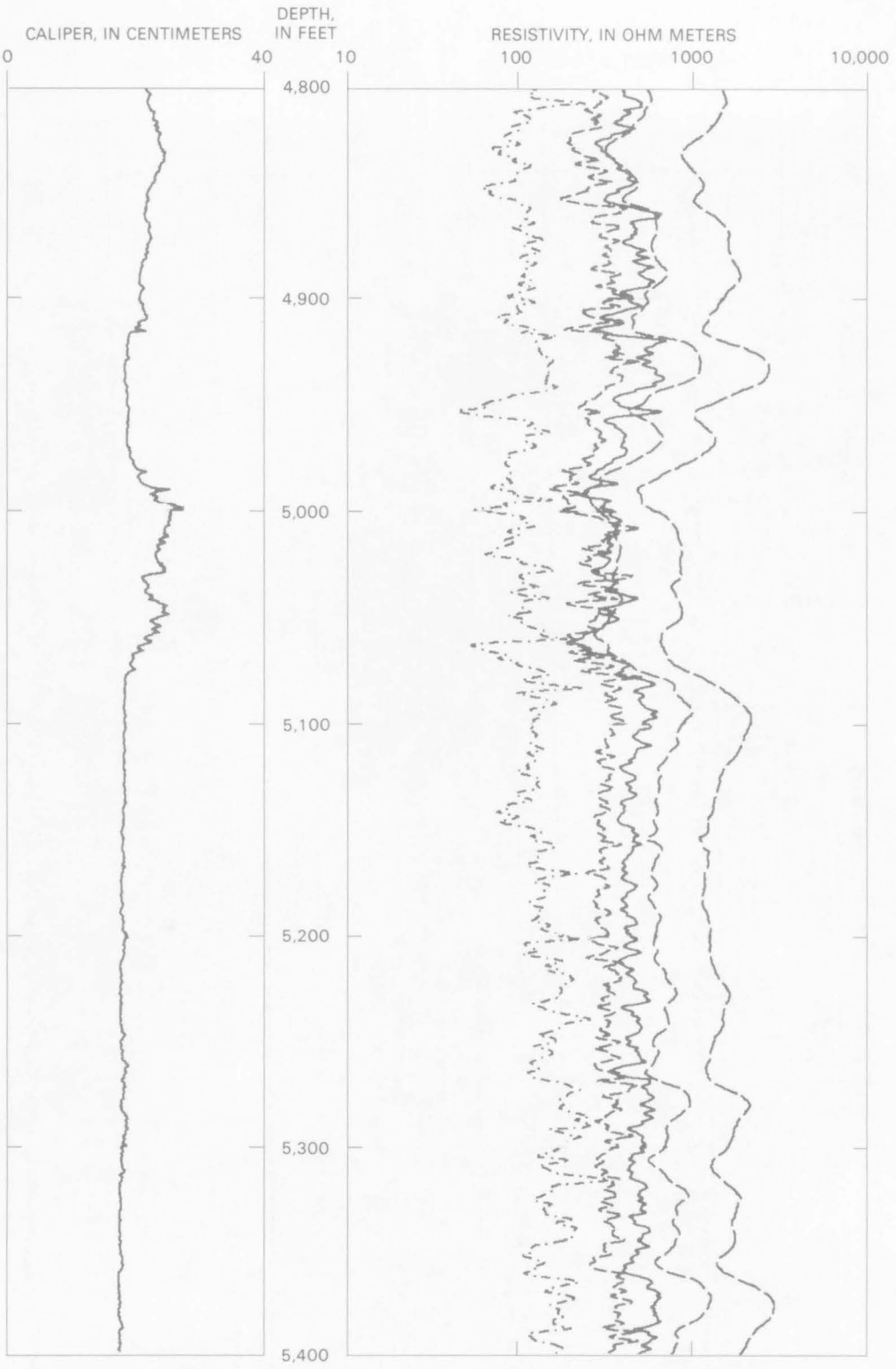

Figure 7. Five resistivity logs of dolomite in borehole P–1, Yucca Mountain, Nev. From left to right: resistivity log from 47–MHz dielectric tool, and medium-induction, deep-induction, short-normal, and long-normal logs. Bit size is 6.8 in. (17.2 cm).

LOG CHARACTERISTICS

We will discuss some log characteristics within the context of specific problems that can be examined by means of the logs: lithologic correlation, the determination of porosity, partial saturation, and permeability to fluid flow. This discussion is intended to provide an overview of problem areas that can then be addressed in more detail.

Lithologic Controls

The degree of welding and the degree and type of alteration are two important controls on log characteristics that can be described from observation of core. Both parameters were coded from descriptions of GU–3 and G–3 core by Scott and Castellanos (1984) and plotted in log format in figure 8. Increased welding is expected to reduce porosity and increase the bulk density, but even so the correlation between degree of welding and the density log is remarkable considering that estimates of the degree of welding are based on flattening of pumice clasts. Density is almost always low in bedded tuffs and in nonwelded to poorly welded ash-flow tuffs and increases as welding becomes moderate or dense. The correspondence is particularly good in the upper 2,500 ft of the hole. Compaction due to overburden may have a more pronounced effect below 2,500 ft.

Borehole GU–3 is one of the holes that was filled with water for logging, permitting normal resistivity logging. The resistivity log is similar in many respects to the density log, but resistivity is low where clays and zeolites are abundant, as they are in the intervals 1,750–2,000, 2,600–2,700, and 3,200–5,000 ft. One should expect the resistivity to drop even lower in the interval 4,250–4,420 ft, where both zeolites and clays are abundant, but abundant calcite, which typically plugs pore space and increases resistivity, was also observed in this interval.

Lithologic Correlation

To show the use of logs for lithologic correlation, we selected the gamma-ray, magnetic field, density, and resistivity logs for boreholes along a north-south profile (figs. 10–13). A geological perspective of this profile shown in figure 9 illustrates the general uniformity of the major tuff units. Logs from the deeper G- and H-series boreholes were selected in order to show the deeper lithologic units. Boreholes H–5, H–3, and G–3 are located on the ridge crest of Yucca Mountain; G–1, G–4, and H–4 are located in washes at the eastern edge of Yucca Mountain, and borehole G–2 is located on a ridge to the north. The logs were shifted to align the depths at the top of the Prow Pass Member of the Miocene Crater Flat Tuff. The depth scale applies to H–5 only, which was not shifted.

As an aid to the reader, a summary of pertinent characteristics of the lithologic units is given in table 5, and a summary of our observations of log character and correlation is given in table 6.

Gamma-Ray Logs

The large offsets due to casing and borehole fluid, already discussed under "Hole Eccentricity," were removed from the logs of figure 10. The negative spikes in boreholes H–5, G–4, H–4, H–3, and G–3 are caused by casing joints, where the increased steel thickness attenuates gamma rays. Logs from G–1 and G–2 were smoothed by applying a 15-point (7.5-ft) unweighted average. These few modifications ease the task of visual correlation.

Perhaps the most obvious indicator of change in lithology is the relatively uniform gamma-ray response in the Topopah Spring Member, with pronounced changes at the top and bottom of the unit. A few other correlations within units are noteworthy: the blocky anomaly at the top of the Prow Pass Member, which is seen in five of the seven boreholes, the definitive character of the Bullfrog Member of the Crater Flat Tuff in H–3 and G–3, and the demarcation of the upper and lower units of the Tram Member of the Crater Flat Tuff in all but G–2. But, overall, the gamma-ray log is much less useful for characterizing lithology here than it is in a clastic rock sequence.

Magnetic Logs

Either magnetic-field logs or measurements of remanent magnetization on core were available in six of the seven holes on the profile (fig. 11). The magnetization data were corrected in this figure for inclination, so that they and the magnetic field track together. Only for G–3 are both a magnetic-field log and remanent-magnetization data available, but the magnetic-field log for G–3 is discontinuous and noisy. Nevertheless, the overlay of remanent magnetization and total field is quite good, showing that most of the character of the magnetic field is due to variations in remanent magnetization, not to fields induced by varying susceptibility. Where the magnetic field (or remanent magnetization) swings to positive, the remanent vector points upward in the formation (reversed polarization) and the remanent contribution augments the Earth's

field in the borehole. Conversely, normal remanent polarization causes a reduction in magnetic field in the borehole.

Most spectacular are the signatures of reduced amplitude (normal polarization) in the Bullfrog and the signatures of large, enhanced amplitude (reversed polarization) of the upper part of the Tram. These signatures are excellent correlation markers. Their absence in G–2 is attributed to the absence of the upper lithic-poor unit in that hole and to missing sections in the Bullfrog Member (Maldonado and Koether, 1983).

Another excellent marker is the smaller, but persistent, reduction of magnetic field at the top of the Prow Pass Member. Above it, the Calico Hills unit shows little or no variation in remanent magnetization, but the Topopah Spring Member produces a signature that is more erratic and has higher spatial frequency than do the underlying rock units. This is more clearly shown in the four magnetic logs on an east-west profile in figure 14, the magnetic field being presented on a more sensitive scale. Here the anomaly at the top of the Prow Pass Member is again present and the erratic, high-spatial-frequency character of the Topopah Spring Member can be more clearly seen. Note the consistency of the normal remanent magnetization (reduced field) at the bottom of the Topopah Spring.

Variations in magnetic-field logs are clearly useful for lithologic correlation. These variations are a function of the iron-bearing minerals and the Earth's field at the time of cooling. Magnetic susceptibility, on the other hand, is also dependent upon iron-bearing minerals but is independent of the Earth's paleofield. Magnetic-susceptibility logs were acquired in only a few boreholes (table 2), and over a limited depth range, so we were unable to assess their general applicability for correlation. However, in four of the shallow boreholes in Drill Hole Wash, A–4 through A–7 (plates 34 through 37), the susceptibility logs for the top of the Topopah Spring Member are highly correlative with one another. This correlation does not carry over to the susceptibility logs from nearby boreholes A–1 or WT–14. At this point it appears that magnetic susceptibility is informative if collected routinely, but this expectation remains to be tested.

Density and Resistivity

Density and resistivity (figs. 12 and 13) are considered together to facilitate the discussion of degree of welding and alteration. As we have seen, both density and resistivity increase with the degree of welding, but resistivity can decrease dramatically with increased mineral alteration. Thus, they generally tend to vary systematically. It is expected that these properties can be exploited quantitatively to aid in the definition of lithology and alteration. For now, we offer some observations regarding these two logs and rock character.

Resistivity of the Topopah Spring Member is high, usually greater than 200 ohm meters, not only because the saturation is less than 100 percent, but because it is predominantly densely welded, with (presumably) consequent reduction in pore connectivity. This occurs despite the presence of lithophysae, which comprise large amounts of pore space. These cavities are expected to be drained (Montazer and Wilson, 1984) and to decrease the effective matrix porosity and permeability. Inspection of figure 8 does not show any unusual resistivity effect where lithophysae are abundant.

By way of contrast, both the density and electrical resistivity are much reduced in the underlying Calico Hills unit, which is nonwelded to partially welded and zeolitized. These reductions are manifest regardless of the position of the static water level with respect to lithology. The logs show that these characteristics of the Calico Hills unit are consistent from north to south along Yucca Mountain.

The Prow Pass Member contains a highly resistive zone in its upper part that correlates well across all boreholes. In G–1 this zone is moderately welded and devitrified, in G–2 it is densely to moderately welded and devitrified, and in G–4 it is nonwelded to partially welded and devitrified. In the case of the upper part of the Prow Pass Member, the lack of clays and zeolites appears to be a more important control than the degree of welding.

Zeolitized bedded tuffs are present at the top and bottom of the Bullfrog Member, producing marked decreases in resistivity at the upper and lower boundaries of the Bullfrog. Density and resistivity tend to be high within the Bullfrog, but neither density nor resistivity correlates particularly well across the profile, this poor correlation indicating some lateral variability in the degree of welding and alteration in the Bullfrog. The logs from boreholes H–4, H–3, and G–3 appear to be somewhat better correlated with one another even though the Bullfrog is above static water level in H–3 and G–3.

On the basis of all four types of logs shown in figures 10–13, the Tram Member is subdivided into an upper and lower unit, with the exception of G–2 where the upper subunit of the Tram is missing. Density, resistivity, and gamma-ray readings are higher in the

Figure 8 (facing page). Three logs and geological description from Scott and Castellanos (1984) for borehole GU-3/G-3, Yucca Mountain, Nev. Static water level (SWL) is shown in left track. Resistivity is taken from the induction log (solid curve, upper) and the short-normal log (dashed, lower).

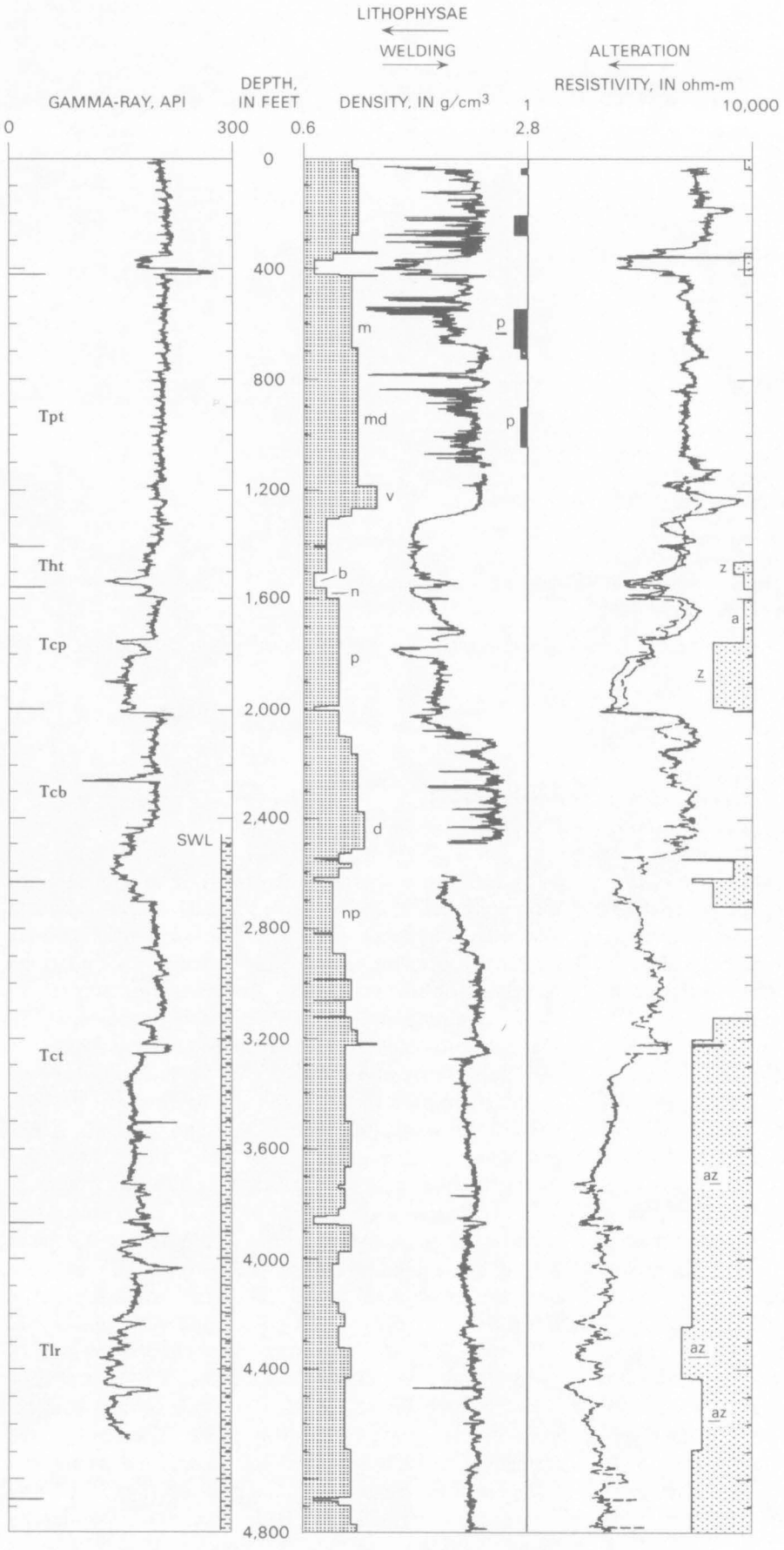

EXPLANATION

Degree of welding

- b Bedded
- n Nonwelded
- p Partially welded
- np Nonwelded to partially welded
- m Moderately welded
- md Moderately to densely welded
- d Densely welded
- v Vitrophyre

Abundance of lithophysae

- p Sparse (1–5 percent of rock)
- p̲ Common to abundant (≥5 percent of rock)

Type and degree of alteration— Sparse if symbol is not underlined; common to abundant if symbol is underlined

- a Clays
- z Zeolites

- Tpt Topopah Spring Member of Paintbrush Tuff
- Tht Tuffs and lavas of Calico Hills
- Tcp Prow Pass Member of Crater Flat Tuff
- Tcb Bullfrog Member of Crater Flat Tuff
- Tct Tram Member of Crater Flat Tuff
- Tlr Lithic Ridge Tuff

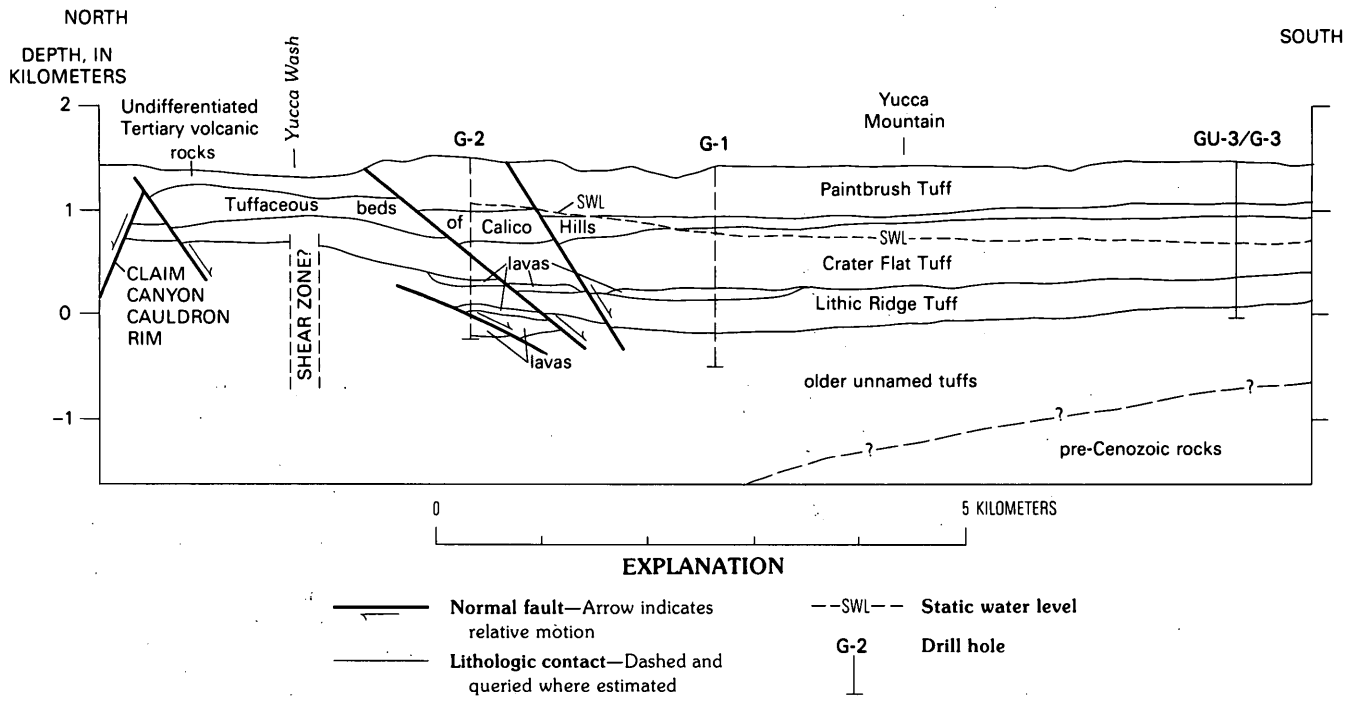

Figure 9. Generalized north-south geologic section along crest of Yucca Mountain, Nev., from Scott and Castellanos (1984).

upper part of the Tram than in the lower part. The electrical resistivity is particularly consistent from hole-to-hole in the southern half of the profile. In G–1 the upper unit is described as moderately welded and devitrified while the lower unit is nonwelded to partially welded and zeolitized, or zeolitized and argillic. From the consistent correlation of resistivity across the profile we infer that this description generally applies to the Tram from G–1 on the north to G–3 on the south.

Unit Tll in G–1 is unaltered flow breccia, so the low resistivity in this hole is attributed to pore structure rather than to clay and zeolites. Mafic minerals probably cause the high bulk density in the unit. Lack of correlation of the resistivity log from borehole G–1 to borehole H–5 reflects the lateral variability of the flow breccia. Unit Tll in borehole H–1 (pl. 9) located only 1,500 ft from G–1, is much more resistive than it is in G–1, so we infer that the unit is unbrecciated in borehole H–1 as well as in H–5.

Densities and resistivities exhibit little change from the lower part of the Tram to the Lithic Ridge Tuff in boreholes H–4, H–3, and G–3. We infer that extensively altered rock extends deeper into the Lithic Ridge Tuff, consistent with observations in G–1 by Spengler and others (1981) and in G–3 by Scott and Castellanos (1984) that below the approximate midpoint of the Tram most rocks show intermittent to pervasive alteration to clay minerals and zeolites.

Mineralogy

Lithologic correlations observed in the logs are ultimately due to variations in porosity, mineralogy, and chemistry. Porosity is usually the most important control on density, neutron, velocity, and resistivity logs, although we have seen that resistivity is low wherever zeolites and clays are abundant. In other cases one or two minerals play an inordinate role in the response of a log. These are commonly fairly subtle and require further consideration of the petrological and chemical data to see if the logs suggest the spatial variation of selected minerals. A few examples of the effect of a few minerals on log characteristics are worth mentioning here.

Feldspar and quartz are the most abundant minerals in the unaltered tuffs (for example, Vaniman and others, 1984; Caporuscio and others, 1982) and have densities in the range 2.57–2.65 g/cm^3. Also present in the tuffs are tridymite and cristobalite with densities of 2.26 and 2.30 g/cm^3, the zeolite clinoptilolite (2.20 g/cm^3), and glass, also of low density. We have already inferred from figure 8 that degree of welding controls bulk density through porosity. This is true, but the interval of low density from 1,300–2,100 ft does contain a large fraction of glass and clinoptilolite (fig. 3 of Vaniman and others, 1984). The impact of low-density minerals on the density log merits close study.

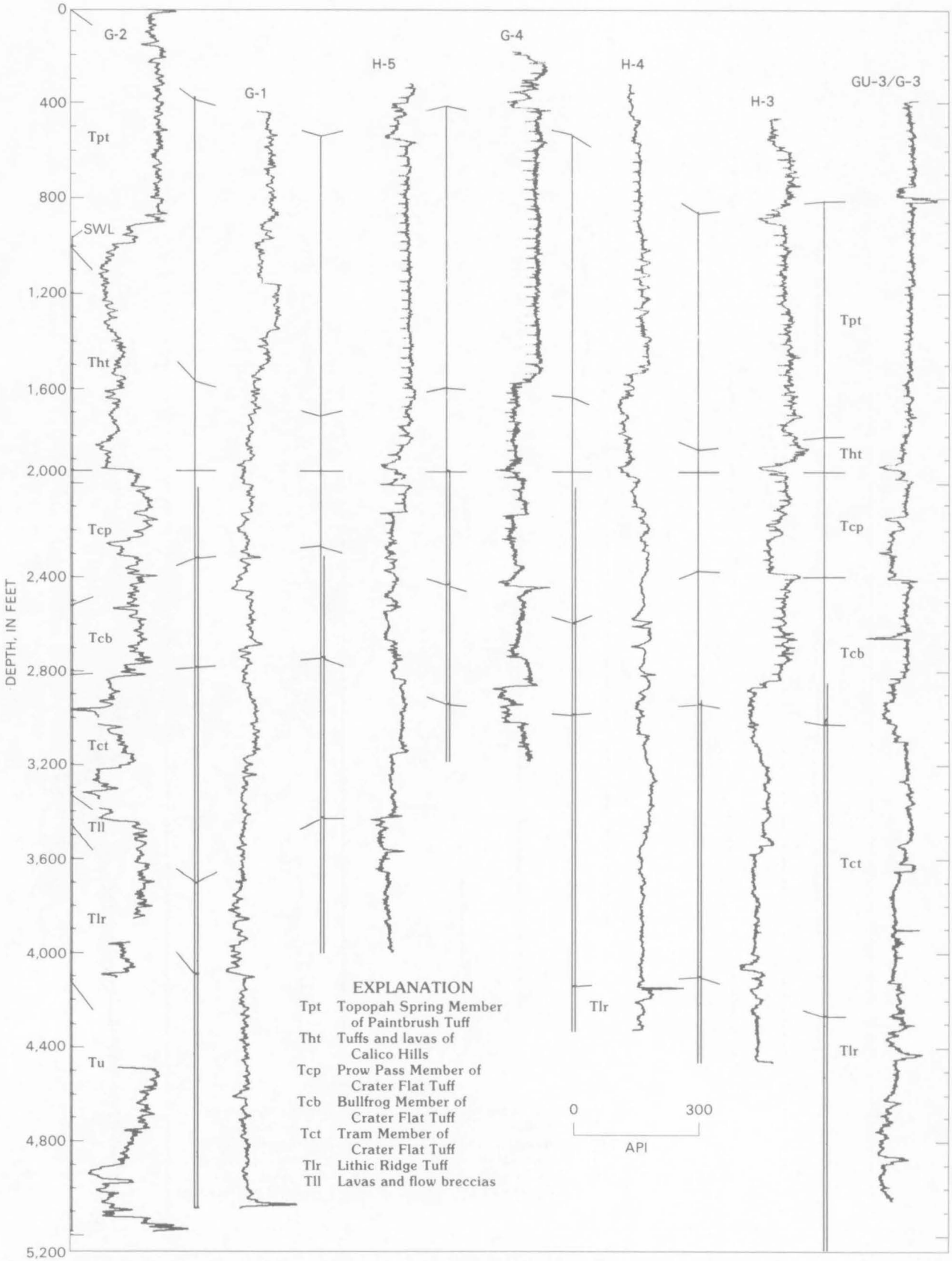

Figure 10. Gamma-ray logs for seven boreholes along north-south line at crest of Yucca Mountain, Nev. Depth of logs has been shifted to align at top of Prow Pass Member. Depth scale applies only to borehole H–5. Effects of casing and borehole fluid have been removed from gamma-ray logs. Tie points show stratigraphic correlations (refer to table 5) based on geological observation. Second vertical line shows extent of the static water level (SWL).

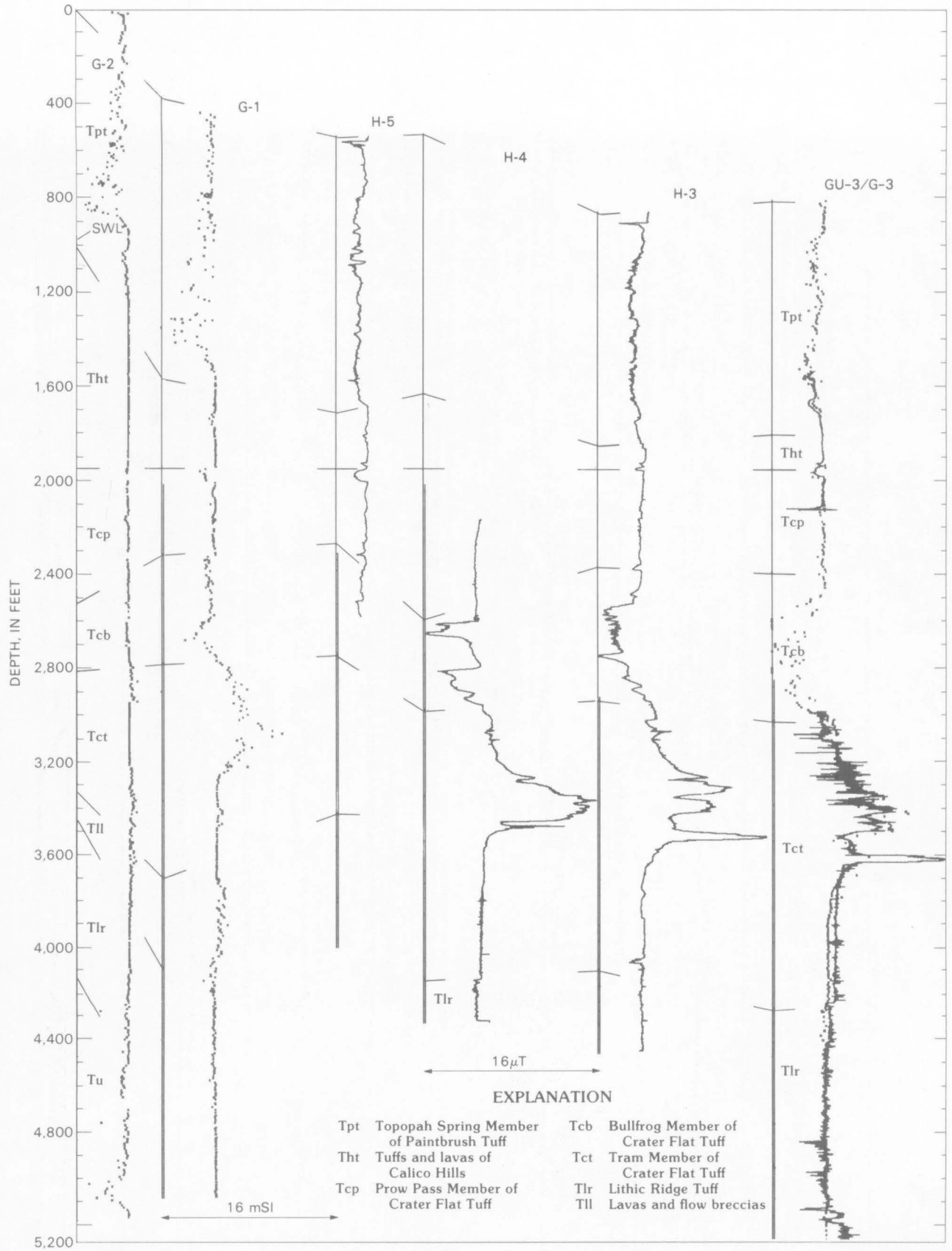

Figure 11. Magnetic-field logs (solid line) and measurements of remanent magnetization on core (dots) from six boreholes along north-south line at crest of Yucca Mountain, Nev. Depth scale applies only to borehole H–5. Tie points show stratigraphic correlations (refer to table 5) based on geological observation. Second vertical line shows extent of the static water level (SWL).

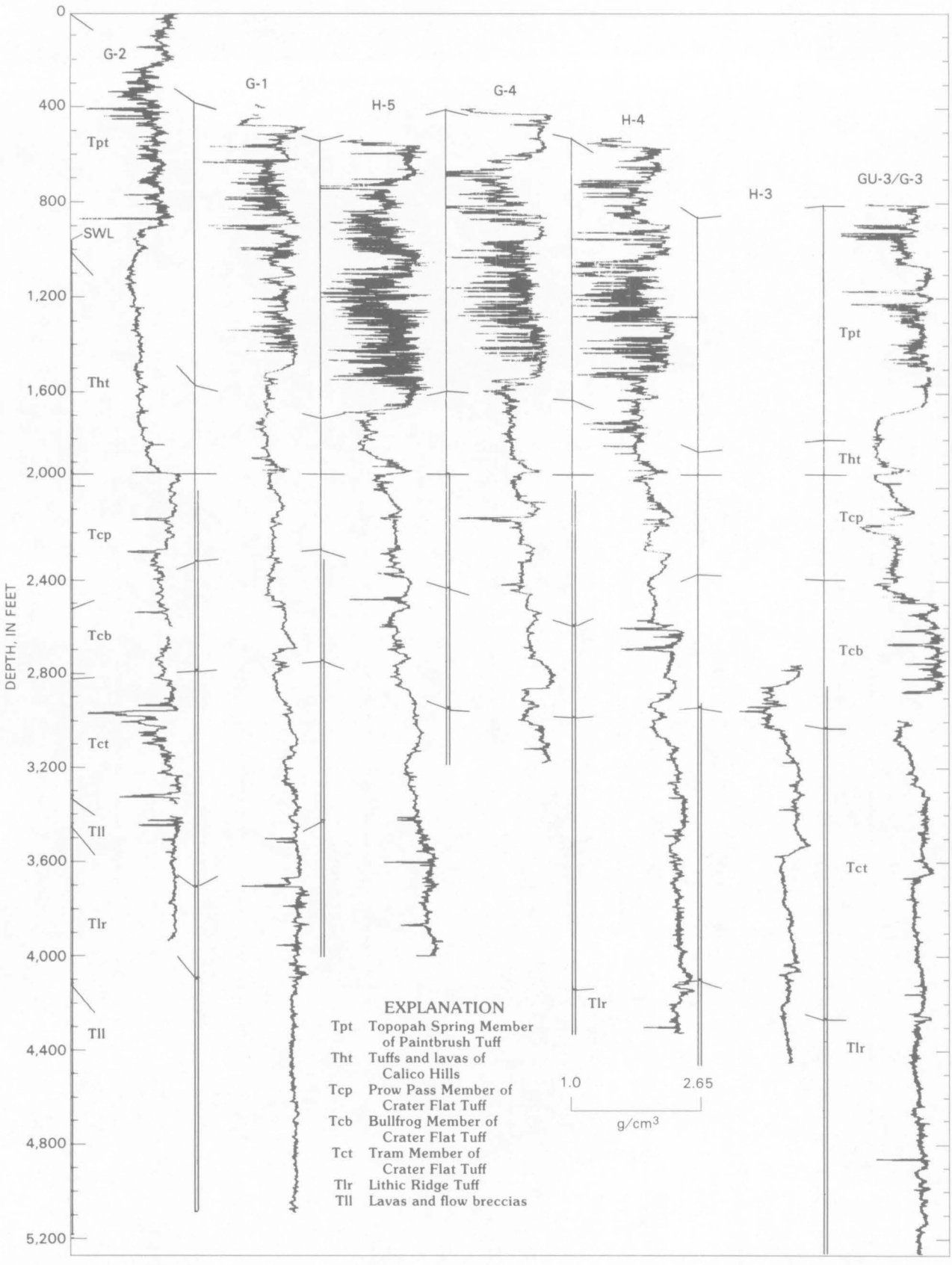

Figure 12. Density logs for seven boreholes along north-south line at crest of Yucca Mountain, Nev. Depth scale applies only to borehole H–5. Tie points show stratigraphic correlations (refer to table 5) based on geological observation. Second vertical line shows extent of the static water level (SWL).

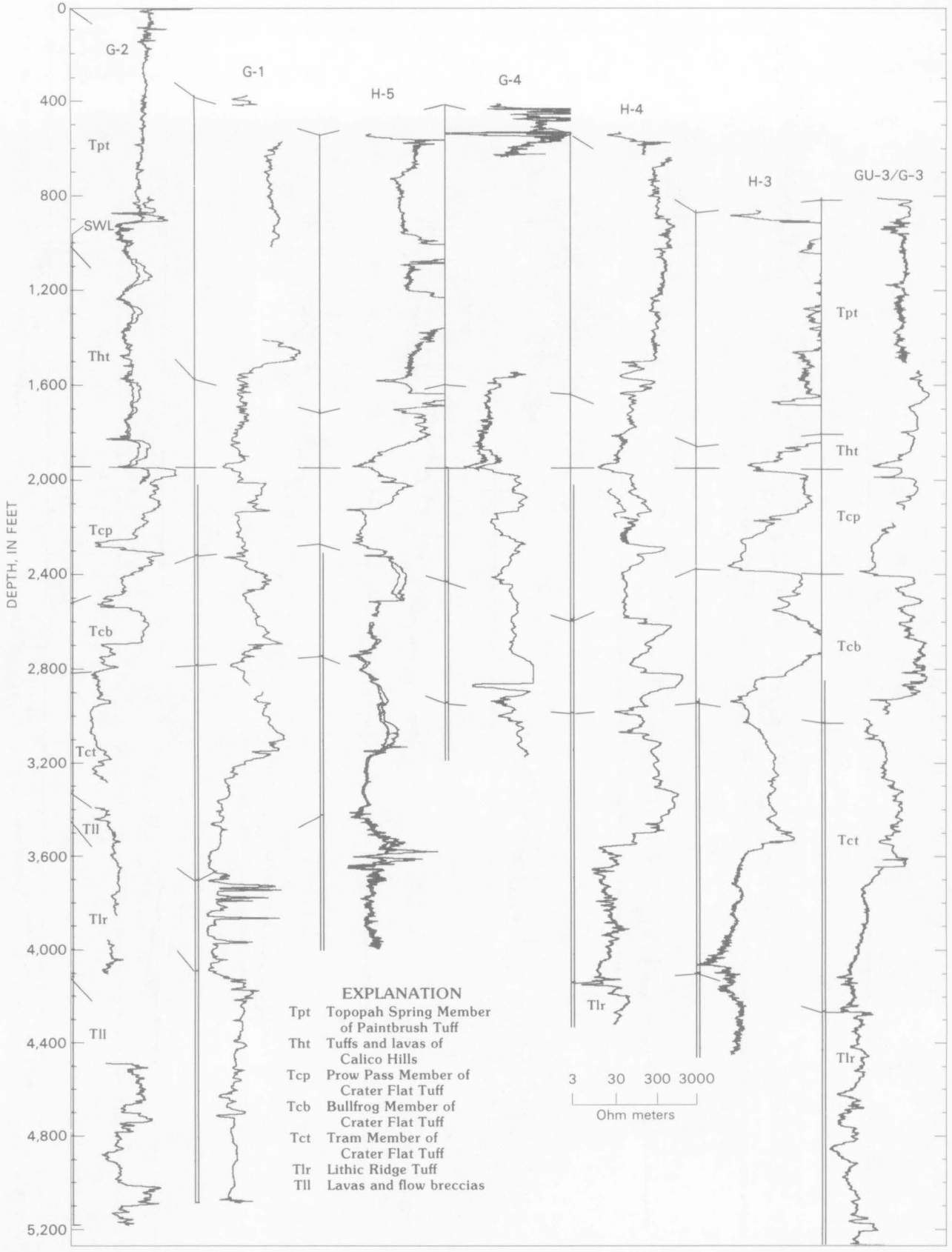

Figure 13. Electrical-resistivity logs for seven boreholes along north-south line at crest of Yucca Mountain, Nev. Depth scale applies only to borehole H–5. Tie points show stratigraphic correlations (refer to table 5) based on geological observation. Second vertical line shows extent of the static water level (SWL). Induction logs are presented for the interval above the static water level, short-normal logs below.

Table 5. Summary description of geology and alteration of volcanic units, Yucca Mountain, Nev., after Spengler and others (1981), Maldonado and Koether (1983), Scott and Castellanos (1984), and Spengler and Chornack (1984)

Geologic unit	Description	Alteration
Topopah Spring Member (Tpt).	Nonwelded glassy top and bottom; thick, densely welded, devitrified center; two or three lithophysal subunits.	Unaltered except for zeolites in nonwelded units below vitrophyre.
Tuffs and lavas of Calico Hills (Tht).	Massive, homogeneous, nonwelded ash-flow tuffs; mostly crystal poor.	North: 60–80% zeolitized over entire zone. South: vitric.
Prow Pass Member (Tcp).	Similar to Bullfrog Member	Top and bottom altered to clay and zeolites. Locally zeolitized.
Bullfrog Member (Tcb).	Nonwelded to partly welded units enclose welded core; compound units in south.	Top and bottom altered to clay and zeolites.
Tram Member (Tct).	Moderately welded to nonwelded; quartz phenocrysts as much as 30%; upper unit is lithic poor; lower unit is lithic rich.	Upper unit: zeolites and clays scarce. Lower unit: zeolites, clays, pyrite south and east of borehole G–1.
Lavas and flow breccias (Tll).	Dacite lava and flow breccias; prominent mafic minerals.	Moderate to intensely altered to clays and zeolites.
Lithic Ridge Tuff (Tlr).	Nonwelded to moderately welded ash-flow.	Extensively altered to smectite clays and zeolites.

The high gamma radiation, generally greater than 150 API units, is attributed to the potassium in the alkali feldspars and in their alteration products. Feldspar amounts to as much as 80 weight percent of the rock matrix. The spectral gamma-ray log deserves much more attention than it has received thus far, with regard to both its calibration and utility. Neutron activation analysis, yielding quantitative estimates of potassium, uranium, and thorium, has thus far been carried out only on core material from borehole G–1 (Broxton and others, 1986). Unfortunately, a spectral gamma-ray log was not obtained in G–1.

Identification of zeolite zones is of great interest because of their sorptive properties. It was reasonable to expect that induced-polarization logging would be diagnostic of zeolites, but this does not appear to be so. Inspection of the induced-polarization data for GU–3/G–3 shows a highly variable response through the

Table 6. Qualitative character and correlation of logs by lithologic unit, Yucca Mountain, Nev.

[Bedded units (Tba) have been ignored. Rating of hole-to-hole correlation excludes G–2. N, no correlation rating for Tll and Tlr due to insufficient number of boreholes]

Geologic unit	Log character	Hole-to-hole correlation
Topopah Spring Member (Tpt).	Gamma: high amplitude and very uniform	Excellent
	Density: variable and spiky due to rough hole	Good
	Resistivity: high amplitude; limited data	Poor
	Magnetic: low amplitude with high-frequency ripple.	Fair
Tuffs and lavas of Calico Hills (Tht).	Gamma: low	Poor
	Density: low	Fair
	Resistivity: low, decreasing with depth in holes above the static water level.	Good
	Magnetic: unperturbed	Fair
Prow Pass Member (Tcp).	Gamma: blocky character	Good
	Density: moderate amplitude, variable	Poor
	Resistivity: high amplitude in upper, variable in lower unit.	Good
	Magnetic: normal remanent magnetization at top of unit.	Excellent
Bullfrog Member (Tcb).	Gamma: high to moderate amplitude	Fair
	Density: erratic, increasing with depth	Poor
	Resistivity: erratic, increasing with depth	Poor
	Magnetic: large normal remanent magnetization	Excellent
Tram Member (Tct).	Gamma: high amplitude in upper, moderate amplitude and uniform in lower unit	Good
	Density: moderate to high amplitude, increasing with depth.	Fair
	Resistivity: high amplitude in upper, low to moderate amplitude in lower unit.	Excellent
	Magnetic: large reverse remanent magnetization	Excellent
Lavas and flow breccias (Tll).	Gamma: low amplitude	N
	Density: high amplitude	N
	Resistivity: no consistency	N
	Magnetic: no data	N
Lithic Ridge Tuff (Tlr).	Gamma: moderate amplitude	N
	Density: insufficient data	N
	Resistivity: low amplitude	N
	Magnetic: no data	N

entire 5,000 ft of hole, with no obvious correlation with the major zeolitized intervals. This lack of correlation was also noted at Rainier Mesa on the Nevada Test Site (Carroll, 1990).

Density and Porosity

The density log is the only "porosity" log obtained in both the saturated and unsaturated zones of almost all

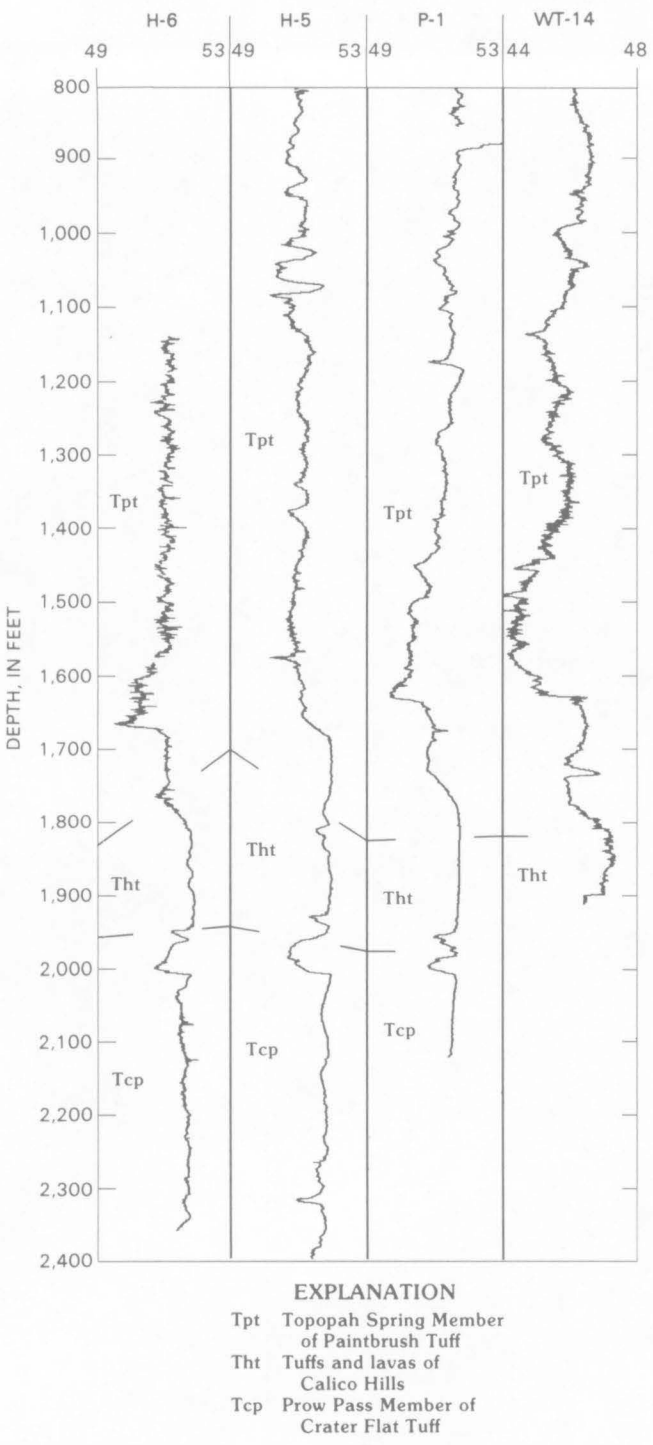

Figure 14. East-west profile of magnetic-field logs (in microteslas) from four boreholes, Yucca Mountain, Nev. Vertical field is displayed for WT–14; other three are total fields. Logs have been shifted to tie to anomaly at top of Prow Pass Member, at 2,000 ft. Depth scale tied to H–5.

Yucca Mountain boreholes. Density data are useful for designing and interpreting gravity surveys, for engineering design purposes, and for estimating porosity. In all these uses, the accuracy of the log needs to be assessed by comparison with gravity and core data.

Figure 15 provides an excellent comparison between the density log and core measurements from borehole G–3. In this case, conditions for such a comparison are ideal: the borehole is of uniform diameter with only minor rugosity, and the log was run in a water-filled hole in the saturated zone, so the density of saturated core samples can be compared with the density log. This is advantageous because the water content can be controlled by resaturating to make up any losses occurring during core recovery.

In the unsaturated zone, there is no control over the saturation conditions in either the core or the formation. Where mud is the drilling fluid, presumably mud filtrate invades both core and formation. Nevertheless, a comparison of core density and the density log for borehole G–4 (fig. 18) shows a good correspondence between saturated core and the density log (except in the "invaded" zones, 1,792–1,947 and 2,250–2,530 ft, which are discussed under "Air Invasion"). The gravity log shows a greater density than the density log by about 0.04 g/cm^3, a discrepancy attributed to the uncertainty in free-air gradient, as discussed under "Gravity."

Although statistical tests are needed to confirm more rigorously the correspondence between the core and density logs, these two examples and others shown on plates 1–40 indicate that the density log is a good measurement of in-situ density. One might then assume that the density log can easily provide good estimates of porosity, but this is not the case. To calculate porosity from a density log, one must have a good estimate of grain density and also know that it is reasonably constant. Figure 18 shows that grain density varies considerably in the tuffs, so the density log alone is not reliable for estimating porosity except for cored wells for which grain density data are available. The problem is not so serious in the saturated zone, in which case the resistivity, neutron, and acoustic logs can also be used to estimate porosity. However, in the unsaturated zone, for which fewer logs are available, the variations in grain density make the estimation of porosity and water saturation even more difficult.

Water Saturation

Electrical resistivity, dielectric constant, and neutron moderation are the common logging techniques for detecting and measuring the amount of water present in rock. None of these properties is easy to measure in the unsaturated zone at Yucca Mountain. Under "Static Water Level and Air-filled Boreholes," we mentioned the environmental restrictions of an air-filled borehole.

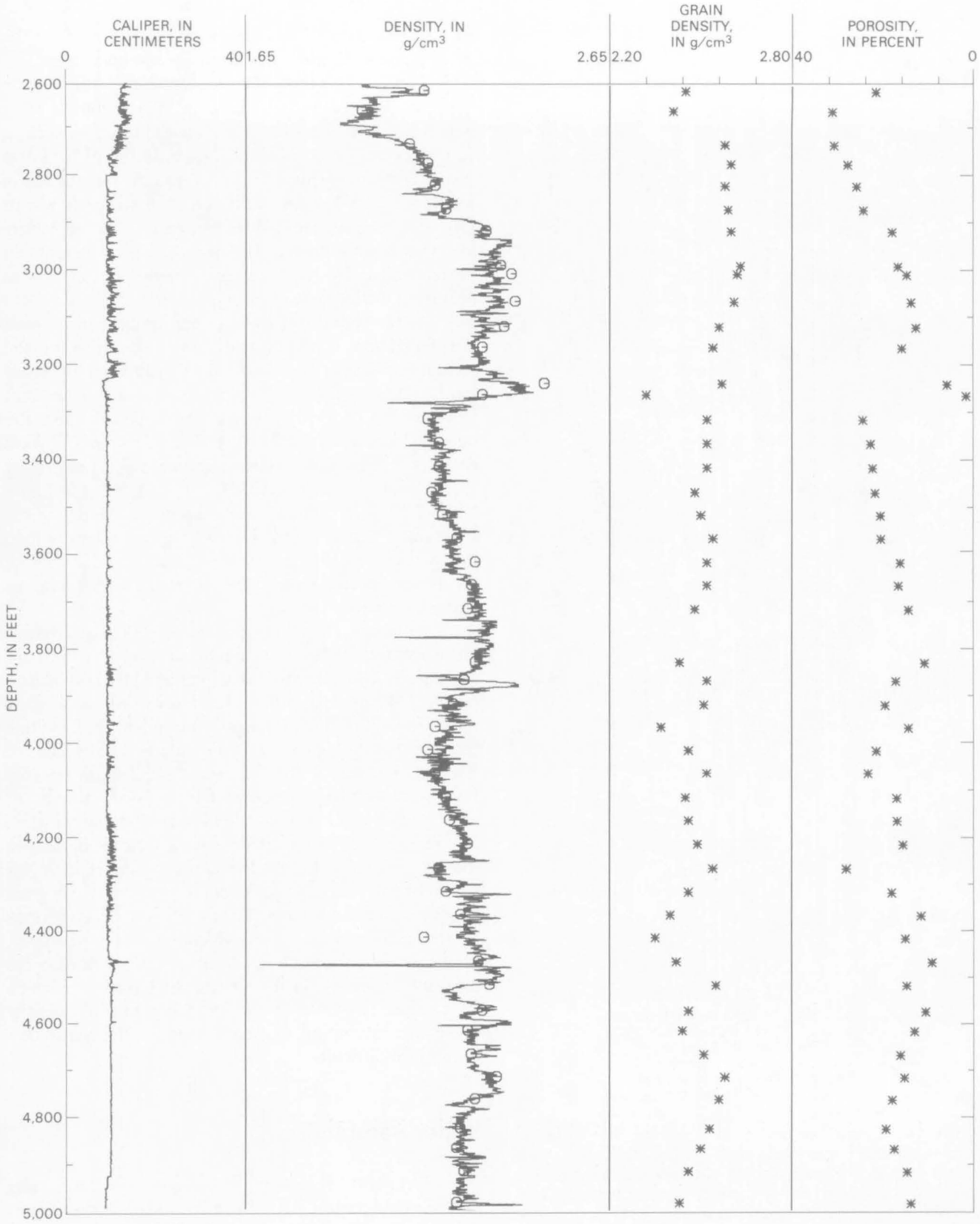

Figure 15. Caliper and density logs for borehole G-3, Yucca Mountain, Nev., with core measurements of saturated bulk density (open circles plotted with density log), grain density, and porosity from Anderson (1984).

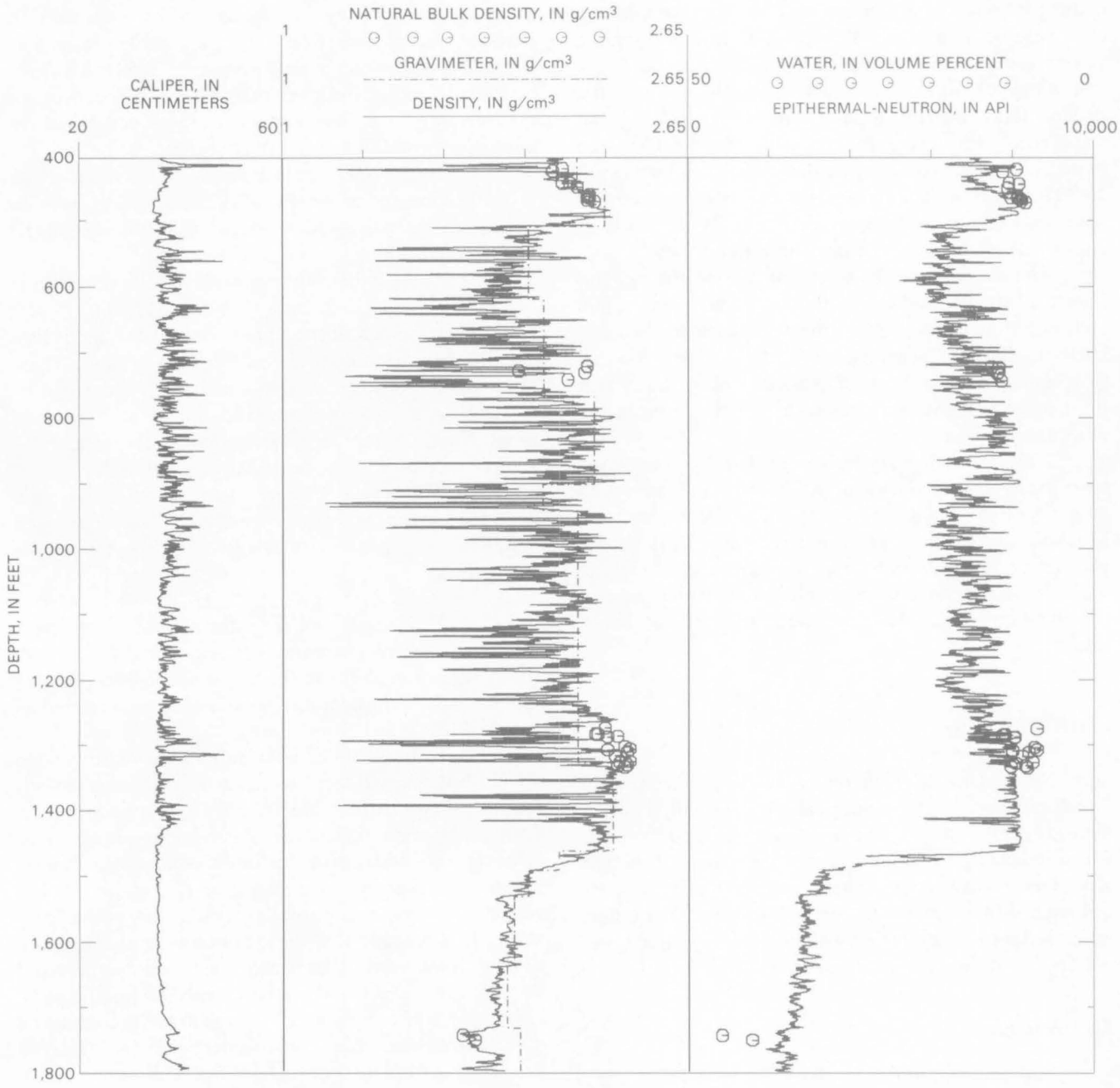

Figure 16. Log and core data for borehole H–1. Horizontal scales in track 3 (at right) were adjusted to show correspondence between water content and epithermal-neutron log.

The high resistivity limits the accuracy of the induction tool. The lack of fluid in the borehole means the compensated neutron tool cannot be operated. Tools that can be used are the epithermal-neutron tool, which requires special calibration for an air-filled borehole, and the dielectric tool, which operates at reduced resolution in the high-resistivity environment and which also requires special calibration.

There are two approaches to calibration. A calibration "pit" or test facility can be designed and built in which the parameter of interest, in this case water content, is controlled or measured during fabrication. This approach has been followed by workers at LLNL (for example, Axelrod and Hearst, 1984), who established that sonde gap, water content, and density control the epithermal neutron count. Their work resulted in calibration formulas for holes of large diameter.

A second approach to calibration is to determine the water content of core samples, requiring that the

drilling fluid does not contaminate the core sample and that there be no significant loss of fluid from the sample during retrieval and transport to the laboratory. These conditions are difficult to assure, especially if mud is the drilling fluid. Figure 16 shows an epithermal log and water content of core in the unsaturated zone. The large increase in water content and decrease in tool counts at 1,470 ft occurs at the interface between an altered porous zone and a low-porosity welded zone. Calibration is easier if there are large changes in water content.

The dielectric tool also responds to water content. Figure 17 shows good correlation between dielectric and epithermal-neutron logs as one would expect because both tools are sensitive to total water content. Correlation of both these logs with density shows that total water content increases with porosity, even in the unsaturated zone.

Unfortunately, very little core data were obtained from the holes drilled with air, so there are not many data with which to calibrate the epithermal-neutron tool. Most dielectric runs were in uncored wells, so there are even fewer core data with which to calibrate the dielectric tool. The ability to estimate water content depends on obtaining more core data from holes to be drilled in the future.

Permeability

No logging tool currently available furnishes a direct measurement of permeability. Instead, indirect measurements of permeability have evolved, two of which indicate permeable zones in the Yucca Mountain area. One measurement, which involves the invasion of drilling fluid into the formation, is fortuitous. The other, which is done in conjunction with pump or injection tests, is effective at delineating zones of relatively high flow.

Air Invasion

Two unusual zones in borehole G–4 (pl. 5) are shown in expanded format in figure 18. Note that both zones are below the static water level. In oil-well logging parlance, these zones (1,792–1,947 ft and 2,250–2,530 ft) would be termed "gas zones" on the basis of differences between the neutron and density logs. (A condition of low "neutron-porosity" and high "density-porosity" (that is, low density) exists when gas rather than fluid fills the pore space, but gas is not expected in this environment.) Several other observations can be made:

1. Except for these two zones, the density derived from the borehole gravimeter agrees with the log and core density data at all depths, although there is a small offset of about 0.04 g/cm^3. Taking the gravimeter density as nearly correct, we see that within the two zones in question, the density log reads erroneously high in porosity and the neutron log reads erroneously low. Because the gravimeter measurement is affected by rock at greater radial distance than either the density or neutron log, this discrepancy can be attributed to anomalous conditions near the borehole.

2. Both zones are concordant with vapor-phase crystallization zones within units described to be non-welded to partially welded, as shown by the geological description in the left-hand track.

3. The low-density zones can also be observed in holes H–4, C–1, C–2, and C–3 (pls. 11, 14, 15, 16, respectively), again in the upper parts of the Prow Pass and Bullfrog Members of the Crater Flat Tuff. These occurrences convince us that the phenomenon can be ascribed to a rock property and not to an artifact of measurement. Moreover, inspection of the caliper log assures us that it is not caused by a rough hole.

4. The grain density actually increases, not decreases, in the two zones in question. This rules out the possibility of micron-size air-filled pores in pumice fragments.

5. Holes C–1, C–2, C–3, H–4, and G–4 were drilled with air foam over the intervals discussed here.

6. Core measurements (tracks 3 and 4 of fig. 18) show that permeability in the two zones in question, 2–8 millidarcies, is considerably greater than in surrounding zones of less than 0.1 millidarcy.

On the basis of this information, it is reasonable to attribute these two "gas" zones to invasion of the air-foam drilling mixture into (relatively) permeable rock. This explanation fits all six observations above. It is, however, at odds with hydraulic-conductivity values based on packer-injection slug tests (Lobmeyer, 1986), which do not reveal any greater permeability in the "gas" zones. It is possible that these zones were plugged with drilling fines when the packer tests were conducted because the zones could not be cleaned by pumping (D. Lobmeyer, oral commun., 1989) due to the presence of a much more permeable flow zone deeper in G–4 (refer to the flow log of plate 5 or to fig. 17 of Lobmeyer, 1986). Based on the log and core data, we conclude that a zone having matrix permeability on the order of 5 millidarcies is present in the Prow Pass and upper part of the Bullfrog Members of the Crater Flat Tuff and that it extends over a distance of at least several kilometers.

Water Invasion

The previous example dealt with air invasion of saturated rock below the water table; we now examine a case of permeable rock above the water table encountered in borehole GU–3 and nearby G–3 (fig. 19). As discussed in "Drilling Problems and Related Logging Problems," GU–3 is unusual in that it was drilled with mud instead of air and foam above the static water level.

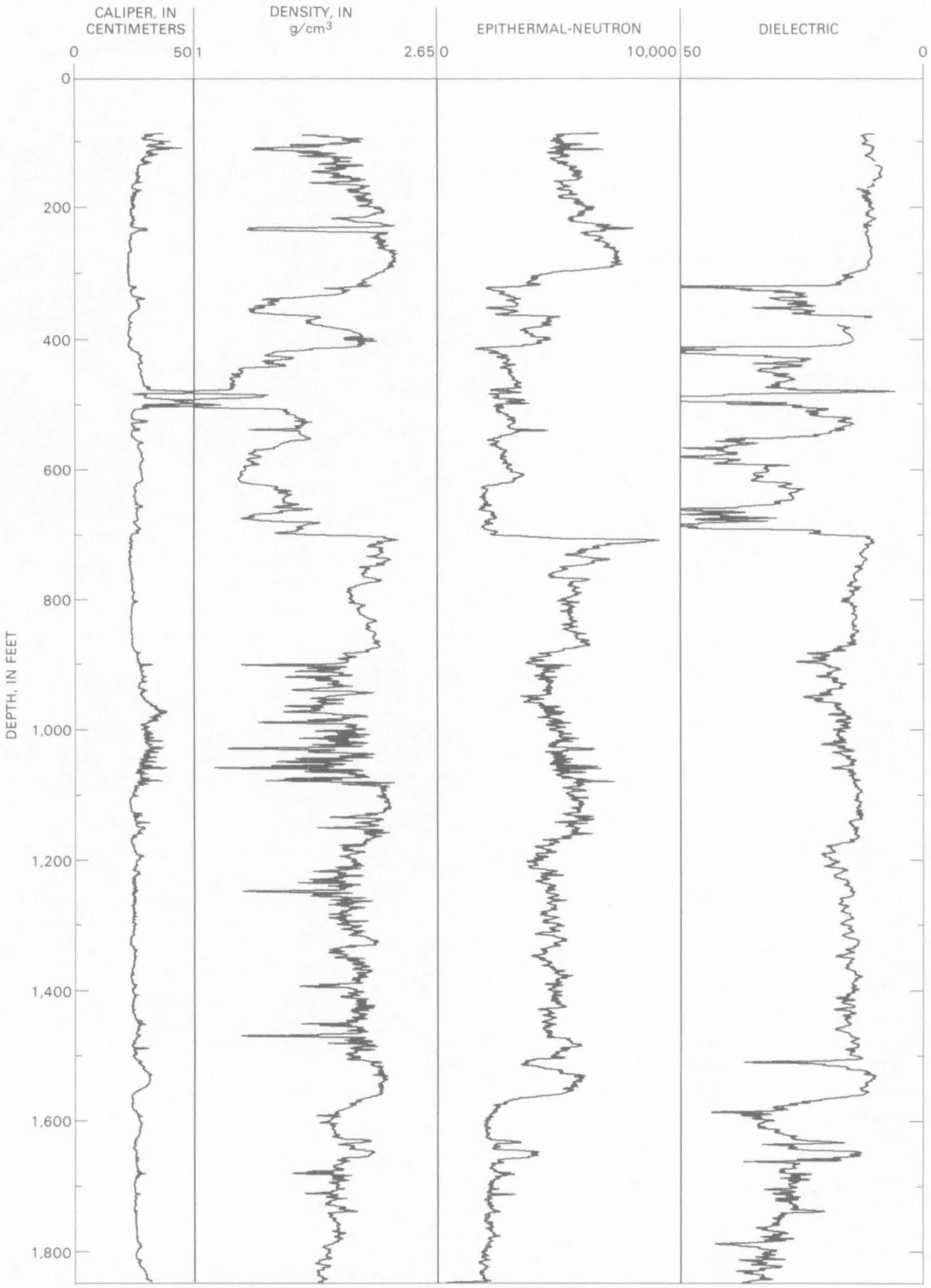

Figure 17. Logs for borehole WT–18, Yucca Mountain, Nev. Correspondence between the epithermal-neutron and dielectric logs indicates their response to water content.

The most striking feature is the contrast between the density and neutron logs between 1,270 and 1,810 ft. As in the case of G–4, just discussed, it has the appearance of a "gas effect." In this case it is attributed to the partial saturation of the nonwelded to poorly welded tuff. Note that the ordering of density measurements in this interval, from low to high, is as follows: gravimeter log, density log, and saturated-core samples. We believe that the gravimeter reads the density accurately for the partially saturated formation, that the density log reads higher because mud filtrate invaded the formation, and that the core data are correct for saturated rock. Shallow invasion of the formation by mud is consistent with the high permeability and high porosity established by core measurements. Pores and pore throats in the tuff must be large enough that capillary retention is poor and water saturation is low. The logs and core data are consistent in revealing a unit in the nonwelded to partially welded tuff having high porosity and high permeability.

Above the strata where the logs correspond poorly, we see excellent agreement among gravimeter, density, and core density in the vitrophyre (1,190–1,270 ft). Above that, in the moderately to densely welded tuff, porosity is low, the saturation state is not well determined, and there was no invasion by drilling mud filtrate. An altered (zeolitic) zone having low permeability and high porosity exists from 1,810 to 2,010 ft. Neutron response indicates that total water content is high. The lack of density-gravimeter separation and the permeability data indicate no invasion. The moderately to densely welded zone below 2,100 ft exhibits low porosity and permeability, probable high saturation, and no invasion.

Flow Logs

The most reliable and consistent indicator of permeability utilized thus far has been the flow profiles obtained with radioactive tracers and reproduced in track 9 of the log plots for boreholes G–4, B–1H, P–1, H–1, H–3, H–4, H–5, and H–6. USGS investigators have established that permeability is controlled by fractures, not by the rock matrix. Evidence of flow through fractures is manifest by virtually every flow log thus far recorded: flow is reduced sharply over fairly narrow intervals of hole rather than exhibiting uniform exodus from the wellbore as it would if matrix porosity were controlling the flow. The porosity logs are much more uniform in character than the flow logs, showing that permeability does not correlate with matrix porosity.

In figure 20 flow profiles from P–1 of Tertiary volcanic rock and Paleozoic dolomites are shown for comparison with uranium, televiewer, and sonic waveform logs. These three logs are generally effective indicators of fractures in sedimentary sequences. The sonic logs were not run above 1,580 ft because of casing, and the televiewer log was not valid above 1,515 ft.

The televiewer log shown in figure 20 is an oriented sonic-reflectance map of the borehole wall. The cylindrical view of the borehole has been cut at the northern edge and unrolled so that the edges of the strip are north, the center is south, and east is left and west is right of center. High reflectance is white, and low reflectance is black. Washouts and elliptical holes cause black and white strips on the record (1,650–1,680 ft, fig. 20). Fractures show up as sinusoidal features. Within the upper flow interval the televiewer reveals a thick fracture dipping west at a low angle just above 1,625 ft and a thin fracture dipping west at a high angle just below. However, these cannot be differentiated from features in the no-flow intervals.

Fracture fillings and coatings commonly concentrate uranium and appear on the logs as spikes or as an overall increase in magnitude through fractured intervals. The uranium values for Yucca Mountain rocks are higher than for most sedimentary rocks elsewhere and seem to mask any effects that might be produced by fractures. There is no evidence for anomalous uranium deposition in the high-flow intervals.

The sonic-waveform log usually shows signals of lower amplitude, lower rock velocity, and a disrupted, noisy wave pattern in fractured intervals. Some of these features can be seen in the waveforms within the two flow intervals, but they cannot be differentiated from similar features in the no-flow intervals.

In summary, the uranium log provides no information regarding fractures. The sonic-waveform logs respond to fractures but do not differentiate between impermeable and permeable fracture zones. Tools that produce images of the borewall seem to work better: the acoustic televiewer and television camera have been used to identify fractures and, with some success, to correlate them with flow zones (Erickson and Waddell, 1985). Tools that work in concert with pump or injection tests are the most effective: temperature and radioactive tracer logs have produced the best evidence of permeable zones. Borewall imaging and sonic-waveform logs can augment the flow logs and are worth refining.

Figure 18 (facing page). Log and core data for borehole G–4. Separation of density and neutron logs indicates air invasion. Welding and alteration taken from Spengler and Chornack (1984), core measurements from Anderson (1984). Static water level (SWL) is at 1,780 ft.

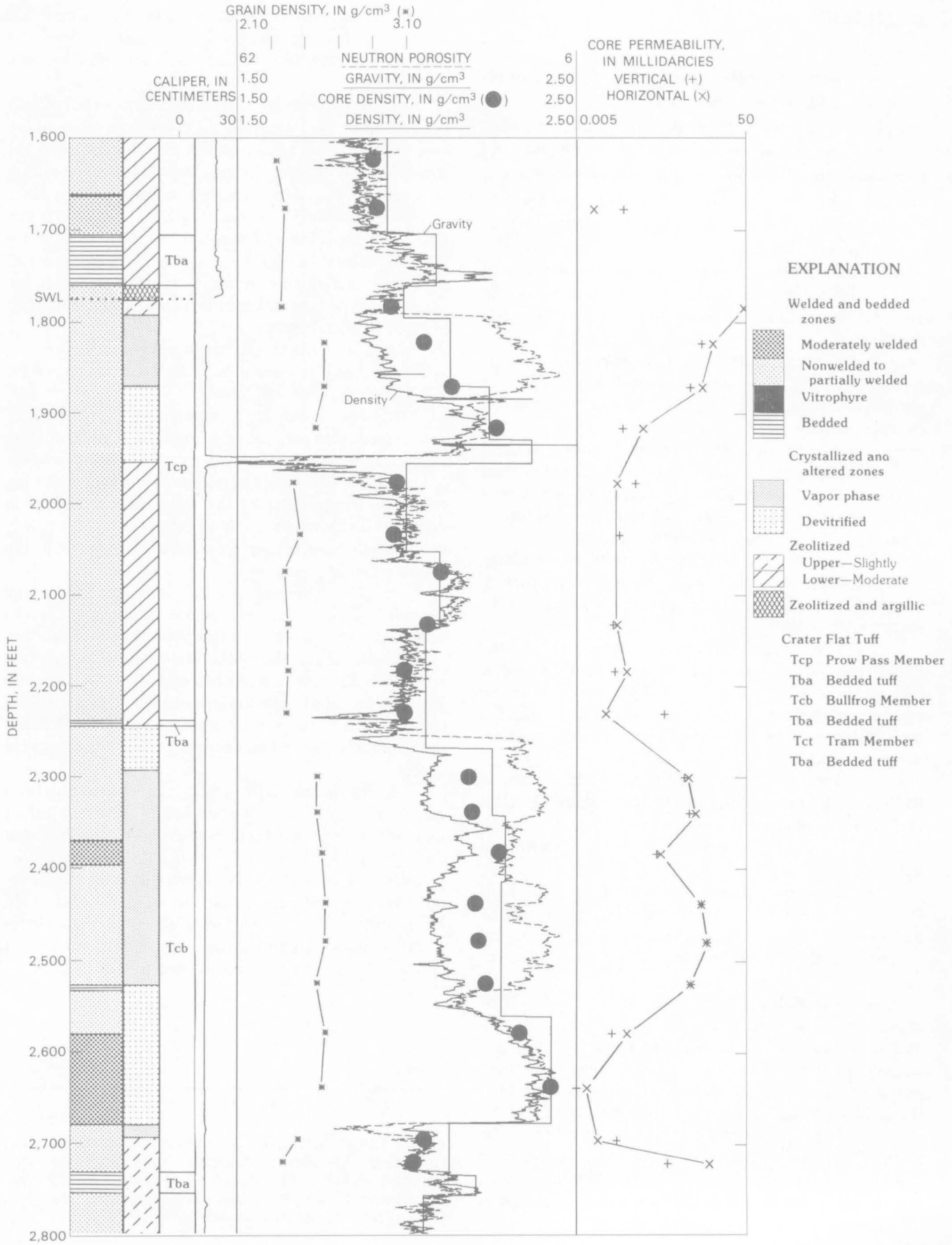
GRAIN DENSITY, IN g/cm3 (*)
2.10
3.10
62
NEUTRON POROSITY
6
CORE PERMEABILITY, IN MILLIDARCIES
CALIPER, IN CENTIMETERS
1.50
GRAVITY, IN g/cm3
2.50
VERTICAL (+)
HORIZONTAL (×)
1.50
CORE DENSITY, IN g/cm3 (●)
2.50
0
30
1.50
DENSITY, IN g/cm3
2.50
0.005
50
DEPTH, IN FEET
1,600
1,700
1,800
1,900
2,000
2,100
2,200
2,300
2,400
2,500
2,600
2,700
2,800
SWL
Tba
Tcp
Tba
Tcb
Tba
Gravity
Density
EXPLANATION
Welded and bedded zones
Moderately welded
Nonwelded to partially welded
Vitrophyre
Bedded
Crystallized and altered zones
Vapor phase
Devitrified
Zeolitized
Upper—Slightly
Lower—Moderate
Zeolitized and argillic
Crater Flat Tuff
Tcp Prow Pass Member
Tba Bedded tuff
Tcb Bullfrog Member
Tba Bedded tuff
Tct Tram Member
Tba Bedded tuff

SUMMARY

The geophysical logs and relevant core measurements from 40 boreholes at Yucca Mountain have been compiled into a single computerized data base, accessible with a commercial log-analysis package. Log quality and continuity varies from hole to hole because of variations in hole size, hole rugosity, and drilling history. The logging suite is more comprehensive and generally of better quality in the saturated zone than in the unsaturated zone because some tools cannot be operated in an air-filled borehole and because drilling in the Topopah Spring Member above the water table creates a rugose hole.

Welding and alteration are two important geologic controls on log response. Increased welding causes porosity to decrease and density to increase. The porosity changes are also manifest in the compressional-velocity, compensated-neutron, and resistivity logs. Mineral alteration (clays and zeolites) imposes a second control on the resistivity and neutron logs, causing a decrease in resistivity and an increase in neutron absorption, resulting in a high apparent neutron porosity.

Taken together, the logs are useful in examining both vertical and lateral variations in rock properties. Some of the prominent vertical, lithologically controlled features are these:

1. The Topopah Spring Member of the Paintbrush Tuff is characterized by a highly uniform, high-intensity gamma-ray log, caliper-log spikes, and erroneous low-density spikes (due to borehole rugosity), high resistivity, and a low-amplitude, normal-remanent magnetic field.

2. The tuff of Calico Hills and the lower part of the Topopah Spring, which are typically altered to clays and zeolites, produce a low-amplitude gamma-ray log, and show low density, low resistivity, and an unperturbed magnetic field.

3. The upper part of the Prow Pass Member of the Crater Flat Tuff is characterized by high resistivity and enhanced gamma-ray activity. A normal-remanent magnetic-field anomaly at the top of the Prow Pass serves as an excellent marker.

4. The Bullfrog Member of the Crater Flat Tuff appears as a zone of high-amplitude gamma radiation and erratically higher density and resistivity, having a large-amplitude, normal remanent magnetic field signature. A decrease in welding at the top and bottom of the Bullfrog Member helps to define it on the logs.

5. The upper unit of the Tram Member of the Crater Flat Tuff is probably the easiest unit to recognize from logs. It is characterized by its very high amplitude, reverse remanent magnetic-field log and by high values of gamma radiation, density, and resistivity.

The lower unit of the Tram, by way of contrast, shows only low-level magnetic-field perturbations and moderate values for gamma radiation, density, and resistivity.

Figures 10–12 show that physical properties of tuffs penetrated by G–2 are quite different from those of the same stratigraphic units penetrated in boreholes to the south. Lateral variations in log character could be caused by pinching out of a unit, changes in type and abundance of mineral alteration, or mineralogical gradients at the time of deposition. Explanation of this particularly dramatic lateral change requires study of the logs and core. Documentation of other lateral changes within the site requires posting and examination of logs in a number of cross sectional views.

With regard to the determination of porosity, saturation, and permeability from the logs, we have established the following points:

1. The density log compares well with densities determined from core samples. In the unsaturated zone, log quality is marred by low-density spikes due to borehole rugosity. Estimation of porosity from the density log would be complicated by the substantial variations in grain density. Neutron, sonic-velocity, and resistivity logs would contribute to the estimation of porosity in the saturated zone.

2. The determination of water content in the unsaturated zone depends on the epithermal-neutron and dielectric logs, which at this point appear to produce "reasonable" data. The epithermal-neutron logging tool requires calibration in a test facility. Use of the dielectric log requires laboratory study of dielectric properties of tuff. Ultimately, confidence in their application depends on good sampling and measurement of water content of cores.

3. From radioactive-tracer logs, it has already been established that flow is dominated by fractures rather than by matrix permeability. However, the logs show that during drilling there was significant invasion of the formation by air over a few intervals within the Prow Pass and Bullfrog Members of the Crater Flat Tuff. Permeability values in these intervals are on the order of 5 millidarcies, according to core measurements. It appears that matrix permeability cannot be ignored.

Figure 19 (facing page). Log and core data for borehole GU–3/G–3. Separation of density and gravimeter logs indicates invasion. All data from GU–3 except gravimeter from nearby G–3. Open circles are saturated bulk densities. Permeability scale is logarithmic.

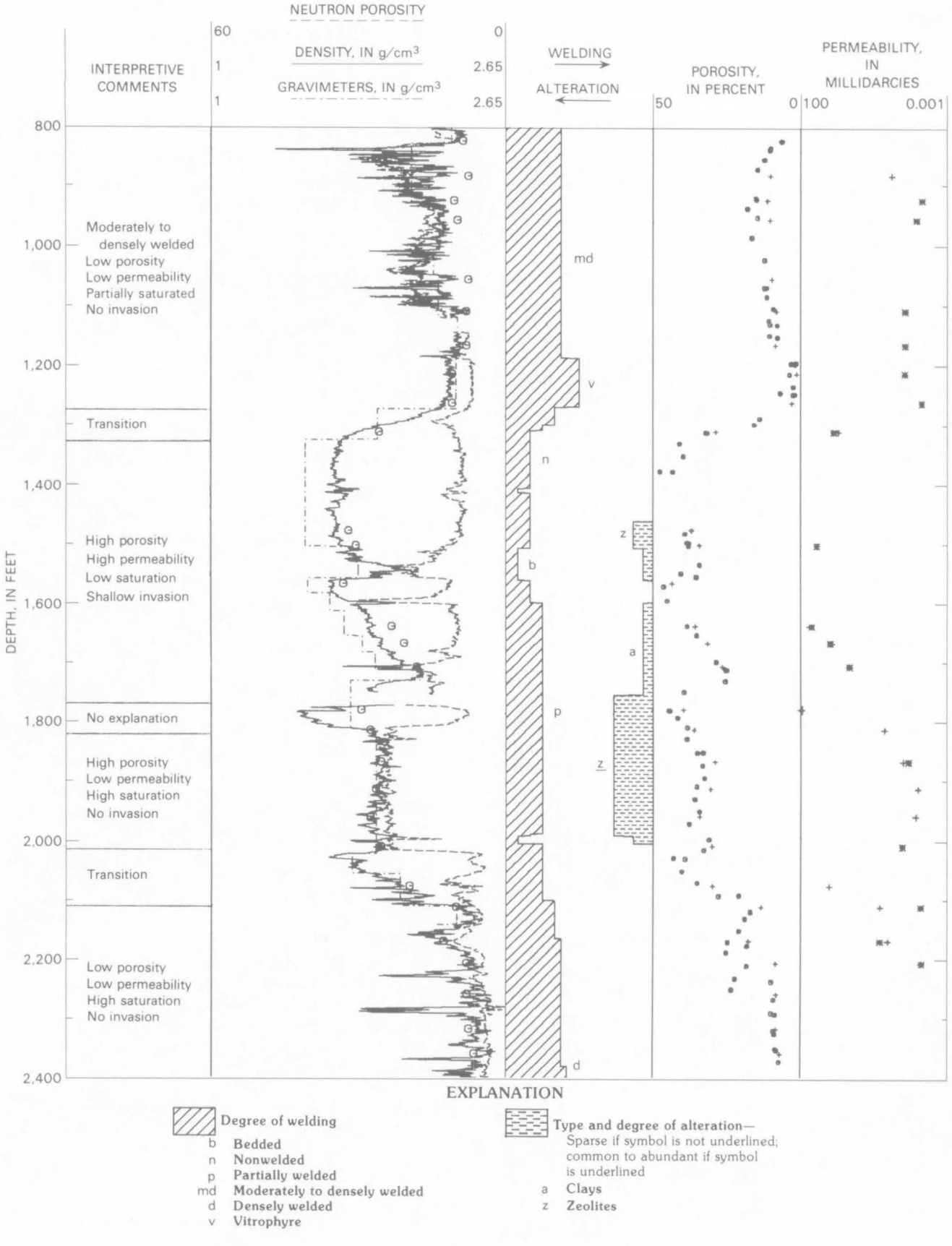
NEUTRON POROSITY
60
0
DENSITY, IN g/cm3
1
2.65
GRAVIMETERS, IN g/cm3
1
2.65
INTERPRETIVE COMMENTS
WELDING
ALTERATION
POROSITY, IN PERCENT
50
0
PERMEABILITY, IN MILLIDARCIES
100
0.001
DEPTH, IN FEET
800
1,000
1,200
1,400
1,600
1,800
2,000
2,200
2,400
Moderately to densely welded
Low porosity
Low permeability
Partially saturated
No invasion
Transition
High porosity
High permeability
Low saturation
Shallow invasion
No explanation
High porosity
Low permeability
High saturation
No invasion
Transition
Low porosity
Low permeability
High saturation
No invasion
md
v
n
b
z
a
p
z
d
EXPLANATION
Degree of welding
b Bedded
n Nonwelded
p Partially welded
md Moderately to densely welded
d Densely welded
v Vitrophyre
Type and degree of alteration—
Sparse if symbol is not underlined; common to abundant if symbol is underlined
a Clays
z Zeolites

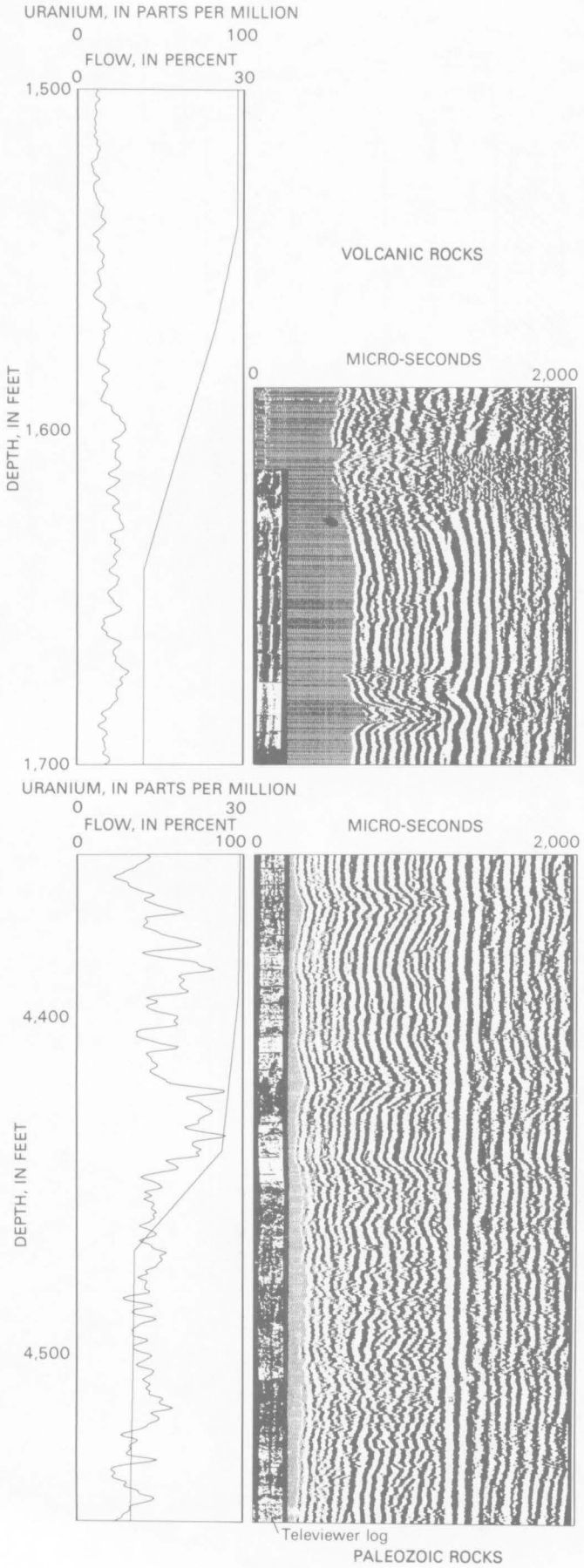

ACKNOWLEDGMENTS

We thank Len Anderson for discussions and the contribution of unpublished core data. Steve Prensky and Ray Obuch provided access to computer facilities and software support. Mel Millett of Lawrence Livermore National Laboratory provided computer tapes of unpublished magnetic-field logs.

REFERENCES CITED

Anderson, L.A., 1981a, Rock property analysis of core samples from Yucca Mountain UE25a–1 borehole, Nevada Test Site, Nevada: U.S. Geological Survey Open-File Report 81–1338, 36 p.

_____ 1981b, Rock property analysis of core samples from the Calico Hills UE25a–3 borehole, Nevada Test Site, Nevada: U.S. Geological Survey Open-File Report 81–1337, 33 p.

_____ 1984, Rock property measurements on large-volume core samples from Yucca Moutain USW GU–3/G–3 and USW G–4 boreholes, Nevada Test Site, Nevada: U.S. Geological Survey Open-File Report 84–552, 39 p.

Axelrod, M.C., and Hearst, J.R., 1984, Calibration of a neutron log in partially saturated media IV—Effects of sonde-wall gap: Transactions of Society of Professional Well Log Analysts Twenty-Fifth Annual Logging Symposium, Paper Q, 17 p.

Baldwin, M.J., and Jahren, C.E., 1982, Magnetic properties of drill core and surface samples from the Calico Hills area, Nye County, Nevada: U.S. Geological Survey Open-File Report 82–536, 27 p.

Benson, L.V., and McKinley, P.W., 1985, Chemical composition of ground water in the Yucca Mountain area, Nevada, 1971–84: U.S. Geological Survey Open-File Report 85–484, 10 p.

Benson, L.V., Robison, J.H., Blankennagel, R.K., and Ogard, A.E., 1983, Chemical composition of ground water and the locations of permeable zones in the Yucca Mountain area, Nevada: U.S. Geological Survey Open-File Report 83–854, p. 19.

Bentley, C.B., 1984, Hydrologic data for well USW G–4, Yucca Mountain area, Nye County, Nevada: U.S. Geological Survey Open-File Report 84–063, 53 p.

Bentley, C.B., Robison, J.H., and Spengler, R.W., 1983, Geohydrologic data for well USW H–5, Yucca Mountain area, Nye County, Nevada: U.S. Geological Survey Open-File Report 83–853, 38 p.

Bish, D.L., 1981, Detailed mineralogical characterization of the Bullfrog and Tram members in USW–G1, with emphasis on clay mineralogy: Los Alamos National Laboratory Report LA–9021–MS, 21 p.

Figure 20 (facing column). Flow log from radioactive tracer (straight line) compared with uranium, televiewer (narrow strip), and sonic-waveform logs for borehole P-1, Yucca Mountain, Nev.

Broxton, D.E., Vaniman, D.T., Caporuscio, F.A., and Heiken, G.H., 1982, Detailed petrographic descriptions and microprobe data for drill holes USW–G2 and UE25b–1H, Yucca Mountain, Nevada: Los Alamos National Laboratory Report LA–9324–MS, 72 p.

Broxton, D.E., Warren, R.G., Hagan, R.C., and Luedemann, Gary, 1986, Chemistry of diagenetically altered tuffs at a potential nuclear waste repository, Yucca Mountain, Nye County, Nevada: Los Alamos National Laboratory Report LA–10802–MS, 160 p.

Byers, F.M., Jr., 1985, Petrochemical variation of Topopah Spring tuff matrix with depth (stratigraphic level), drill hole USW G–4, Yucca Mountain, Nevada: Los Alamos National Laboratory Report LA–10561–MS, 38 p.

Caporuscio, F.A., Vaniman, D.T., Bish, D.L., Broxton, D.E., Arney, B., Hieken, G.H., Byers, F.M., Gooley, R., and Semarge, E., 1982, Petrologic studies of drill cores USW–G2 and UE25b–1H, Yucca Mountain, Nevada: Los Alamos National Laboratory Report LA–9255–MS, 111 p.

Caporuscio, F.A., Warren, R.G., and Broxton, D.E., 1983, Detailed petrographic descriptions and microprobe data for Tertiary silicic volcanic rocks in drill hole USW–G1, Yucca Mountain, Nevada: Los Alamos National Laboratory Report LA–9323–MS, 76 p.

Carr, W.J., 1982, Volcano-tectonic history of Crater Flat, southwestern Nevada, as suggested by new evidence from drill hole USW–VH–1 and vicinity: U.S. Geological Survey Open-File Report 82–457, 23 p.

Carr, W.J., and Parrish, L.D., 1985, Geology of drill hole USW VH–2, and structure of Crater Flat, southwestern Nevada: U.S. Geological Survey Open-File Report 85–475, 41 p.

Carr, M.D., Waddell, S.J., Wick, G.S., Stock, J.M., Monsen, S.A., Harris, A.G., Cork, B.W., and Byers, F.M., Jr., 1986, Geology of drill hole UE25p#1—A test hole into pre-Tertiary rocks near Yucca Mountain, southern Nevada: U.S. Geological Survey Open-File Report 86–175, 87 p.

Carroll, P.I., Caporuscio, F.A., and Bish, D.L., 1981, Further description of the petrology of the Topopah Spring member of the Paintbrush Tuff in drill holes UE25A–1 and USW–G1 and of the lithic-rich tuff in USW–G1, Yucca Mountain, Nevada: Los Alamos National Laboratory Report LA–9000–MS, 26 p.

Carroll, R.D., 1990, Electric logging and electrical properties of rock in the Rainier Mesa area, Nevada Test Site, Nevada: U.S. Geological Survey Open-File Report 90–31, 90 p.

Chipera, S.J., and Bish, D.L., 1988, Mineralogy of drill hole UE–25p#1 at Yucca Mountain, Nevada: Los Alamos National Laboratory Report LA–11292–MS, 24 p.

Craig, R.W., and Johnson, K.A., 1984, Geohydrologic data for test well UE25p#1, Yucca Mountain area, Nye County, Nevada: U.S. Geological Survey Open-File Report 84–450, 63 p.

Craig, R.W., Reed, R.L., and Spengler, R.W., 1983, Geohydrologic data for well USW H–6, Yucca Mountain Area, Nye County, Nevada: U.S. Geological Survey Open-File Report 83–856, 39 p.

Craig, R.W., and Robison, J.H., 1984, Geohydrology of rocks penetrated by test well UE–25p#1: U.S. Geological Survey Water-Resources Investigations Report 84–4248, 57 p.

Daniels, J.J., and Scott, J.H., 1980, Borehole geophysical measurement for hole UE25a–3, Nevada Test Site, Nuclear Waste Isolation Program: U.S. Geological Survey Open-File Report 80–126, 30 p.

Daniels, J.J., Scott, J.H., and Hagstrum, J.T., 1981, Interpretation of geophysical well-log measurements in drill holes UE25a–4, –5, –6, –7, Yucca Mountain, Nevada Test Site: U.S. Geological Survey Open-File Report 81–615, 29 p.

Douglas, A.C., and Millett, M.R., 1978, Total intensity magnetometer logging as a stratigraphic tool in Tertiary volcanic rock: Lawrence Livermore National Laboratory Report UCRL–52617, 11 p.

Dresser-Atlas, 1985, Log interpretation charts: Houston, Texas, Dresser Industries, Inc., 157 p.

Ellis, D.V., 1987, Well logging for earth scientists: New York, Elsevier, 532 p.

Ellis, W.L., and Swolfs, H.S., 1983, Preliminary assessment of in-situ geomechanical characteristics in drill hole USW G–1, Yucca Mountain, Nevada: U.S. Geological Survey Open-File Report 83–401, 18 p.

Erickson, J.R., and Waddell, R.K., 1985, Identification and characterization of hydrologic properties of fractured tuff using hydraulic and tracer tests—Test Well H–4: U.S. Geological Survey Water-Resources Investigations Report 85–4066, 30 p.

Hagstrum, J.T., Daniels, J.J., and Scott, J.H., 1980a, Interpretation of geophysical well-log measurements in drill hole UE25a–1, Nevada Test Site, Radioactive Waste Program: U.S. Geological Survey Open-File Report 80–941, 32 p.

_____ 1980b, Analysis of the magnetic susceptibility well log in drill hole UE25a–5, Yucca Mountain, Nevada Test Site: U.S. Geological Survey Open-File Report 80–1263, 33 p.

Healey, D.L., Clutsom, F.G., and Glover, D.A., 1984, Borehole gravity meter surveys in drill holes USW G–3, Ue25p#1, and UE–25c#1, Yucca Mountain area, Nevada: U.S. Geological Survey Open-File Report 84–672, 16 p.

_____ 1986, Borehole gravity meter survey in drill hole USW G–4, Yucca Mountain area, Nye County, Nevada: U.S. Geological Survey Open-File Report 86–205, 18 p.

Healy, J.H., Hickman, S.H., Zoback, M.D., and Ellis, W.L., 1984, Report on televiewer log and stress measurements in core hole USW–G1, Nevada Test Site, December 13–22, 1981: U.S. Geological Survey Open-File Report 84–15, 47 p.

Hearst, J.R, and Nelson, P.H., 1985, Well logging for physical properties: New York, McGraw-Hill Book Company, 571 p.

Heiken, G.H., and Bevier, Mary Lou, 1979, Petrology of tuff units from the J–13 drill site, Jackass Flats, Nevada: Los Alamos Scientific Laboratory Report LA–7563–MS, 55 p.

Johnson, R.L., 1982, Thermal analysis for a nuclear waste repository in tuff using USW–G1 borehole data: Sandia National Laboratories Report SAND 82–0170, 50 p.

Lahoud, R.G., Lobmeyer, D.H., and Whitfield, M.S., Jr., 1984, Geohydrology of volcanic tuff penetrated by test well UE–25b#1, Yucca Mountain, Nye County, Nevada: U.S. Geological Survey Water-Resources Investigations Report 84–4253, 44 p.

Lappin, A.R., Van Buskirk, R.G., Enniss, D.O., Butters, S.W., Prater, F.M., Muller, C.S., and Bergosh, J.L., 1982, Thermal conductivity, bulk properties, and thermal stratigraphy of silicic tuffs from the upper portion of hole USW–G1, Yucca Mountain, Nye County, Nevada: Sandia National Laboratories Report SAND 81–1873, 48 p.

Levy, S.S., 1983, Petrology of samples from drill holes USW–H3, H4, H5, Yucca Mountain, Nevada: Los Alamos National Laboratory Report LA–9706–MS, 80 p.

Lobmeyer, D.H., 1986, Geohydrology of rocks penetrated by test well USW G–4, Yucca Mountain, Nye County, Nevada: U.S. Geological Survey Water-Resources Investigations Report 86–4015, 38 p.

Lobmeyer, D.H., Whitfield, M.S., Jr., Lahoud, R.R., and Bruckheimer, L., 1983, Geohydrologic data for test well UE–25b#1H, Nevada Test Site, Nye County, Nevada: U.S. Geological Survey Open-File Report 83–855, 52 p.

Maldonado, Florian, and Koether, S.L., 1983, Stratigraphy, structure, and some petrographic features of Tertiary volcanic rocks at the USW G–2 Drill Hole, Yucca Mountain, Nye County, Nevada: U.S. Geological Survey Open-File Report 83–732, 83 p.

Maldonado, Florian, Muller, D.C., and Morrison, J.N., 1979, Preliminary geologic and geophysical data of the UE25a–3 exploratory drill hole, Nevada Test Site, Nevada: U.S. Geological Survey Report USGS–1543–6, 43 p.

Montazer, Parviz, and Wilson, W.E., 1984, Conceptual hydrologic model of flow in the unsaturated zone, Yucca Mountain, Nevada: U.S. Geological Survey Water-Resources Investigations Report 84–4345, 55 p.

Muller, D.C., and Kibler, J.E., 1983, Commercial geophysical well logs from the USW G–1 drill hole, Nevada Test Site, Nevada: U.S. Geological Survey Open-File Report 83–321, 7 p.

_____ 1984, Preliminary analysis of geophysical logs from drill hole UE–25p#1, Yucca Mountain, Nye County, Nevada: U.S. Geological Survey Open-File Report 84–649, 14 p.

_____ 1986, Preliminary analysis of geophysical logs from the WT series of drill holes, Yucca Mountain, Nye County, Nevada: U.S. Geological Survey Open-File Report 86–46, 30 p.

Nimick, F.B., and Schwartz, B.M., 1987, Bulk, thermal, and mechanical properties of the Topopah Spring Member of the Paintbrush Tuff, Yucca Mountain, Nevada: Sandia National Laboratories Report SAND 85–0762, UC–70, 251 p.

Peters, R.R., Klavetter, E.A., Hall, I.J., Blair, S.C., Heller, P.R., and Gee, G.W., 1984, Fracture and matrix hydrologic characteristics of tuffaceous materials from Yucca Mountain, Nye County, Nevada: Sandia National Laboratories Report SAND 84–1471, UC–70, 184 p.

Price, R.H., 1983, Analysis of rock mechanics properties of volcanic tuff units from Yucca Mountain, Nevada Test Site: Sandia National Laboratories Report SAND 82–1315, UC–70, 81 p.

Robbins, S.L., Schmoker, J.W., and Hester, T.C., 1982, Principal facts and density estimates for borehole gravity stations in exploratory wells Ue4ah, Uelh, Uelq, Ue2co, and USW H–1 at the Nevada Test Site, Nye County, Nevada: U.S. Geological Survey Open-File Report 82–277, 18 p.

Robison, J.H., 1984, Ground-water level data and preliminary potentiometric-surface maps, Yucca Mountain and vicinity, Nye County, Nevada: U.S. Geological Survey Water-Resources Investigations Report 84–4197, 8 p.

Robison, J.H., Stephens, D.M., Luckey, R.R., and Baldwin, D.A., 1988, Water levels in periodically measured wells in the Yucca Mountain area, Nevada, 1981–1987: U.S. Geological Survey Open-File Report 88–468, 132 p.

Rosenbaum, J.G., and Rivers, W.C., 1984, Paleomagnetic orientation of core from drill hole USW GU–3, Yucca Mountain, Nevada—Tiva Canyon Member of the Paintbrush Tuff: U.S. Geological Survey Open-File Report 85–48, 116 p.

Rosenbaum, J.G., and Snyder, D.B., 1984, Preliminary interpretation of paleomagnetic and magnetic property data from drill holes USW G–1, G–2, GU–3, G–3, and VH–1 and surface localities in the vicinity of Yucca Mountain, Nye County, Nevada: U.S. Geological Survey Open-File Report 85–49, 73 p.

Rush, F.E., Thordarson, William, and Bruckheimer, Laura, 1983, Geohydrologic and drill-hole data for test well USW H–1, adjacent to Nevada Test Site, Nye County, Nevada: U.S. Geological Survey Open-File Report 83–141, 38 p.

Rush, F.E., Thordarson, William, and Pyles, D.G., 1984, Geohydrology of test well USW H–1, Yucca Mountain, Nye County, Nevada: U.S. Geological Survey Water-Resources Investigations Report 83–4032, 56 p.

Sass, J.H., Lachenbruch, A.H., Dudley, W.W., Jr., Priest, S.S., and Munroe, R.J., 1988, Temperature, thermal conductivity, and heat flow near Yucca Mountain, Nevada: Some tectonic and hydrologic implications: U.S. Geological Survey Open-File Report 87–649, 118 p.

Sass, J.H., Lachenbruch, A.H., and Mase, C.W., 1980, Analysis of thermal data from drill holes UE25a–3 and UE25a–1, Calico Hills and Yucca Mountain, Nevada Test Site: U.S. Geological Survey Open-File Report 80–826, 25 p.

Scott, J.H., and Olson, G.G., 1986, Development of a 3-component borehole magnetometer probe with gyroscopic orientation, *in* Killeen, P.G., ed., Borehole geophysics for mining and geotechnical applications: Geological Survey of Canada Paper 85–27, p. 251–259.

Scott, J.H., Seeley, R.L., and Barth, J.J., 1981, A magnetic susceptibility well-logging system for mineral exploration: Society of Professional Well Log Analysts Twenty-Second Annual Logging Symposium, Transactions, paper CC, 21 p.

Scott, R.B., and Castellanos, Mayra, 1984, Stratigraphic and structural relations of volcanic rocks in drill holes USW GU–3 and USW G–3, Yucca Mountain, Nye County, Nevada: U.S. Geological Survey Open-File Report 84–491, 121 p.

Spengler, R.W., Byers, F.M., Jr., and Warner, J.B., 1981, Stratigraphy and structure of volcanic rocks in drill hole USW–G1, Yucca Mountain, Nye County, Nevada: U.S. Geological Survey Open-File Report 81–1349, 50 p.

Spengler, R.W., and Chornack, M.P., 1984, Stratigraphic and structural characteristics of volcanic rocks in core hole USW G–4, Yucca Mountain, Nye County, Nevada, *with a section on* Geophysical logs by D.C. Muller and J.E. Kibler: U.S. Geological Survey Open-File Report 84–789, 77 p.

Spengler, R.W., Muller, D.C., and Livermore, R.B., 1979, Preliminary report on the geology and geophysics of drill hole UE25a–1, Yucca Mountain, Nevada Test Site: U.S. Geological Survey Open-File Report 79–1244, 43 p.

Spengler, R.W., and Rosenbaum, J.G., 1980, Preliminary interpretations of geologic results obtained from boreholes UE25a–4, –5, –6, and –7, Yucca Mountain, Nevada Test Site: U.S. Geological Survey Open-File Report 80–929, 33 p.

Stock, J.M., Healy, J.H., and Hickman, S.H., 1984, Report on televiewer log and stress measurements in core hole USW G–2, Nevada Test Site, October-November 1982: U.S. Geological Survey Open-File Report 84–172, 31 p.

Stock, J.M., Healy, J.H., Svitek, J., and Mastin, L., 1986, Report on televiewer log and stress measurements in holes USW G–3 and UE–25p#1, Yucca Mountain, Nye County, Nevada: U.S. Geological Survey Open-File Report 86–369, 91 p.

Sykes, M.L., Heiken, G.H., and Smyth, J.R., 1979, Mineralogy and petrology of tuff units from UE25a–1 drill site, Yucca Mountain, Nevada: Los Alamos National Laboratory Informal Report LA–8139–MS, 76 p.

Thordarson, William, 1983, Geohydrologic data and test results from well J–13, Nevada Test Site, Nye County, Nevada: U.S. Geological Survey Water-Resources Investigations Report 83–4171, 57 p.

Thordarson, William, and Howells, Lewis, 1987, Hydraulic tests and chemical quality of water at well USW VH–1, Crater Flat, Nye County, Nevada: U.S. Geological Survey Water-Resources Investigations Report 86–4359, 20 p.

Thordarson, William, Rush, F.E., and Waddell, S.J., 1985, Geohydrology of test well USW H–3, Yucca Mountain, Nye County, Nevada: U.S. Geological Survey Water-Resources Investigations Report 84–4272, 38 p.

Vaniman, D.T., Bish, D.L., Broxton, D.E., Byers, F.M., Jr., Heiken, G.H., Carlos, B.A., Semarge, R.E., Caporuscio, F.A., and Gooley, R.C., 1984, Variations in authigenic mineralogy and sorptive zeolite abundance at Yucca Mountain, Nevada, based on studies of drill cores USW–GU3/G3: Los Alamos National Laboratory Report LA–9707–MS, 71 p.

Warren, R.G., Byers, F.M., Jr., and Caporuscio, F.A., 1984, Petrography and mineral chemistry of units of the Topopah Spring, Calico Hills and Crater Flats Tuffs, and older volcanic units, with emphasis on samples from drill hole USW G–1, Yucca Mountain, Nevada Test Site: Los Alamos National Laboratory Report LA–10003–MS, 78 p.

Waters, A.C., and Carroll, P.R., ed., 1981, Preliminary stratigraphic and petrologic characterization of core samples from USW–G1, Yucca Mountain, Nevada: Los Alamos National Laboratory Report LA–8840–MS, 66 p.

Weeks, E.P., and Wilson, W.E., 1984, Preliminary evaluation of hydrologic properties of cores of unsaturated tuff, test well USW H–1, Yucca Mountain, Nevada: U.S. Geological Survey Water-Resources Investigations Report 84–4193, 30 p.

Whitfield, M.S., Jr., Eshom, E.P., Thordarson, William, and Schaefer, D.H., 1985, Geohydrology of rocks penetrated by test well USW H–4, Yucca Mountain, Nye County, Nevada: U.S. Geological Survey Water-Resources Investigations Report 85–4030, 33 p.

Whitfield, M.S., Jr., Thordarson, William, and Eshom, E.P., 1984, Geohydrologic and drill-hole data for test well USW H–4, Yucca Mountain, Nye County, Nevada: U.S. Geological Survey Open-File Report 84–449, 39 p.

Wichmann, P.A., McWhirter, V.C., and Hopkinson, E.C., 1975, Field results of the natural gamma spectrolog: Society of Professional Well Log Analysts Sixteenth Annual Logging Symposium, Transactions, paper O, 13 p.

APPENDIXES 1 AND 2

APPENDIX 1. INDEX TO PUBLISHED SOURCES OF LOG, CORE, AND TEST DATA FOR YUCCA MOUNTAIN BOREHOLES

This index lists published reports that present data obtained from drill holes at Yucca Mountain, including observations and measurements on core, hydrological tests, and borehole measurements. Publications that review, interpret, and synthesize results are not included unless they contain original data. Some reports of "preliminary" data may not appear here if such data are included in a subsequent "final" report.

With two exceptions, all boreholes penetrate alluvium and tuff. Borehole UE–25a#3 penetrates argillite of the Eleana Formation, not tuff. Borehole UE–25p#1 penetrates pre-Tertiary rocks below Tertiary tuff units.

A lack of a bibliographic reference does not necessarily indicate a lack of data, as some data had not been reported at the time this index was compiled. Obviously, many logs presented for the first time in this report are not referenced in the index. Temperature logs were obtained in most boreholes (Sass and others, 1988) but, to avoid repetition, are not listed in the index. However, thermal conductivity values obtained by Sass and others (1988) are referenced in column 4 of the index.

[NA, no data or data not published]

Borehole	Geology, petrology, mineralogy	Hydrology	Well logs, gravimetry, in-situ stress	Core tests
USW G-1	Bish, 1981 Carroll and others, 1981 Spengler and others, 1981 Waters and Carroll, 1981 Caporuscio and others, 1983 Warren and others, 1984 Broxton and others, 1986	NA	Ellis and Swolfs, 1983 Muller and Kibler, 1983 Healy and others, 1984.	Rosenbaum and Snyder, 1984 Nimick and Schwartz, 1987 Johnson, 1982 Lappin and others, 1982 Price, 1983 Sass and others, 1988
USW G-2	Broxton and others, 1982 Caporuscio and others, 1982 Maldonado and Koether, 1983 Broxton and others, 1986	Robison and others, 1988	Stock and others, 1984	Rosenbaum and Snyder, 1984 Nimick and Schwartz, 1987 Sass and other, 1988
USW GU-3	Scott and Castellanos, 1984 Broxton and others, 1986	Vaniman and others, 1984	NA	Rosenbaum and Snyder, 1984 Anderson, 1984 Peters and others, 1984 Nimick and Schwartz, 1987 Sass and others, 1988
USW G-3	Vaniman and others, 1984 Scott and Castellanos, 1984 Broxton and others, 1986	Robison and others, 1988	Healey and others, 1984	Anderson, 1984 Rosenbaum and Snyder, 1984 Stock and others, 1986 Sass and others, 1988
USW G-4	Spengler and Chornack, 1984 Byers, 1985 Broxton and others, 1986	Bentley, 1984 Lobmeyer, 1986 Robison and others, 1988	Spengler and Chornack, 1984 Healey and others, 1986	Anderson, 1984 Nimick and Schwartz, 1987 Peters and others, 1984 Sass and others, 1988
UE-25a#1	Spengler and others, 1979 Sykes and others, 1979 Carroll and others, 1981 Broxton and others, 1986	Spengler and others, 1979 Robison and others, 1988	Hagstrum and others, 1980a Sass and others, 1980	Anderson, 1981a Price, 1983 Nimick and Schwartz, 1987
UE-25b#1	Broxton and others, 1982 Caporuscio and others, 1982 Broxton and others, 1986	Lobmeyer and others, 1983 Lahoud and others, 1984 Robison and others, 1988	NA	NA
UE-25p#1	Carr and others, 1986 Chipera and Bish, 1988 Broxton and others, 1986	Craig and Johnson, 1984 Robison and others, 1988	Healey and others, 1984 Muller and Kibler, 1984 Stock and others, 1986	Sass and others, 1988

Borehole	Geology, petrology, mineralogy	Hydrology	Well logs, gravimetry, in-situ stress	Core tests
USW H-1	NA	Rush, 1983 Rush, 1984 Weeks, 1984 Robison and others, 1988	NA	NA
USW H-3	Levy, 1983	Thordarson and others, 1985 Robison and others, 1988	NA	NA
USW H-4	Levy, 1983	Erickson and Waddell, 1985 Whitfield and others, 1984 Whitfield and others, 1985 Robison and others, 1988	NA	NA
USW H-5	Levy, 1983	Bentley and others, 1983 Robison and others, 1988	NA	NA
USW H-6	NA	Craig and others, 1983 Robison and others, 1988	NA	NA
UE-25c#1	NA	NA	Healey and others, 1984	NA
UE-25c#2	NA	NA	NA	NA
UE-25c#3	NA	NA	NA	NA
USW WT-1	NA	Robison and others, 1988	Muller and Kibler, 1986	NA
USW WT-2	NA	Robison and others, 1988	Muller and Kibler, 1986	NA
UE-25WT#3	NA	Robison and others, 1988	Muller and Kibler, 1986	NA
UE-25WT#4	NA	Robison and others, 1988	Muller and Kibler, 1986	NA
UE-25WT#6	NA	Robison and others, 1988	Muller and Kibler, 1986	NA
USW WT-7	NA	Robison and others, 1988	Muller and Kibler, 1986	NA
USW WT-10	NA	Robison and others, 1988	Muller and Kibler, 1986	NA
USW WT-11	NA	Robison and others, 1988	Muller and Kibler, 1986	NA
UE-25WT#12	NA	Robison and others, 1988	Muller and Kibler, 1986	NA

Borehole	Geology, petrology, mineralogy	Hydrology	Well logs, gravimetry, in-situ stress	Core tests
UE-25WT#13	NA	Robison and others, 1988	Muller and Kibler, 1986	NA
UE-25WT#14	NA	Robison and others, 1988	Muller and Kibler, 1986	NA
UE-25WT#15	NA	Robison and others, 1988	Muller and Kibler, 1986	NA
UE-25WT#16	NA	Robison and others, 1988	Muller and Kibler, 1986	NA
UE-25WT#17	NA	Robison and others, 1988	Muller and Kibler, 1986	NA
UE-25WT#18	NA	Robison and others, 1988	Muller and Kibler, 1986	NA
USW UZ-1	NA	NA	NA	NA
USW UZ-6	NA	NA	NA	NA
UE-25a#3	Maldonado and others, 1979	NA	Maldonado and others, 1979 Sass and others, 1980 Daniels and Scott, 1980	Baldwin and Jahren, 1982 Anderson, 1981b
UE-25a#4	Spengler and Rosenbaum, 1980	NA	Daniels and others, 1981	NA
UE-25a#5	Spengler and Rosenbaum, 1980	NA	Hagstrum and others, 1980b Daniels and others, 1981	NA
UE-25a#6	Spengler and Rosenbaum, 1980	NA	Daniels and others, 1981	NA
UE-25a#7	Spengler and Rosenbaum, 1980	NA	Daniels and others, 1981	NA
J-13	Heiken and Bevier, 1979 Broxton and others, 1986	Thordarson, 1983 Robison and others, 1988	NA	NA
USW VH-1	Carr, 1982	Thordarson and Howells, 1987 Robison and others, 1988	NA	Rosenbaum and Snyder, 1984
USW VH-2	Carr and Parrish, 1985	NA	NA	NA

APPENDIX 2. DENSITY AND POROSITY DETERMINATIONS FROM CORE

Plotted in figures 21–30 are measurements of grain density, dry bulk density, and saturated bulk density as a function of depth in the borehole. Also plotted is the porosity determined from these density measurements. Density is given in g/cm^3; porosity is given as a percent of rock volume. These core properties were measured by Holmes and Narver, Terra Tek, Sandia Laboratories, and the USGS. Not included are measurements by Core Laboratories on a small number of samples from several different boreholes.

Label prefixes "GD," "SBD," "DBD," and "POR" designate grain density, saturated bulk density, dry bulk-density, and porosity, respectively. The letter "C" follows to indicate that these measurements are derived from core rather than from logs. The suffix letter(s) identifies the source of the data. Data by Lennart Anderson of the USGS are denoted with a subscript "A," as in "SBDCA." "GS" designates data by USGS analysts other than L. Anderson. "N" designates data from Sandia Laboratories reports; properties were measured by Sandia, Terra Tek, and Holmes and Narver. "HN" designates data from Holmes and Narver data sheets. "S" designates measurements by Sandia Laboratories, from Sandia reports or data sheets. "TT" refers to measurements by Terra Tek and reported by Sandia. References are cited in Appendix 1 under the appropriate borehole.

The stratigraphic chart to the right shows the geologic unit symbols used in figures 21–30.

Name of unit	Symbol
Quaternary and younger Tertiary	
Alluvium	Qac
Alluvium and colluvium	QTac
Miocene	
Basalt	Tb
Timber Mountain Tuff	
Ammonia Tanks Member	Tma
Rainier Mesa Member	Tmr
Bedded tuff	Tba
Paintbrush Tuff	
Tiva Canyon Member	Tpc
Bedded tuff	Tba
Yucca Mountain Member	Tpy
Bedded tuff	Tba
Bedded tuff (ash flow)	Tpb
Bedded tuff	Tba
Pah Canyon Member	Tpp
Bedded tuff	Tba
Topopah Spring Member	Tpt
Bedded tuff	Tba
Rhyolite of Calico Hills	
(tuffs and lavas of Calico Hills)	Tht
Crater Flat Tuff	
Prow Pass Member	Tcp
Bedded tuff	Tba
Bullfrog Member	Tcb
Bedded tuff	Tba
Tram Member	Tct
Bedded tuff	Tba
Lavas and flow breccias	Tll
Bedded tuff	Tba
Lithic Ridge Tuff	Tlr
Bedded tuff	Tba
Lava	Tll
Bedded tuff	Tba
Older tuffs in borehole USW G-1	Tt
Unit A	Tta
Unit B	Ttb
Unit C	Ttc
Older units	
Sedimentary deposits	Tsd
Calcified tuff	Tca
Tuff of Yucca Flat(?)	Tyf
Lone Mountain Dolomite	Slm
Roberts Mountain Formation	Srm

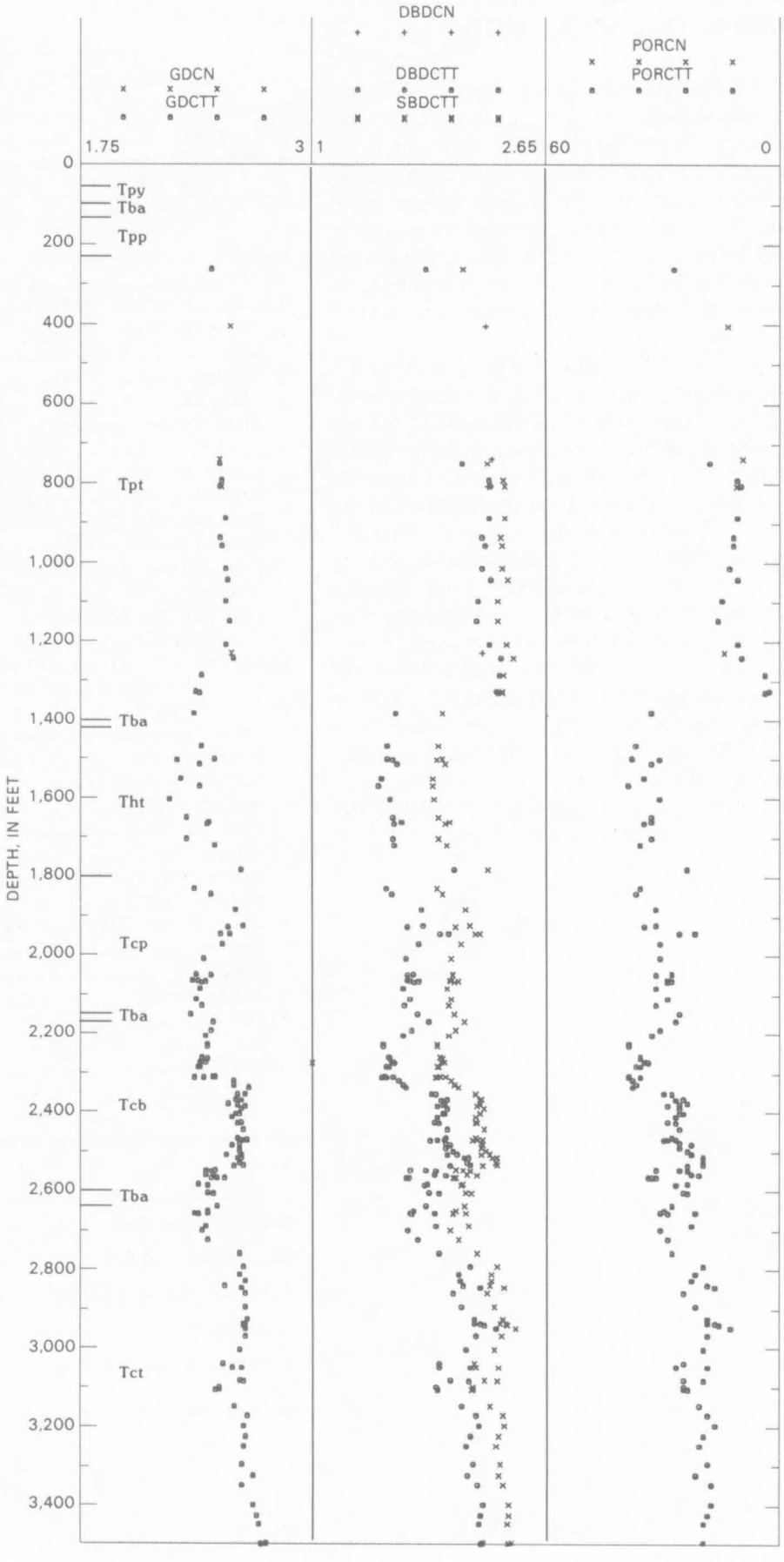
DBDCN
GDCN
GDCTT
DBDCTT
SBDCTT
PORCN
PORCTT
1.75
3
1
2.65
60
0
0
200
400
600
800
1,000
1,200
1,400
1,600
1,800
2,000
2,200
2,400
2,600
2,800
3,000
3,200
3,400
DEPTH, IN FEET
Tpy
Tba
Tpp
Tpt
Tba
Tht
Tcp
Tba
Tcb
Tba
Tct

Figure 21 (facing page). Determinations of grain density, dry bulk density, saturated bulk density, and porosity on core from borehole G-1, Yucca Mountain, Nev. Symbols are explained in introduction to Appendix 2.

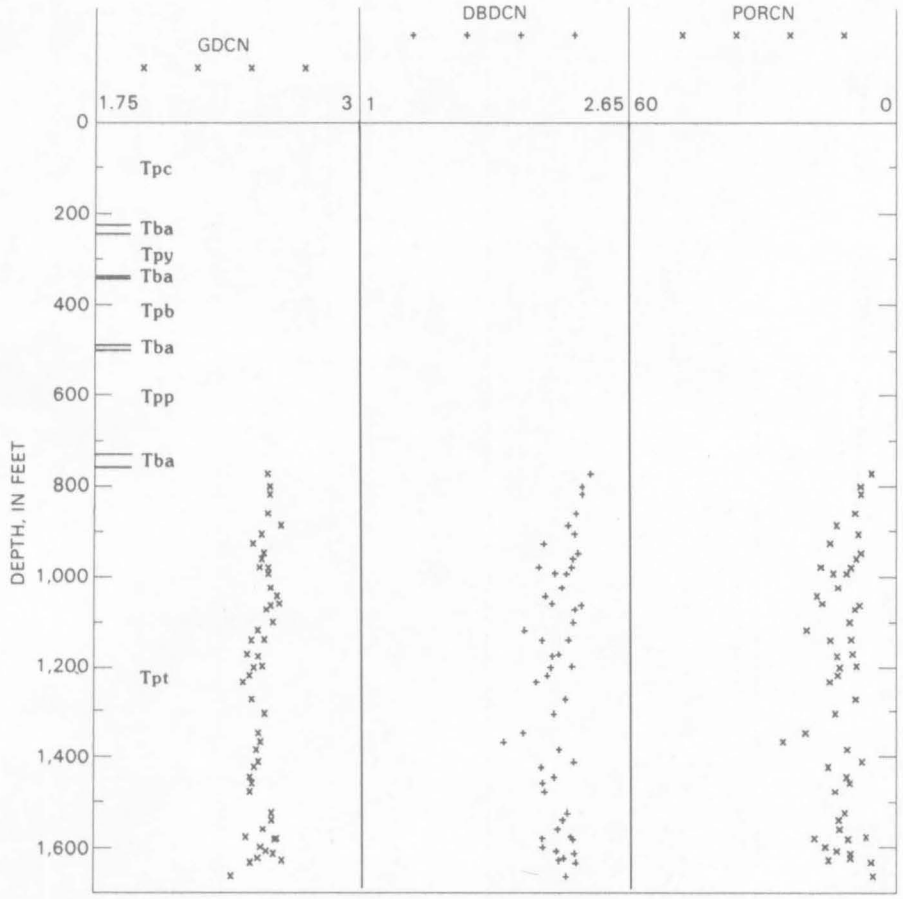

Figure 22. Determinations of grain density, dry bulk density, and porosity on core from borehole G-2, Yucca Mountain, Nev. Symbols are explained in introduction to Appendix 2.

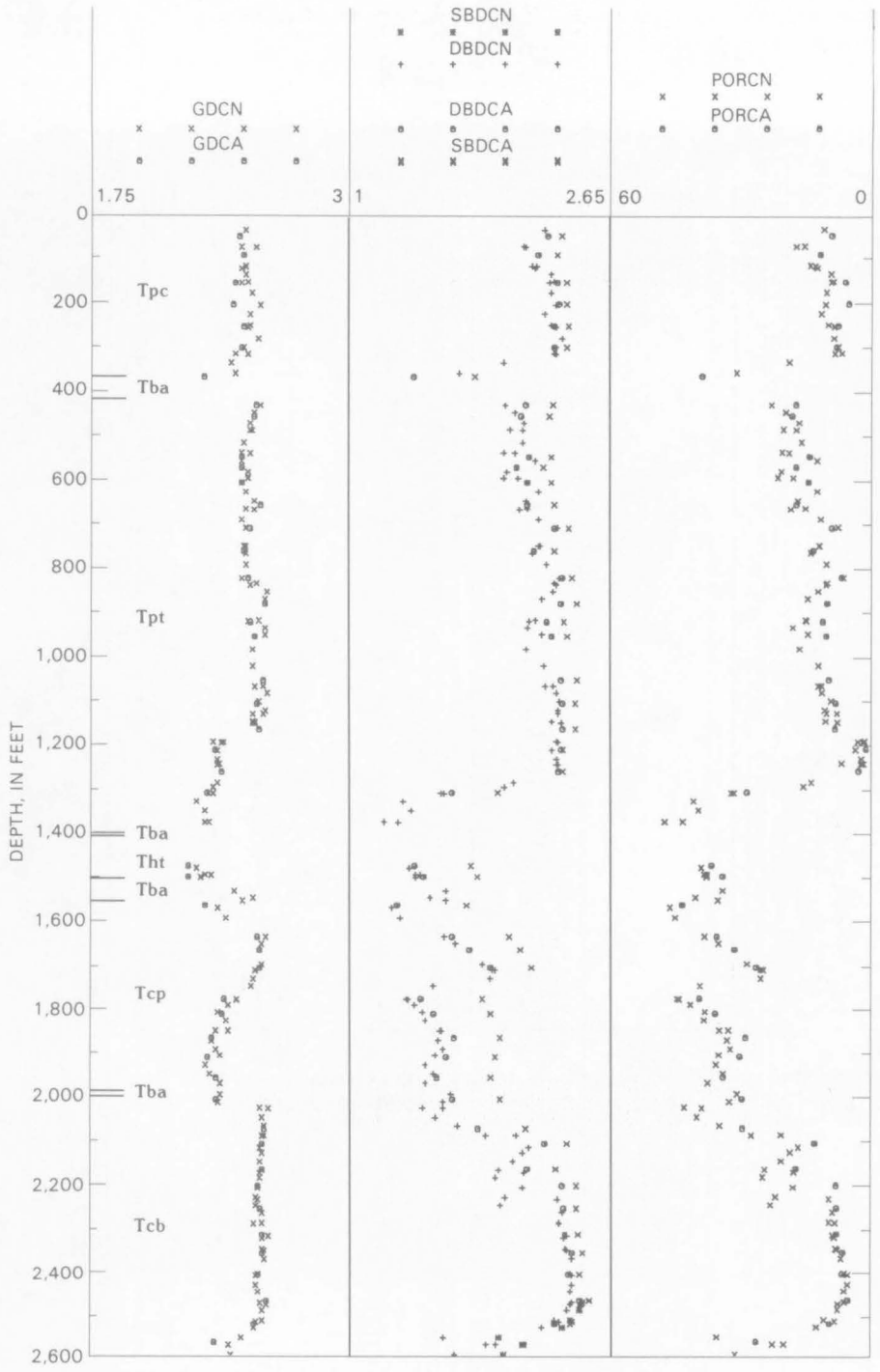

Figure 23. Determinations of grain density, dry bulk density, saturated bulk density, and porosity on core from borehole GU-3, Yucca Mountain, Nev. Symbols are explained in introduction to Appendix 2.

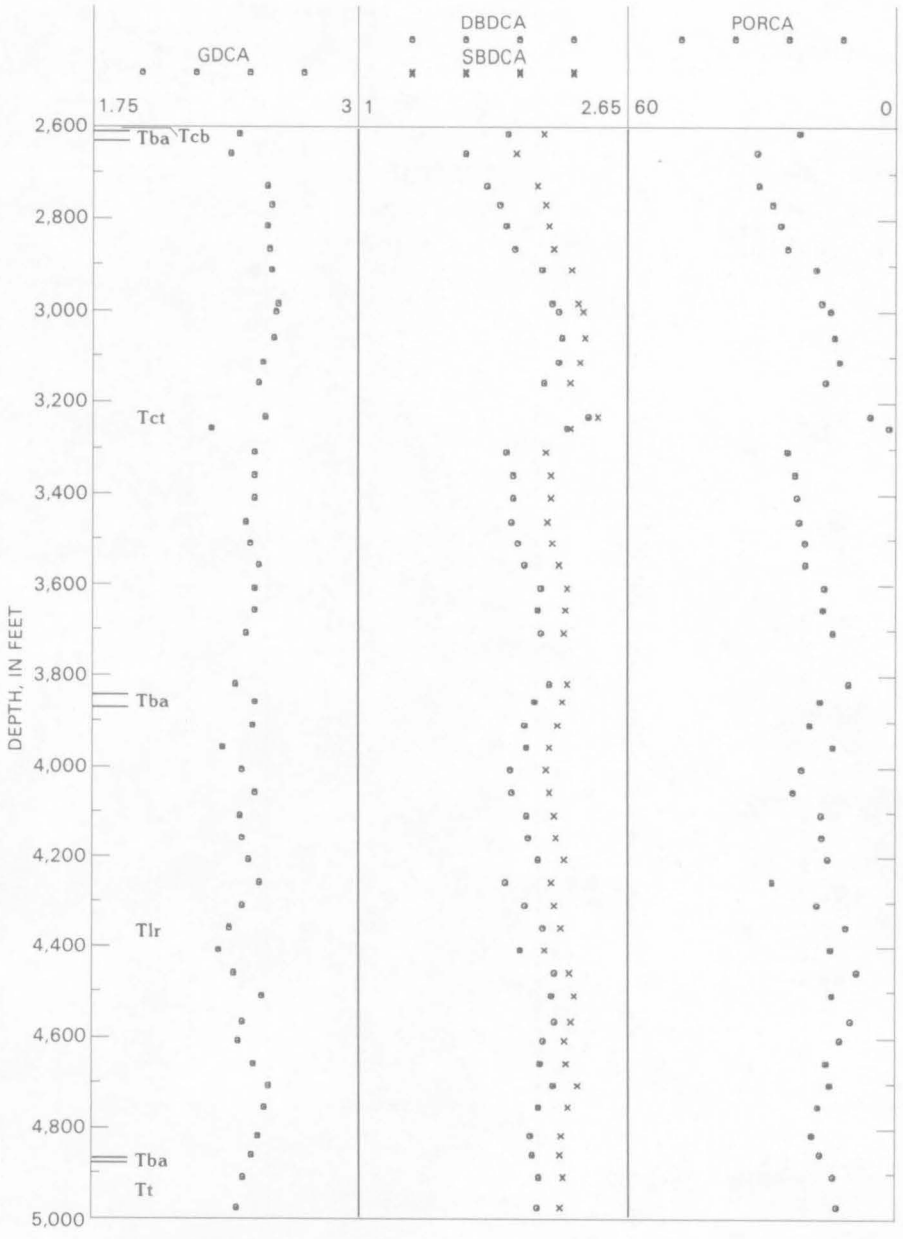

Figure 24. Determinations of grain density, dry bulk density, saturated bulk density, and porosity on core from borehole G-3, Yucca Mountain, Nev. Symbols are explained in introduction to Appendix 2.

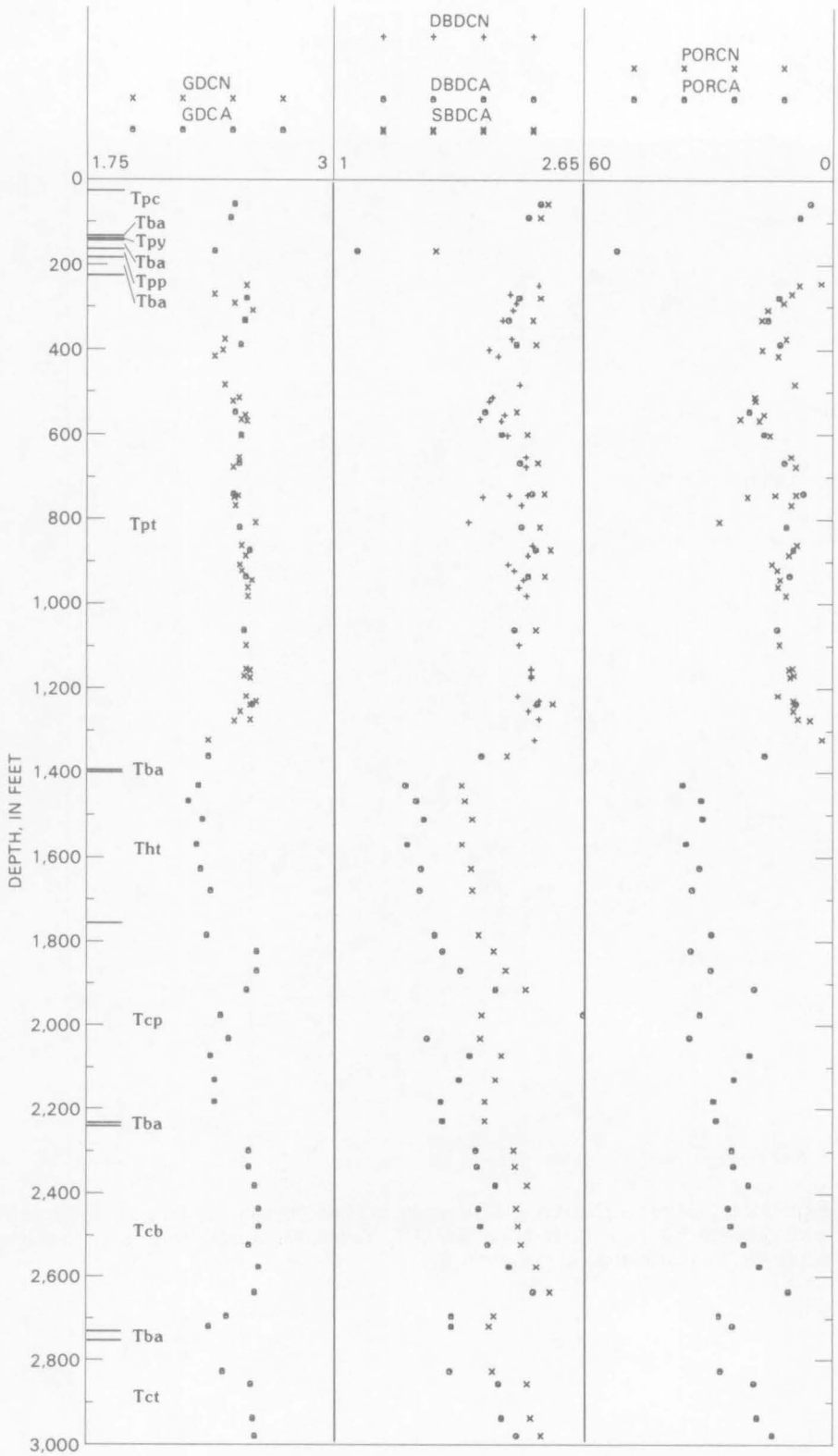

Figure 25. Determinations of grain density, dry bulk density, saturated bulk density, and porosity on core from borehole G-4, Yucca Mountain, Nev. Symbols are explained in introduction to Appendix 2.

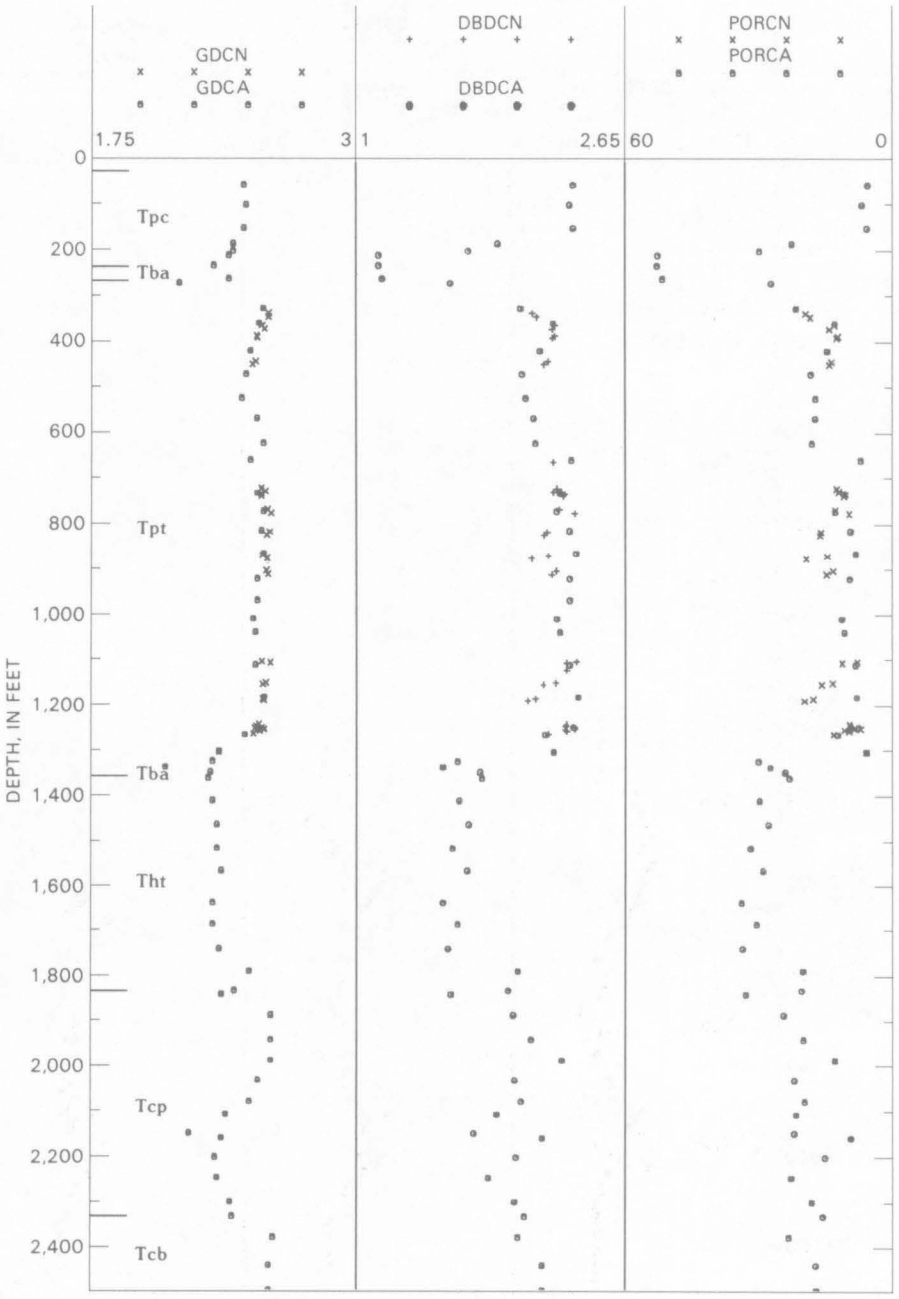

Figure 26. Determinations of grain density, dry bulk density, and porosity on core from borehole A-1, Yucca Mountain, Nev. Symbols are explained in introduction to Appendix 2.

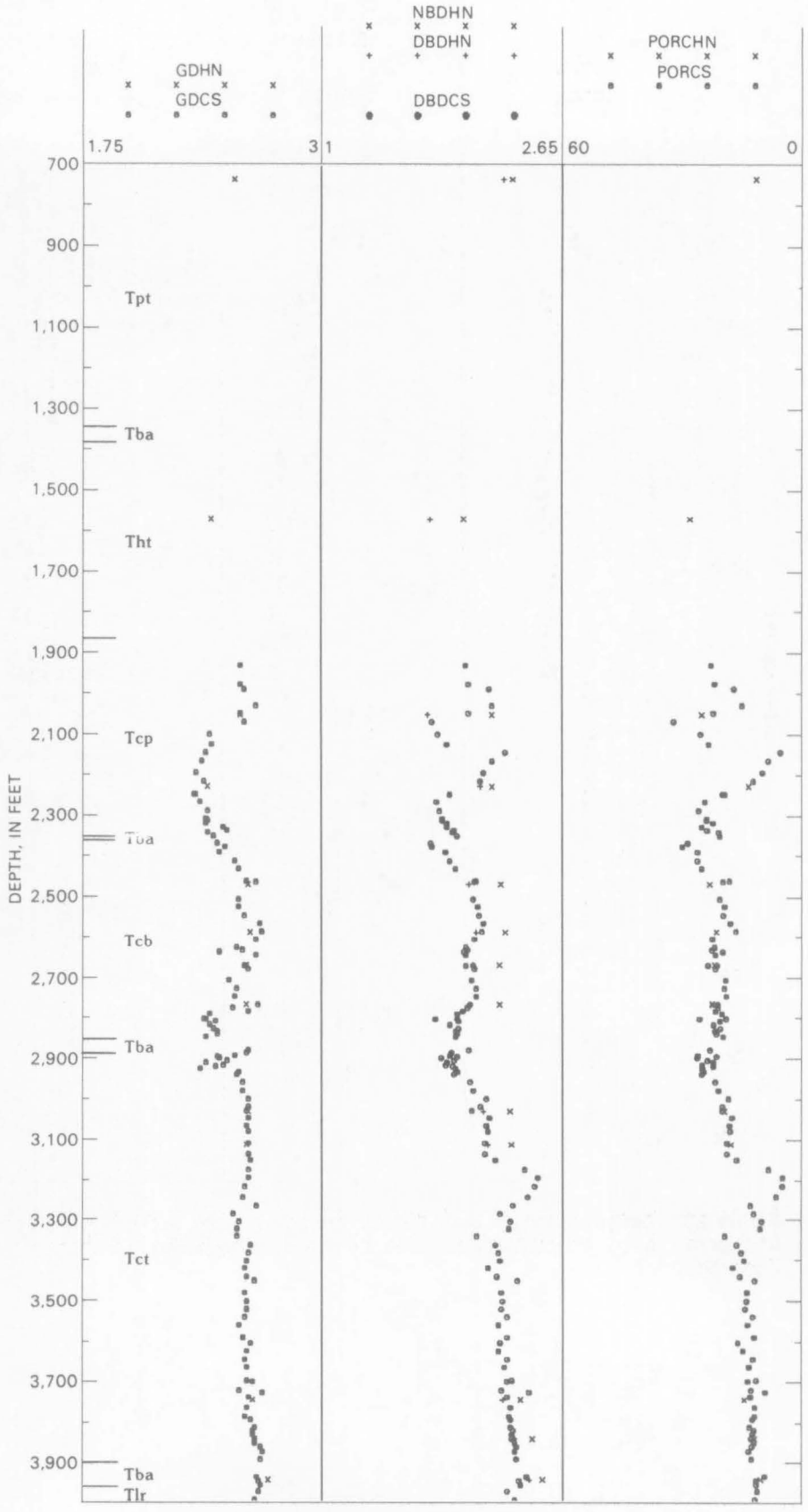

Figure 27. Determinations of grain density, dry bulk density, saturated bulk density, and porosity on core from borehole B-1H, Yucca Mountain, Nev. Symbols are explained in introduction to Appendix 2.

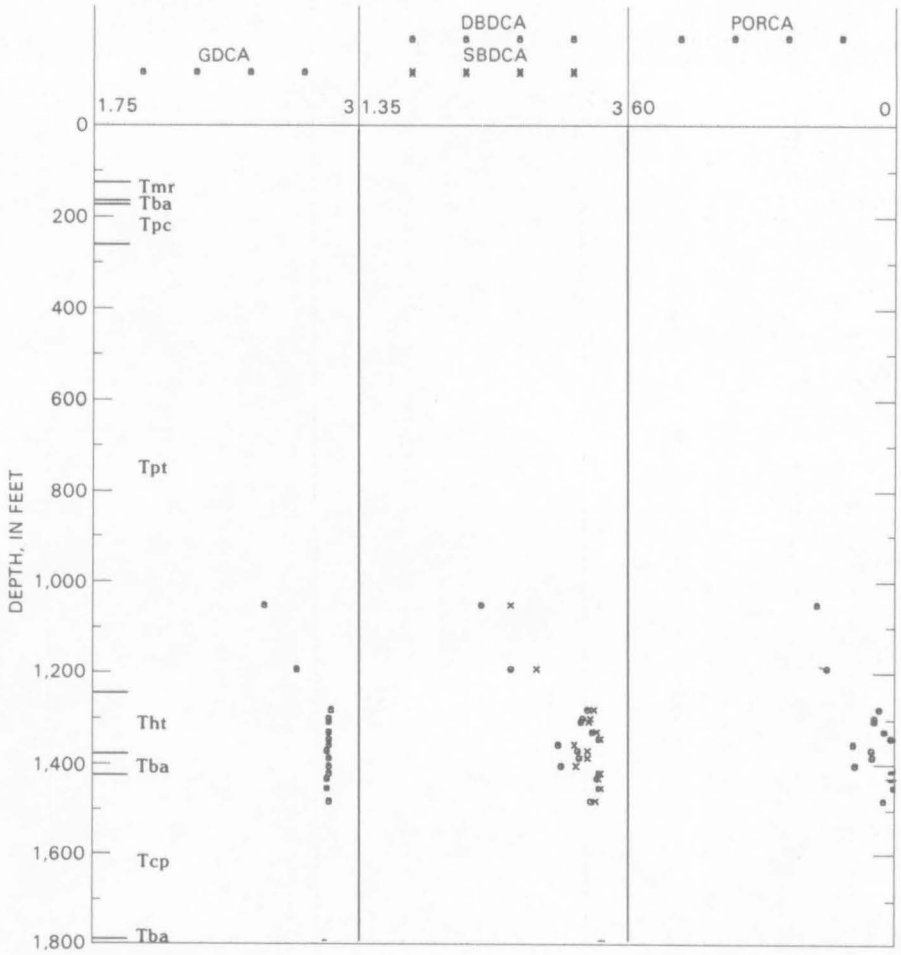

Figure 28. Determinations of grain density, dry bulk density, saturated bulk density, and porosity on core from borehole P–1, Yucca Mountain, Nev. Symbols are explained in introduction to Appendix 2.

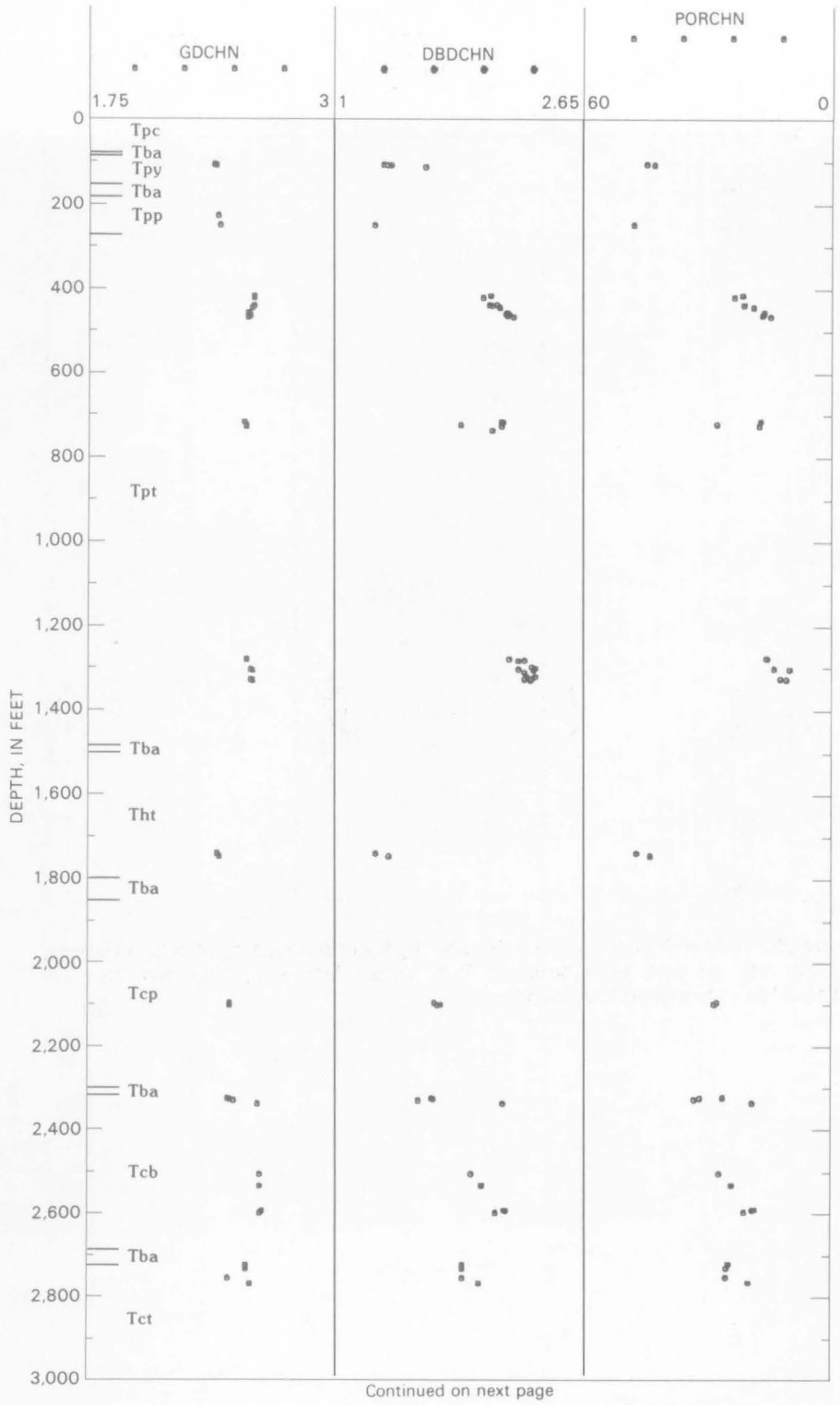

Continued on next page

Figure 29 (above and facing page). Determinations of grain density, dry bulk density, and porosity on core from borehole H–1, Yucca Mountain, Nev. Symbols are explained in introduction to Appendix 2.

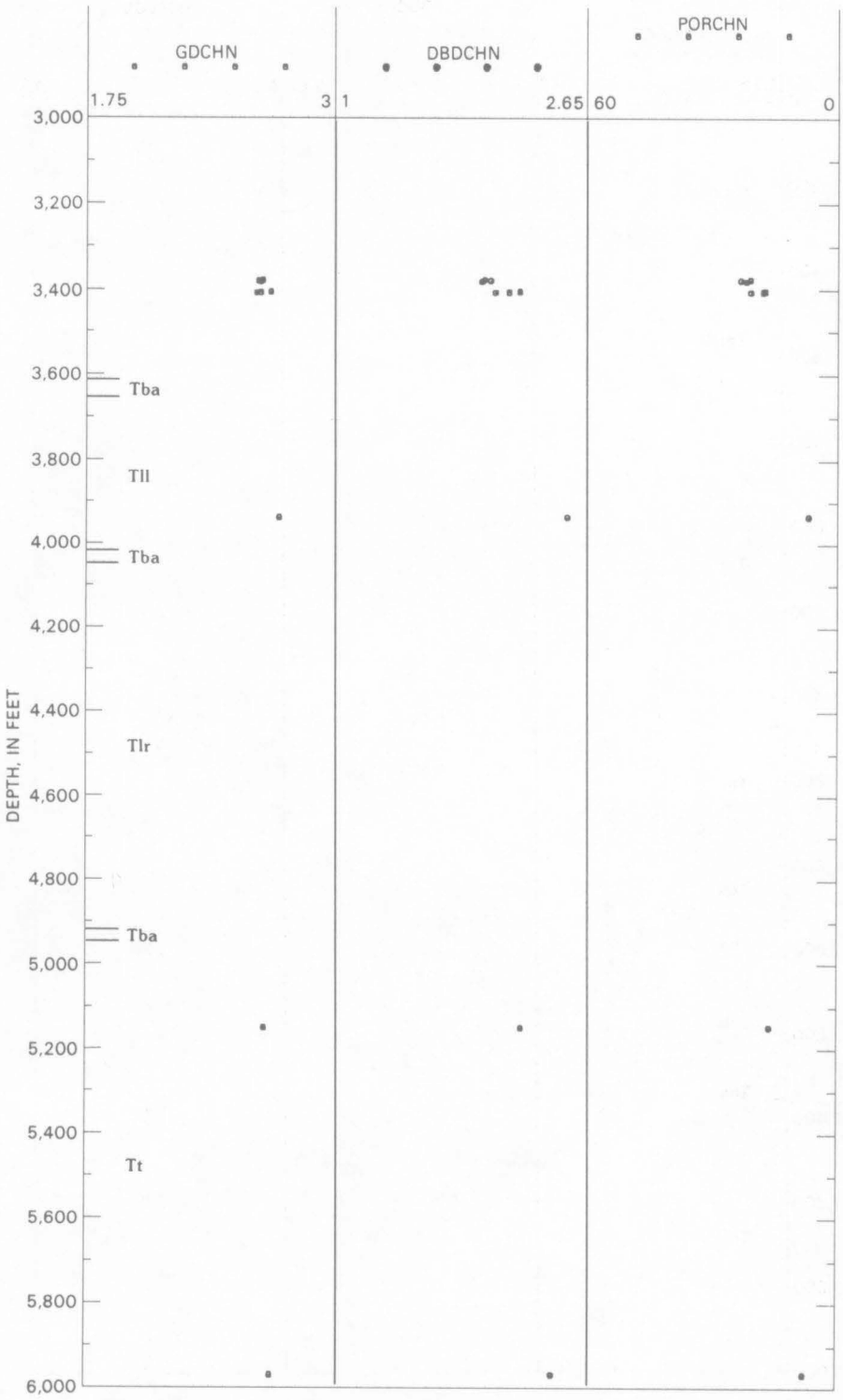
GDCHN
DBDCHN
PORCHN
1.75
3
1
2.65
60
0
3,000
3,200
3,400
3,600
3,800
4,000
4,200
4,400
4,600
4,800
5,000
5,200
5,400
5,600
5,800
6,000
DEPTH, IN FEET
Tba
Tll
Tba
Tlr
Tba
Tt

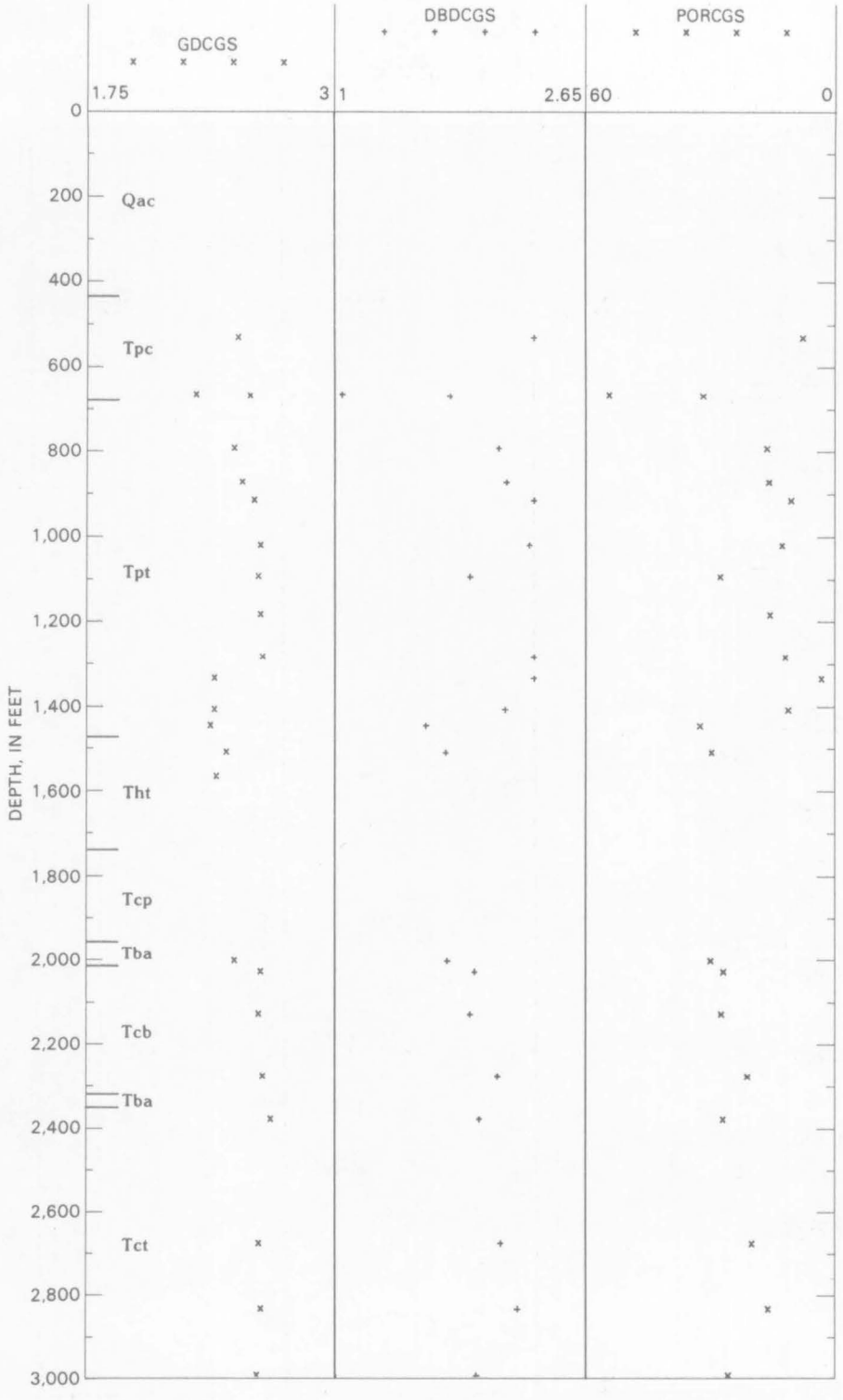

Figure 30. Determinations of grain density, dry bulk density, and porosity on core from borehole J–13, Yucca Mountain, Nev. Symbols are explained in introduction to Appendix 2.

*U.S. GOVERNMENT PRINTING OFFICE: 1991--524-370/40459